ADDIS ABABA UNIVERSITY
ADDIS ABABA INSTITUTE OF TECHNOLOGY
SCHOOL OF MECHANICAL AND INDUSTRIAL ENGINEERING
GRADUATE PROGRAM IN RAILWAY ENGINEERING

Structural Analysis of Addis Ababa City Light Railway Transit Tram Car Body Using Steel and Aluminum Honeycomb Sandwich material

A thesis submitted to the
School of Graduate Studies of Addis Ababa University
in partial fulfillment of the requirements for the award of the degree of
Master of Science in Mechanical Engineering (Rolling Stock Engineering)

By
Benyam Adane

Advisor
Dr. Ing zewdu Abdi

Co-Advisor

Ato Tollosa Debrie

September, 2014

Addis Ababa, Ethiopia

Addis Ababa Institute of Technology

School of Mechanical and Industrial Engineering

Structural Analysis of Addis Ababa City Light Railway Transit Tram Car Body Using Steel and Aluminum Honeycomb Sandwich material

By

Benyam Adane

Approved by Board of Examiners

Birhanu Beshah (Dr-Ing) ______________ ____________

Head, Railway center Signature Date

Zewdu Abdi (Dr-Ing) ______________ ____________

(Advisor) Signature Date

Tollossa Debrie _________ ____________

(Co-advisor) Signature Date

Tsegaye Feleke __________ ____________

Internal examiner Signature Date

Habtamu Tikubet ______________ ____________

External examiner Signature Date

DECLARATION

I hereby declare that the work which is being presented in this thesis entitled as "Structural Analysis of Addis Ababa City Light Railway Transit Tram Car Body Using Steel and Aluminum Honeycomb Sandwich material" is original work of my own. The work contained in this thesis has not been previously submitted for a degree or diploma at any other higher education institution. To the best of my knowledge and belief, the thesis contains no material previously published or written by another person except where due reference is made and all the resource materials used for this thesis had been accordingly acknowledged.

________________________	____________________
Benyam Adane	Date

This is to certify that the above declaration made by the candidate is correct to the best of my knowledge.

________________________	____________________
Dr.-Ing Zewdu Abdi (Advisor)	Date
________________________	____________________
Ato Tollosa Debrie (Co-Advisor	Date

Abstract

The structural design of railway vehicle bodies depends on the loads they are subject to and the Characteristics of the materials they are manufactured from. In this study structure analysis of Addis Ababa city tram passenger car made of the exact steel material and aluminum honeycomb material are analyzed. Finite element method is used to assess the static structure behavior of the tram car by ANSYS 14.5 software. For 3D modeling used solidwork11 and to simplify the core material selection process and to design the layers for aluminum honeycomb material by ANSYS Composite Prep Post (ACP). The result of the finite element analysis (FEA) shows that the structural analysis of the tram car using Aluminum Honeycomb reduce the gross weight by 12.14% with almost the same maximum principal stress and also its stress and deformation result of tensile, compression, lateral and vertical loading condition result validated against Structural requirements of railway vehicle bodies stated under EN 12663 and EN 15227 standard. The finite element result value of aluminum honeycomb and steel maximum principal stress of minimum variation but due to compression load applied on tram car using Aluminum Honeycomb higher compare to steel material to reduce the variation multi- material approach used to further reduce the stress and the deflection.

ACKNOWLEDGMENT

I would like to express my gratitude towards my advisor Dr. Zewdu Abdi and Ato Tollosa Debrie for his invaluable guidance, encouragements and inspiration during the path of this work. I would like to extend my special thanks to all my families and friends for their kind help and cooperation in various ways during this thesis work. I also would like to extend my respect and appreciation to all staff of Addis Ababa Institute of Technology and Ethiopia Railway Corporation, Mechanical Engineering department, Librarians and administrative workers of both AAIT and ERC: without their support, this thesis would not have been possible.

BENYAM ADANE

LIST OF CONTENTS

Abstract III
Acknowledgement IV
Table of contents V
List of figures VII
List of tables XI
Notations XII

CHAPTER ONE 1

1. Introduction 1

1.1 Background 1
1.2 Objective of the study 2
1.2.1General objective 2
1.2.2 Specific objective 3
1.3 Scope of the study 3
1.4 Methodology used 3
1.5 Organization of the research 4

CHAPTER TWO 5

2. Literature review 5

2.1 Introduction 5
2.2 Composite materials 7
2.3 Sandwich material 8
2.3.1 Face Materials 10
2.3.2 Core Materials 11

2.4 Application of sandwich material 14
2.5 Sandwich structures in rail vehicles 15
  2.5.1 C20 FICAS 16
  2.5.2 Korean Tilting Train Express, TTX 17
2.6 past work 17
2.7 Finite element formulation of sandwich panel 20
  2.7.1 Problem Formulation 20
  2.7.2 Stress strain relation in sandwich panel 23
  2.7.3 Finite element shape function 27
  2.7.4 The static analysis of sandwich panel 28
CHAPTER THREE 32
3. Creating finite element model 32
3.1 FE Analysis method of steel tram car 32
  3.1.1 FE modeling of steel tram car 32
  3.1.2 Define material property 33
  3.1.3 Mesh generation 34
  3.1.4 Boundary condition 34
  3.1.5 support and load 35
3.2 FE Analysis method of aluminum honeycomb tram car 38
  3.2.1 Aluminum honeycomb tram car model 38
  3.2.2 Define Engineering Data 39
  3.2.3 Generate Mesh 40
  3.2.4 ANSYS composite preprocess (ACP) 40
  3.2.5 Define Boundary Conditions and loading condition 41

3.3 Static stress analysis 41
3.3.1 Result of steel tram car due to tensile force at buffers 41
3.3.2 Result of steel tram car due to compression force at buffers 43
3.3.3 Result of steel tram car due to right turn 45
3.3.4 Result of steel tram car due to operating load 47
3.3.5 Result of aluminum honeycomb tram car due to tensile force at buffer 499
3.3.6 Result of aluminum honeycomb tram car due to compression force at buffer 51
3.3.7 Result of aluminum honeycomb tram car due to right turn 53
3.3.8 Result of aluminum honeycomb tram car due to operating load 55
CHAPTER FOUR **58**
4. Result and discussion **58**
CHAPTER FIVE **61**
5. Conclusion,recommendations and future work **61**
5.1 conclusions 61
5.2 Recommendations 62
5.3 Future work 62
References **63**
Appendix 66
ANSYS input file data for modeling aluminum honeycomb in ACP **66**

List of figures

Figure 2.1 Vehicle body carriage subassemblies 5
Figure 2.2 Exemplary percentage distributions of the main assemblies 5
Figure 2.3 Chronology of the development of car bodies 7
Figure 2.4 A sandwich structure 9
Figure 2.5 The Sandwich Effect. Because of the low density core, the weight difference between the structures 9
Figure 2.6 Shear deformation of sandwich material 10
Figure 2.7 Tensile strength and elastic modules comparison of different face material 11
Figure 2.8 Comparison of shear properties, left: shear modulus, right: shear Strength of different core material 12
Figure 2.9 Nomenclature of aluminum honeycomb 13
Figure 2.10 Honeycomb core in plan view 13
Figure 2.11 Schematic of sandwich construction 14
Figure 2.12 Application of sandwich structure in helicopter 14
Figure 2.13 Cross –section view of typical sandwich section for the C20FICAS 16
Figure 2.14 Vehicle configuration of TTX 17
Figure 2.15 The nomenclature of sandwich material 21
Figure 2.16 Displacement u for sandwich element oriented along the x-axis 22
Figure 2.17 Deformation of core element in the xz plane 22
Figure 2.18 The face and the core stress 23
Figure.2.19 Stress resultants and stress couples for a sandwich element 23
Figure 2.20 Ply notation 24
Figure 2. 21 Eight nodded isoperimetric shell element 27
Figure 2.22 Cross section of Addis Ababa city tram 31
Figure 3.1 Modeling of steel tram C-section using solid work 33
Figure 3.2 Meshing of steel vehicle body 34
Figure 3.3 boundary conditions of the FE model 34

Figure 3.4 Tensile force at the buffer 36
Figure 3.5 Compression force at the buffer 36
Figure 3.6 Load due to right turn and left turn 37
Figure 3.7 Load due to operating load 37
Figure 3.8 Finite element procedure used in ACP 38
Figure 3.9 Aluminum honeycomb model 39
Figure 3.10 Mashing of aluminum sandwich tram car 40
Figure 3.11 Total deformation due to tensile force at buffers 41
Figure 3.12 Directional deformation due to tensile force at buffers 42
Figure 3.13 Equivalent von-moises stress due to tensile force at buffers 42
Figure 3.14 Maximum principal stress due to tensile force at the buffer 43
Figure 3.15 Total deformation due to compression force at buffers 43
Figure 3.16 Directional deformation due to compression force at buffers 44
Figure 3.17 Equivalent (von-mises) stress due to compression force at buffers 44
Figure 3.18 Maximum principal stress due to compression force at buffers 45
Figure 3.19 Total deflections due to right turn 45
Figure 3.20 Directional deformations due to right turn 46
Figure 3.21 Equivalent von-moises stresses due to right turn 46
Figure 3.22 Maximum principal stresses due to right turn 47
Figure 3.23 Total deformation due to operating load 47
Figure 3.24 Directional deformation due to operating load 48
Figure 3.25 Equivalent (von-mises) stress due to operating load 48
Figure 3.26 Maximum principal stress due to operating load 49
Figure 3.27 Total deformation of aluminum honeycomb due to tensile load 49
Figure 3.28 Directional deformation of aluminum honeycomb due to tensile load 50
Figure 3.29 Equivalent stress of aluminum honeycomb due to tensile load 50
Figure 3.30 Maximum principal stress of aluminum honeycomb due to tensile load 51
Figure 3.31 Total deformation of aluminum honeycomb due to compression load 51

Figure 3.32 Directional deformation of aluminum honeycomb due to compression load 52
Figure 3.33 Equivalent (von-mises) stress of aluminum honeycomb due to compression Load 52
Figure 3.34 Maximum principal stress of aluminum honeycomb due to compression Load 53
Figure 3.35 Total deformations of aluminum honeycomb due to right turn 53
Figure 3.36 Directional deformations of aluminum honeycomb due to right turn 54
Figure 3.37 Equivalent (von-mises) stresses of aluminum honeycomb due to right turn 54
Figure 3.38 Maximum principal stresses due to right turn 55
Figure 3.39 Total deformation of aluminum honeycomb due to operating load 55
Figure 3.40 Directional deformation of aluminum honeycomb due to operating load 56
Figure 3.41 Maximum principal stress of aluminum honeycomb due to operating load 56
Figure 3.42 Equivalent (von-mises) stress of aluminum honeycomb due to operating Load 57

List of table

Table 2.1 Use of Sandwich Construction in Boeing Aircraft 15
Table 3.1 Material property of steel 33
Table 3.2 Material property of sheet metal 33
Table 3.3 Load condition stated under EN 12663 for P-V type locomotive 35
Table 3.4 Mechanical properties of aluminum honeycomb core material A3003-H19 39
Table 3.5 Face material of Aluminum alloy 39
Table 4.1 Maximum principal stress 58
Table 4.2 Total deformation value 58

NOTATIONS

F_x	Vehicle force in longitudinal direction
F_y	Vehicle force in lateral direction
F_z	Vehicle force in vertical direction
E	Modules of elasticity
ν	Poisons ratio
ρ	Density
S_1	Safety factor for yield and proof strength
R	Material yield (ReH) or 0. 2 % proof stress (N/mm^2)
S_2	Safety factor for ultimate failure
Rm	Material ultimate stress
σ_C	Calculated stress
ERC	Ethiopian Railways Corporation
AREMA	American Railway Engineering and Maintenance of Way Association
EN	European nation standard
FE	Finite Element
ACP	ANSYS composite Prep Post
ASTM	American Society for Testing and Materials

CHAPTER ONE

1. Introduction

1.1 Background

The most visible parts of a rail transit operating system are the track ways, rolling stock (rail vehicles) and stations. The rail vehicle consists of the main load carrying structure above all truck suspension units such as the running gears, Car body structure and equipment (like propulsion, interior, car body completion, etc.)[7].

The car body of rail vehicles refers to the load carrying structure, doors, windows, interior with seats etc., inner lining and so-called comfort systems for lighting, heat, ventilation and sanitation. The technical equipment for propulsion, braking etc. is not definition not include in the car body, even though this equipment usually is attached /hinged on car body. Sometimes the concept of car body is limited to only the load carrying structure of the vehicle [7].

Railway vehicle structures generally consist of shells, plates and beams and behavior of these members directly affect static structure behaviors of these vehicle. The structural design of railway vehicle bodies depends on the loads they are subject to and the characteristics of the materials the vehicle manufactured [5].Car bodies of modern rail vehicles are designed as lightweight structures with the aim to minimize mass and thus operational energy demand. The central structural design requirements are given by the main static loads.

Before putting a railway vehicle into service, it must be certified. Static tests are performed according to international standards during the certification procedures. Some standards, specifications and requirements for static stress tests, vibration and crashworthiness of rail vehicle structures can be found [1- 2]. Within the scope car body standard, it is intended to provide a uniform basis for structural design of the vehicle body. The loading requirement for the vehicle body structure design and testing are based on proven experience supported by the evaluation of experimental data and published information [1].

Numerical methods and experimental measurements are used to determine the static behavior of railway vehicles. Experimental measurements are very time consuming, expensive and they cannot be used at all stages of design. Hence, today numerical methods are important tools in static analyses of railway vehicles. Although numerical simulations do not have aforementioned disadvantages of experimental methods, they must be verified by experiments to obtain realistic results. FE method is a powerful numerical engineering analysis tool, and widely used in static stress analyses of railway vehicles.

Half-width/half-length and half-width/full-length modeling approaches are used to determine static structural, vibrational depending on the symmetry of vehicle. Nevertheless, half- width / full-length and modeling approaches can be used only for certain types of simple static structural loading such as static symmetrical compression and symmetrical tension loading conditions and cannot be validated for complex static structural loading conditions. Hence, full-length simulations are important for the validation of designs and to provide the greatest possible accuracy.

To obtain static structural behavior of the railway vehicles, i.e. stress and strain distribution, different static loading cases defined in [1, 2] Can be used in FE analyses and be validated against experimental measurement that are taken into account are EN15663 for static analysis [1]. Finite element (FE) method is used to assess the static structural behavior of railway vehicles. Full length detailed railway vehicle models are used in all FE analysis.

In this thesis considering the above mentioned issues, analyses of stress and deformation of railway passenger structures are completed. Full-length detailed and validated FE models are used to assess static structural behaviors of the railway vehicles. To obtain static structural behavior of the railway vehicles, different static loading cases defined in EN15663 standards are used.

Within the scope of this thesis structurally analyzed the tram vehicle body and find the maximum stress and the deflection of the body and also parameterized study was done by varying the material using the exact steel and aluminum honeycomb material.

1.2 Objective of the study

1.2.1General objective

The main objective is the structural analysis of Addis Ababa city light railway transit vehicle body using the exact steel materials and aluminum sandwich material.

1.2.2 Specific objective

- Modeling the vehicle structural and analyzed the structure using ANSYS on the exact steel material and aluminum honeycomb material
- To verify the strength of the structure when subjected to the maximum loads
- To verify that no significant permanent deformation is present after removal of the maximum loads
- Determine the maximum stress area on the vehicle body

1.3 Scope of the study

The scopes of the research is construction of 3D model of the tram car using Solidworks software and for aluminum honey comb material using solidworks plus ANSYS composite post process(ACP) .Finite element analysis using ANSYS14.5.

1.4 Methodology used

Literatures regarding tram car vehicles body and sandwich material are reviewed and also seen the advantage of reducing the vehicle body are studied and reviewed. Technical papers, manuals, journals and publications regarding the current trends of using aluminum honeycomb in the railway industry were reviewed. The data and data sources are from Ethiopian Railways Corporation (ERC), American Railway Engineering and Maintenance of Way Association (AREMA) manual and other acknowledged publications.

Then modeling of the vehicle body with steel and aluminum honeycomb material. There are two levels in the virtual prototype. First in the development of functional modules software for 3d modeling used SOLIDWORK 11 and Finite Element Analysis (FEA) using a software package called ANSYS 14.5 with a full package of ANSYS composite PrepPost (ACP).

1.5 Organization of the research

The research is organized in five parts.

Chapter 1 is the introductory as stated above which contains the general background, objectives of the research, scope of the study and methodology and structure of the thesis.

Chapter two, a review of literature relevant to this thesis work, which has been investigated by different researchers, is given. It also briefly describes the finite element formulation of the sandwich material and finally the raised topics are summarized.

Chapter three shows the simulation process that used finite element method (FEM) to analyze the tram car with steel and aluminum honeycomb material. The results of the finite element modeling of the tram vehicle under different load condition stated under EN 15227 and EN 12663 standards are presented in Chapter 4. It also contains a discussion of the results and presented the main results. Finally, in chapter 5 gives conclusion achieved from this thesis work and proposes future work in this field of study.

CHAPTER TWO

2. Literature review

2.1 Introduction

The vehicle body consists of the main load carrying structure above all truck suspension units. It includes all components that are connected to this structure and contribute directly to its strength, stiffness and stability [6].

A railway carriage can be divided into three main assemblies: the running gears, Car body structure and equipment (like propulsion, interior, car body completion, etc.)

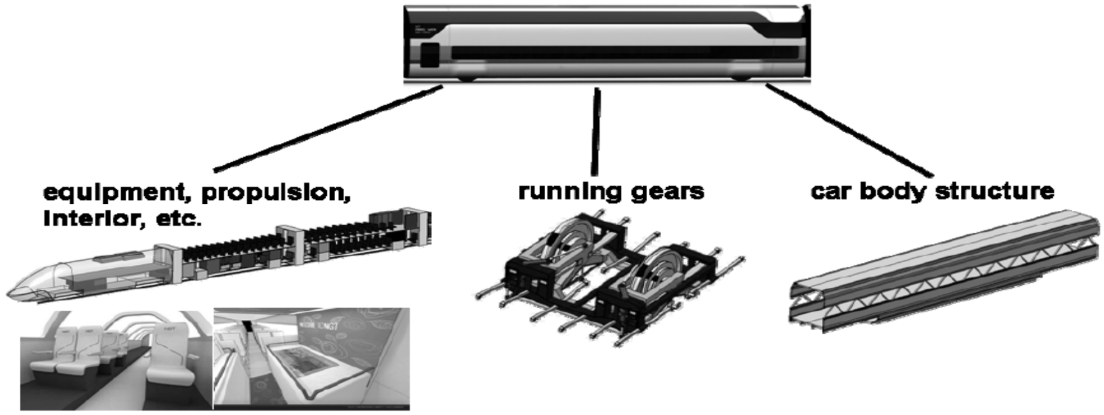

Figure 2.1 Vehicle body carriage subassemblies [3]

It is composed of a large number of diverse subassemblies. These subassemblies are predominantly independent from each other, so they have to be regarded separately [3].

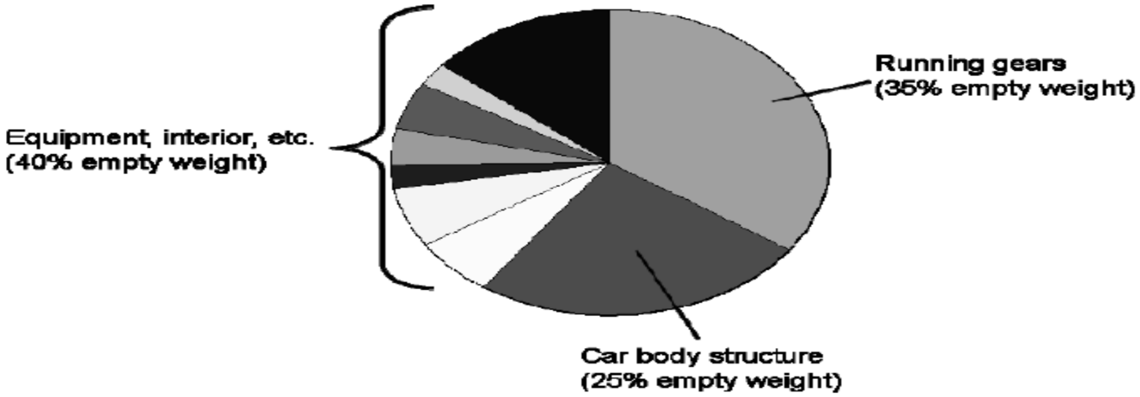

Figure 2.2 Exemplary percentage distributions of the main vehicle assemblies [3]

The car body of rail vehicles refers to the load carrying structure, doors, windows, interior with seats etc., inner lining and so-called comfort systems for lighting, heat, ventilation and sanitation. The technical equipment for propulsion, braking etc. is not definition not include in the car body, even though this equipment usually is attached /hinged on carbody. Sometimes the concept of car body is limited to only the load carrying structure of the vehicle [7]. The car body shall be structurally complete, including flooring if used as part of the primary car body structure, but shall exclude such items as exterior and interior trim, windows, doors, seats, lights, insulation, interior lining, or any other materials that will obscure any structural member of the car body from view. Under floor, roof and ceiling mounted apparatus shall be installed or equivalent weights distributed at their respective locations [6].

Car bodies of modern rail vehicles are designed as lightweight structures with the aim to minimize mass and thus operational energy demand. The central structural design requirements are given by the main static [8].

weight reduction of the vehicle body resulted higher transport capacities and/or enhanced passenger comfort whilst keeping a good energy balance - as well as in the field of urban and sub-urban rolling stock, where weight reduction results in enhanced acceleration and hence, in increased capacity in terms of passenger flow/hour. Lowering the car body weight also means a reduction of the stiffness of the structure, which results in lower natural frequencies [9].

The global weight saving potential resulting of the several rail vehicle equipment is limited. Analyses showed that the mass of the rough car body normally accounts for 15% to 30% of the vehicle's empty weight. Nonetheless the car body structure is in an interaction with Different parameters. This means the car body structure has a direct influence on the weight saving potential of these parameters. Development in the field of railways goes in particular through decreasing the weight of rolling stock vehicles car body structure [3].

To reduce the weight of a rail vehicle body using a global light weight principle, it’s indispensable. The light weight principles can be divided in:

- Material light weight construction,
- Function and system light weight construction
- Shape and form light weight constructions [3].

Rail cars are relatively heavy in comparison to other transportation modes. A comparison of road and rail vehicles reveals that rail vehicles must move more mass per passenger than road vehicles. Reasons for this include high requirements on static load [1] and a configuration of the vehicles for greater mileage.

Railway vehicle bodies shall withstand the maximum loads consistent with their operational requirements and achieve the required service life under normal operating conditions with an adequate probability of survival. The capability of the railway vehicle body to sustain required loads without permanent deformation and fracture [1]. The central structural design requirements are given by the main static loads.

Different research has been done on the materials used for the tram vehicles to get the materials advantage to minimized the stress, vibration, minimize the material deformation and other related to maximize the static nature of the tram car and also done to reduce the weight of the vehicle body. Fig 2.3 show the chronology development of rail vehicle body material from the begging of railcar up to recent history.

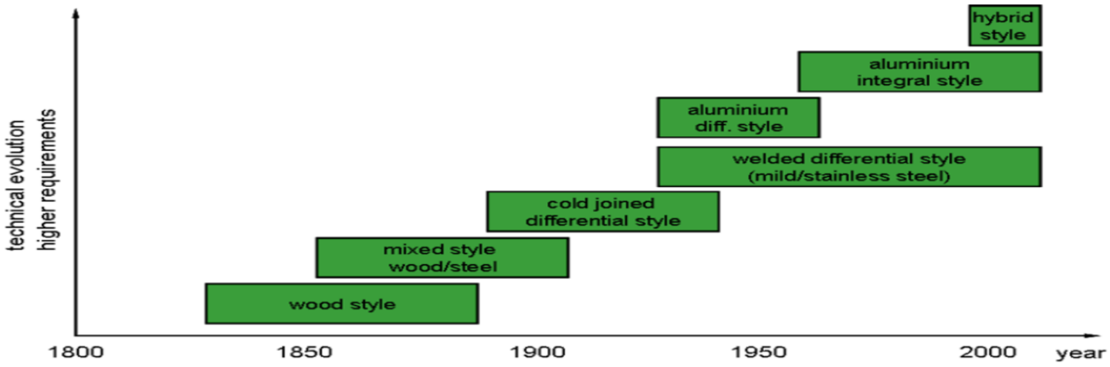

Figure 2.3 Chronology of the development of car bodies [3]

2.2 Composite materials

The word composite in the term composite material signifies that two or more materials are combined on a macroscopic scale to form a useful third material. The advantage of composite materials is that, if well designed, they usually exhibit the best qualities of their components or constituents and often some qualities that neither constituent possesses [10].

Currently, composite materials are rarely used for structural elements of rolling stock vehicles. Studies undertaken in the middle of the nineties have allowed the industry to acquire competence in the field of composite materials. The progress achieved with regard to such materials in addition to the "multi material" approach (composite materials, steel, aluminum) will allow the need for weight lightening to be satisfied at competitive costs [11].

The use of composite materials in vehicle structures could reduce the weight and thereby the fuel consumption of vehicles. As the road safety of the vehicles must be ensured, it is vital that the energy absorbing capability of the composite materials are similar to or better than the commonly used steel structures [12].Composite materials have proven properties in number of engineering fields such as aerospace, automotive and civil engineering. Reason for their getting more popular day-by-day is that they accommodate desirable properties like lightweight, high stiffness to weight and strength to weight characteristics and good corrosion resistance [13].

2.3 Sandwich material

Sandwich structured composites are a special class of composite materials which have become very popular due to high specific strength and bending stiffness. Low density of these materials makes them especially suitable for use in aeronautical, transport engineering, space and marine applications [10]. Sandwich structures are found to be most in case of high specific bending stiffness and strength [13].

The ASTM defines a sandwich structure as follows: A structural sandwich is a special form of a laminated composite comprising of a combination of different materials that are bonded to each other so as to utilize the properties of each separate component to the structural advantage of the whole assembly [14].

A sandwich structure consists of three main elements, two outer faces, or skins, and a center core as shown in Figure 2.4. The outer faces typically consist of a stiffer, higher density material in comparison to the inner core. Practically any structural material can be used for the faces depending on the purpose of the sandwich construction [15].

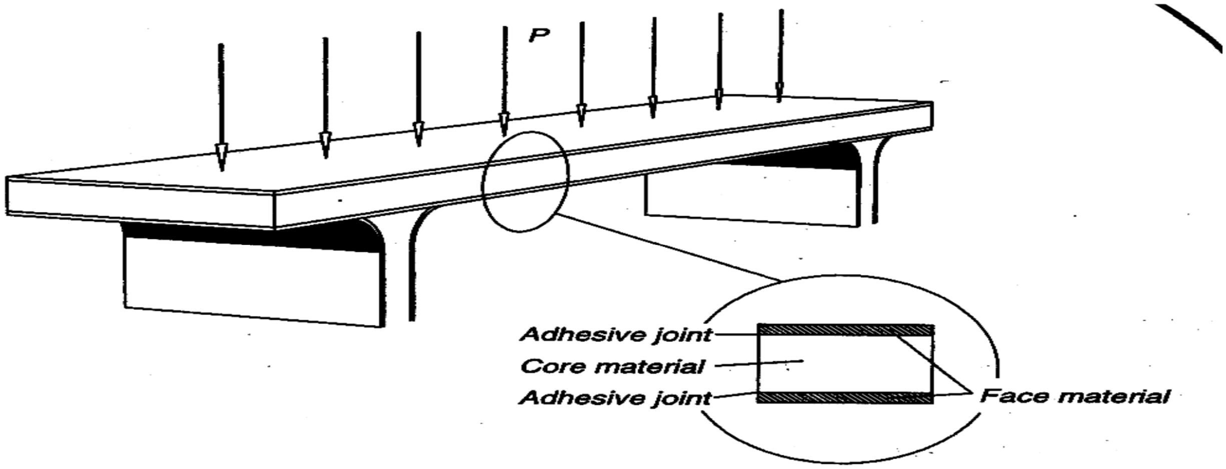

Figure 2.4 A sandwich structure [15]

A sandwich is three layer structure made up of an upper and lower face sheets (skins) and core in between them which are bonded together .The face sheet carries in plane loads, while the core maintains a distance between face sheets [13].If an adhesive is used to bind skins with the core, the adhesive layer can also be considered as an additional component in the structure. The thickness of the adhesive layer is generally neglected because it is much smaller than the thickness of skins or the core. The properties of sandwich composites depend upon properties of the core and skins, their relative thickness and the bonding characteristics between them [10].

Sandwich panels which have high bending stiffness and strength compared to their weight can be used with advantage in vehicle structures.

Thickness:	d	$2d$	$4d$
Weight:	1	~ 1	~ 1
Bending strength:	1	6	12
Flexural rigidity:	1	12	48

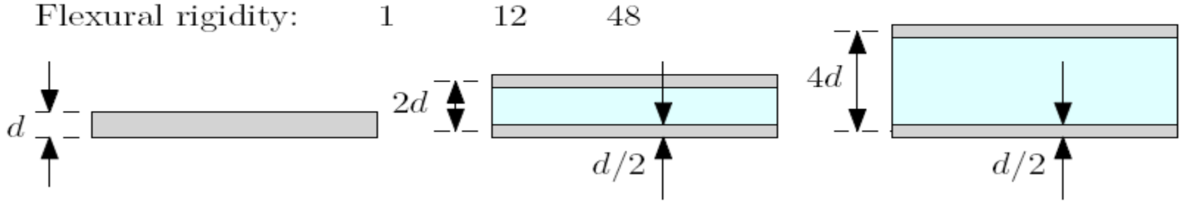

Figure 2.5 The Sandwich Effect because of the low density core, the weight difference between the structures [15]

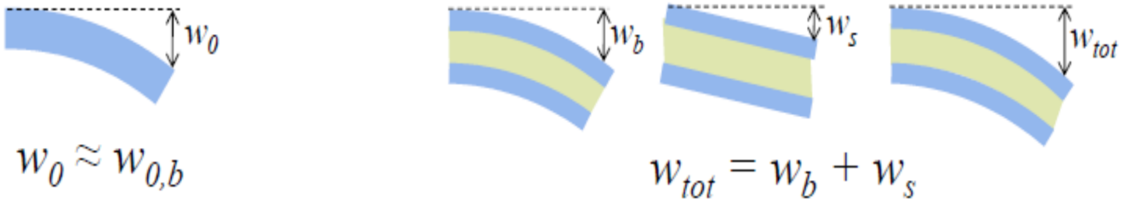

Fig 2.6 Shear deformation of sandwich material [15]

Sandwich structures mainly carry applied bending moments as tensile and compressive stresses in the two face-sheets, whereas applied transverse forces predominantly are carried by the core material as shear stresses [16]. By increasing the core thickness and thereby increasing the distance between the face-sheets the flexural rigidity of the structure is increased with low weight penalty, due to the low density of the core material [12].Sandwich composites have high strength to weight ratio (which results in increase of payload, provides greater range and/or reduced fuel consumption), extended operational life, lower maintenance cost (due to less corrosion), as well as a range of integrated functions, such as thermal and sound insulation, excellent signature properties, fire safety, good energy absorption, directional properties of the face sheets enabling optimized design and production of complex and smooth hydrodynamic surfaces [17].

The face materials are commonly sheet metals or fiber reinforced plastics, i.e. high performance materials, while the core materials are usually of lower density such as balsa wood, honeycomb structures or polymer foams. There are, however, an almost endless amount of combinations and materials that can be used in sandwich construction and each have their own specific benefits and weaknesses [18].

2.3.1 Face Materials

The face-sheets may consist of metal or composite material [12].The local flexural rigidity of each face is typically small and can be ignored. Materials such as steel, stainless steel, aluminum and fiber reinforced polymer materials are often used as materials for the face [14].Almost any structural material which is available in the form of thin sheet may be used to form the faces of a sandwich panel. Panels for high-efficiency aircraft structures utilize steel, aluminum or other metals, although reinforced plastics are sometimes adopted in special circumstances. In any efficient sandwich the faces act principally in direct tension and compression. It is therefore appropriate to determine the modulus of elasticity, ultimate strength and yield or proof stress of the face material in a simple tension test. When the material is thick and it is to be used with a weak core it may be desirable to determine its flexural rigidity [20].

Common sheet metals are, e.g. steel, aluminum and titanium. For composite faces one could consider carbon fiber-, glass fiber- or aramid-laminates. Some of the different characteristics of composite laminates compared to metal sheets Figure 5 gives a comparison of tensile strength and modulus for some epoxy laminates from Hexcel [21].

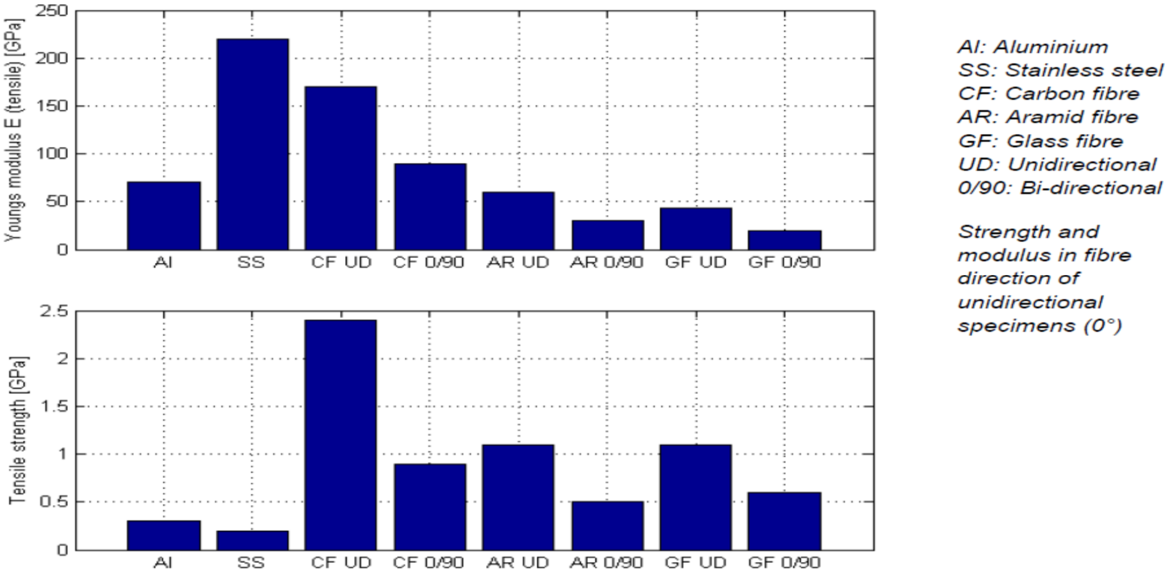

Figure 2.7 Tensile strength and elastic modules comparison of different face material [21]

Comparison of tensile strength and modulus of two metals and some epoxy laminates. Values vary significantly between different types of specific materials, values above are only examples. Fiber volume content of carbon ≈ 60%, Fiber volume content of glass/aramid ≈ 50%

2.3.2 Core Materials

The core has several important functions. It has to be stiff enough to maintain the distance between the two faces constant. It should be also rigid to resist the shear forces and to prevent sliding the faces relative to each other [19]. Most of the cores have densities in the range 120Kg/m^3 to 145Kg/m^3.

Balsa wood is one of the original core materials. It is usually used with the grain perpendicular to the faces of the sandwich. The density is rather variable but the transverse strength and stiffness are good and the shear stiffness moderate. [20]

There are several different material types to choose from when constructing a sandwich with a foam core, e.g. polyurethane foam (PUR), polystyrene foam (PS), polyvinyl chloride foam (PVC), polymethacrylimide foam (PMI), etc. Among these PUR and PS foams are most commonly found as insulation or other non-load bearing applications, whilst PVC and PMI foams offer a higher strength to density ratio and also honeycomb cores come in a variety of materials, e.g. aluminum, aramid, fiber-glass, etc. [20] .The most important characteristics of the core are: low weight, shear modulus, shear strength and stiffness perpendicular to the faces. Below a comparison of the structural properties for different core alternatives from different suppliers [21].

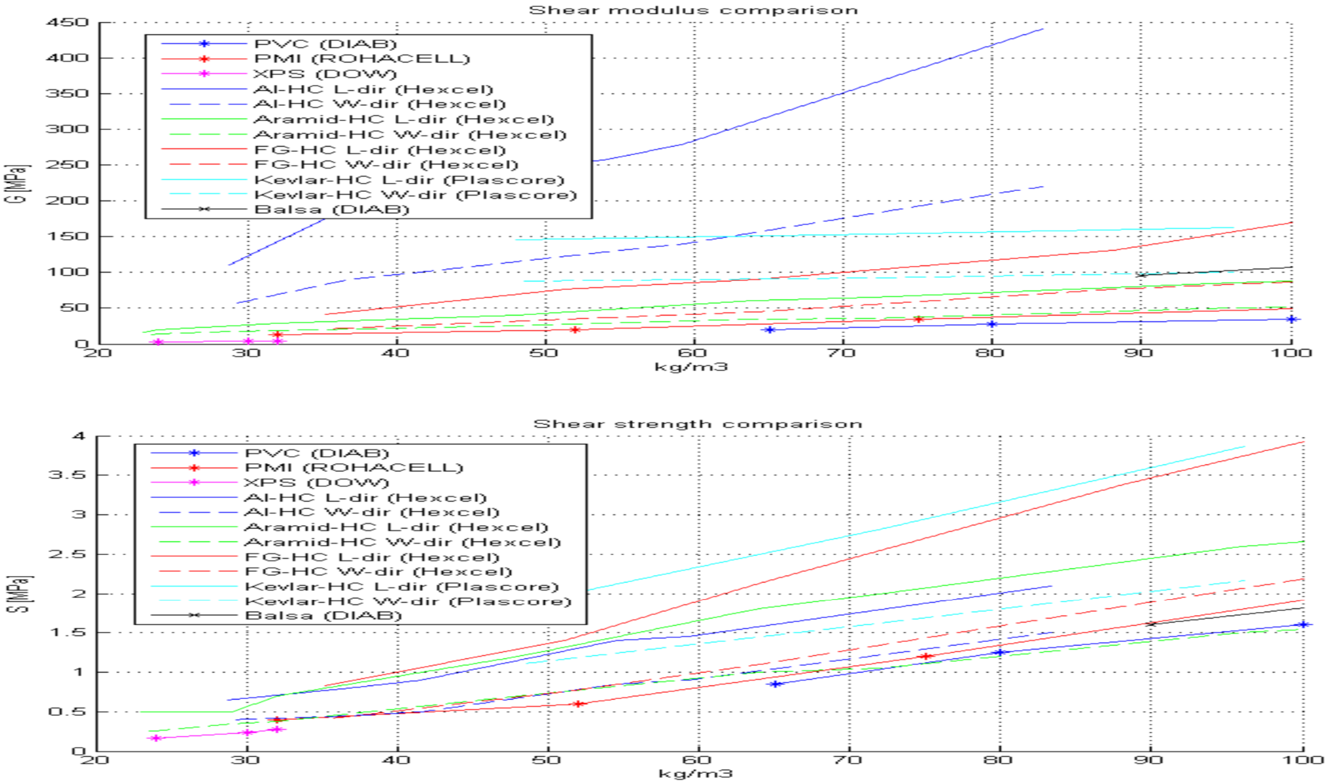

Figure 2.8, Comparison of shear properties, left: shear modulus, right: shear strength. HC = honeycomb, Al = aluminum, FG = fiberglass, XPS = extruded polystyrene Plascore's values from Higher Shear configuration honeycomb [21]

Honeycomb-cored sandwich panels have been used as strength members of satellites or aircraft, thus efficiently reducing their structural weight. In the railroad industry, passenger coaches of high-speed trains such as the TGV have been designed and fabricated using aluminum honeycomb sandwich panels. Recently, attempts to use aluminum sandwich panels as strength members of high-speed vehicle have also been made. [27]

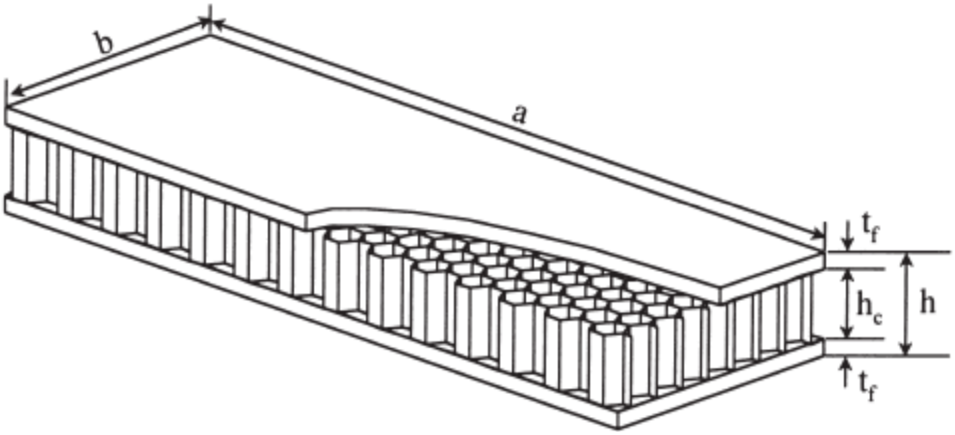

Figure 2.9 Nomenclature of aluminum honeycomb

Aluminum sandwich construction has been recognized as a promising concept for structural design of light weight systems such as wings of aircraft. A sandwich construction, which consists of two thin facing layers separated by a thick core, offers various advantages for design of weight critical structure. [27]

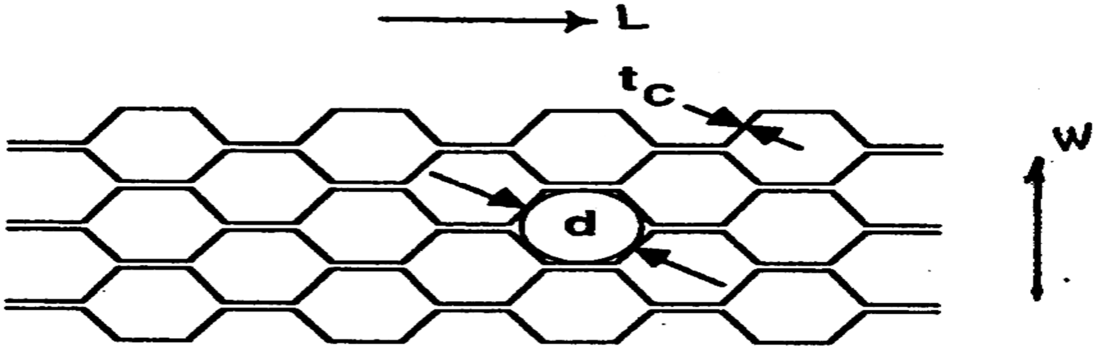

Figure 2.10 Honeycomb core in plan view [27]

The adhesive between the faces and the core must be able to transfer the shear forces between the face and the core. [19]

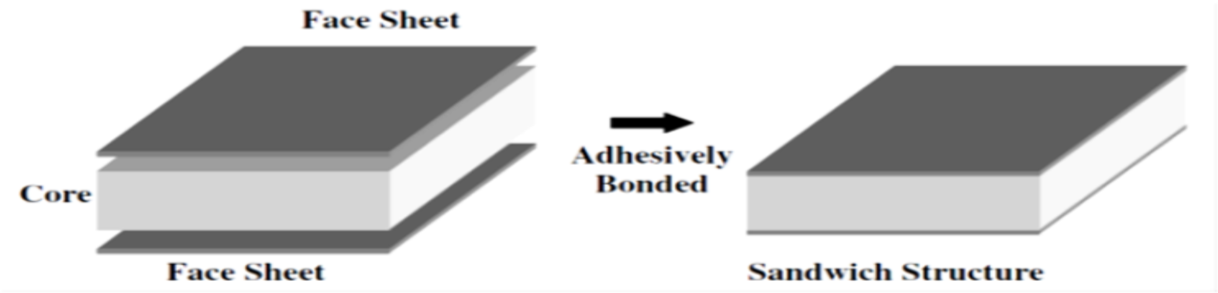

Figure 2.11.Schematic of sandwich construction [19]

2.4 Application of sandwich material

In the past decades various sandwich panels have been implemented in aerospace, marine, architectural and transportation industry. Light-weight, excellent corrosion characteristics and rapid installation capabilities created tremendous opportunities for these sandwich panels in industry.

Sandwich construction is one of the most functional forms of composite structures developed by the composite industry. It is widely employed in aircraft and space vehicles, ships, boats, cargo containers and residential construction [21].

In Aerospace industry various structural designs are accomplished to fulfill the required mission of the aircraft. Since a continually growing list of sandwich applications in aircraft/helicopter (example-Jaguar, Light Combat Aircraft, Advanced Light Helicopter) includes fuselages, wings, ailerons, floor panels and storage and pressure tanks [21].

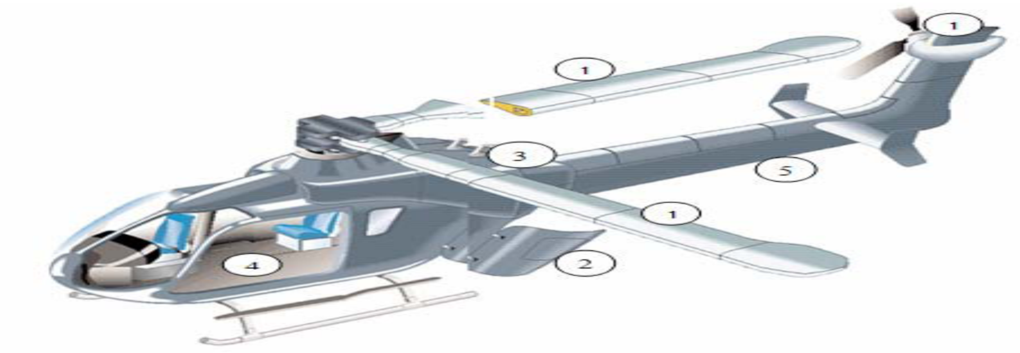

Figure 2.12 Application of sandwich structure in helicopter [21]

Where 1(Rotor Blades), 2(Main and Cargo Doors), 3(Fuselage Panels), 4(Fuselage) and 5(Boom and Tail section)

Table 2.1 Use of Sandwich Construction in Boeing Aircraft [23]

Boeing Aircraft	Percent of wetted surface
702	8
727	18
737	26
747	36
757-767	46
Dreamliner	Over 80%

In the Boeing 747, the fuselage shell, floors, side panels, overhead bins and ceiling are of sandwich construction .[23]Almost half of the wetted surface area of the Boeing 757/767 is honeycomb sandwich and the first non-government funded space ship had, among other things, wings constructed in sandwich with carbon fiber reinforced polymer epoxy skins and honeycomb core.

Architects use sandwich construction made of a variety of materials for walls, ceilings, floor panels, and roofing. Cores for building materials include urethane foam (slab or foam-in-place), polystyrene foam (board or mold), phenolic foam, phenolic-impregnated paper honeycomb, woven fabrics (glass, nylon, silk, metal, etc.), balsa wood, plywood, metal honeycomb, aluminum and ethylene copolymer foam. Facing sheets can be made from rigid vinyl sheeting (fiat or corrugated) ; glass-reinforced, acrylic-modified polyester; acrylic sheeting; plywood; hardwood; sheet metal (aluminum or steel); glass reinforced epoxy; decorative laminate; gypsum; asbestos; and poured concrete [20].

An increasing number of vibration problems must be controlled by damping resonant response. By using a symmetric sandwich panel with a viscoelastic core, various degrees of damping can be achieved, depending on the core material properties, core thickness, and wavelength of the vibration mode [21].

2.5 Sandwich structures in rail vehicles

In ground transportation sandwich structures can be found in cars, busses and trains. Since the 80s front cabs of locomotives have been built with sandwich technology because of its high strength and good impact and energy absorption properties. Some examples of this are the XPT locomotives in Australia, the ETR 500 locomotives in Italy, the French TGV and the Swiss locomotive 2000.

There are also some examples of sandwich paneled rail vehicles; e.g. Schindler's wagons Revvivo, Munico and Neitec, the Korean Tilting Train express [7] and Bombardier's C20 FICAS .The high specific bending stiffness of sandwich structures can with advantage is used in vehicles, provided that the structural behavior during a crash situation is well understood and possible to predict [12].

2.5.1 C20 FICAS

C20 FICAS is among the different sandwich panel rail vehicle. It has been in operation in the Stockholm metro system since July 16 2003. FICA is a Flat package concept, i.e. the car body is made up of several modules that are bolted together. Compared to the conventional C20 the FICA system has introduced large scale lightweight sandwich panels into the load carrying structure. This has increased the aisle space with 30% and reduced the tare weight per passenger by about 8%. The C20 FICA is a 3-car unit with a total length of 46.5 m and an operating speed of 80-90 km/h [7].

The C20 FICA body structure consists of sandwich panels in the sides, roof and floor. End beams where inserted into the sides as supports. The sandwich panels consist of stainless steel face sheets and a Polymethacrylimide foam core.

NO	Component	Material
1	core	PMI foam
2	Face sheets	Stainless steel
3	Inner frame	Stainless steel

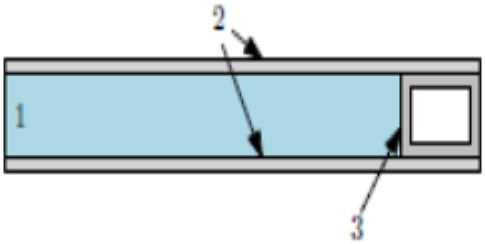

Figure 2.13.Cross –section view of typical sandwich section for the C20 FICAS [7]

2.5.2 Korean Tilting Train Express, TTX

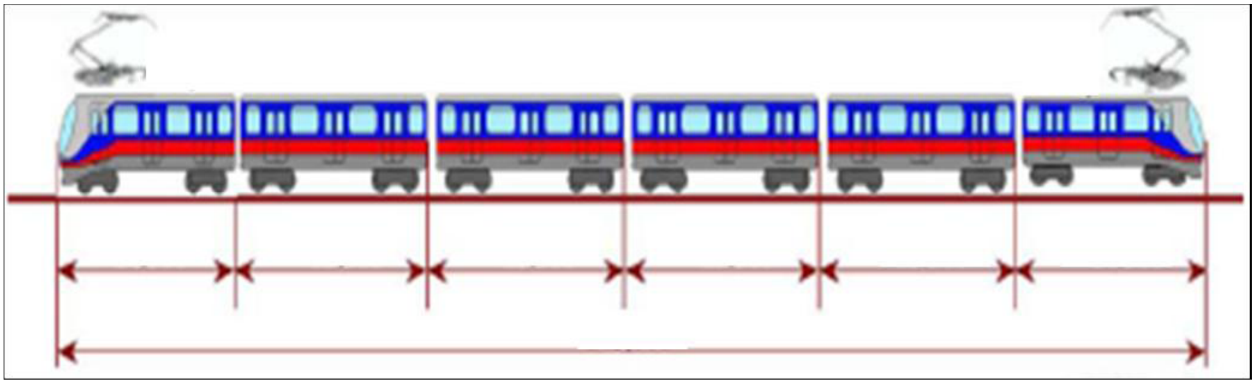

Figure 2.14 Vehicle configuration of TTX [7]

The sandwich structure elements consist of carbon fabric/epoxy prepregs for the faces and an aluminum honeycomb core. The entire car body is manufactured as one single structure. This was accomplished by means of large scale auto-clave. A large mold was built in which the outer face was firstly laid out. The outer face was than cured in the auto-clave. Secondly the inner frame and honeycomb core was placed on top of the outer skin. The core and skin was bonded by use of an adhesive film. After this step followed lay-up of the inner face. Lastly the entire structure was, after appropriate vacuum bagging, cured in the auto-clave. By constructing the entire car body as one structure weak links between panels is eliminated. The only remaining weak link is between the upper body and under frame [7].

The sandwich structure reduced the upper car body weight by 39% compared to a stainless steel car body. The total weight reduction, including under frame, was 28%

2.6 Past work

A number of researches were done on vehicle structural analysis and researches on sandwich materials strength test using simulation software and material labs .Some of the researches related to tram car and sandwich material are found below.

[17] Performed a multi-level approach on weight optimization for a “typical” rail vehicle body shell [7]. Initially the sandwich panel configuration was a 28mm thick polyurethane core with two 8mm thick face sheets of glass fibre reinforced epoxy composite plies giving a total of 16

plies and a lay-up of [0°/±45°/90°]S2. Each ply was 1mm thick. This gave a total panel thickness of 44mm. The panels where supported by a frame of steel stiffeners. The car body was furthermore subjected to a longitudinal compressive force of 1500kN during the optimization.

[18] Investigates how various requirements, such as stiffness, strength, buckling, thickness and area density, influence the choice of load carrying sandwich panels for high-speed rail vehicles. Requirements on the load carrying structure are defined where after various sandwich alternatives are studied to match these requirements. Panels that first pass a general requirement evaluation are further studied by Finite Element Analysis (FEA).

[28] Performed Design and Testing of Sandwich Structures with Different Core Materials the purpose of the study was to design a light-weight sandwich panel for trailers. Strength calculations and selection of different materials were carried out in order to find a new solution for this specific application. 3D FEA was applied to virtually test the selected sandwich structure in real working conditions. Based on FEA results the Pareto optimality concept has been applied and optimal solutions determined.

[25] Studied how environmental ageing affects the structural integrity of the TTX car body [21], mainly by looking at how ageing effects influence the integrity of the composite skins. Tests showed severe decrease in stiffness and strength for the graphite/epoxy specimens except for the transverse tensile stiffness which showed an 8% increase over time due to post-curing effects. The transverse compressive stiffness and transverse tensile strength showed the largest decay over time, -17.5% and -27.74% respectively. The shear strength on the other hand remained relatively constant. By using an electron microscope the authors showed that the decay in strength and stiffness was most likely due to loss of matrix material from the surface of the composite specimens. FE analysis was performed on the car body, with both non-degraded and degraded mechanical properties. Interestingly the maximum stress levels in the composite structure with degraded properties were lower than in the case of non-degraded. The stress levels in the under frame slightly increased but were well within safety values. However, after degradation the car body's maximum deflection under vertical load had increased by about 8%, exceeding the prescribed limit.

[26] Performed an optimization investigation on a rail vehicle with acoustic and mechanical constraints. The lowest natural frequency constraint was set to 9.5Hz and the car body was subjected to a compressive coupler load of 2000kN. Buckling of the floor was designated the most critical failure mode, why local and global buckling stresses of the floor sandwich panels where used as constraints during calculations. The sandwich panels where constructed of quasi-isotropic carbon fiber reinforced polymer laminates with a foam core. Face and core thickness as well as core density was used as design variables in the floor and mechanical properties of the core. For the roof and side walls the core thickness and density was kept constant while the face thickness was the only design variable. An additional acoustic constraint on the sound reduction index was used on the floor.

[23] Developed an expert system to calculate the optimum stiffness design of composite laminates for a train car body by varying the stacking sequence. Optimal stiffness was achieved by quasi-isotropic stacking with design rules such as: avoid grouping of 90° plies, shield primary load carrying plies and do not differ ply angles between adjacent plies more than 45°. These design rules minimized the objective function for most loading situations, however, several other combinations showed good results with a lower number of plies compared to the quasi-isotropic stacking. During uniaxial loading cross-ply stacking was the stacking sequence that, not surprisingly, minimized the objective function.

[10] Performed experimental Test on Sandwich Panel Composite Material. Bending test, tensile test is performed on sandwich panel composite material. Two type of inner core structure is considered for sandwich panel composite material, without hexagonal composite material, and with hexagonal composite material. And it is observed that with hexagonal composite material weight saving is 39% compared with without hexagonal composite material. From tensile test and bending test of composite material, tensile strength and bending strength capacity of with hexagonal composite material is less compare to without hexagonal composite material, but it can be negligible. Hence sandwich panel composite material (with hexagonal structure) is acceptable in Automobile, Aerospace, and Marine engineering.

[28]This paper presents a combined Finite element modeling and experimental analysis of Carbon fiber composite sandwich panel. The core consists of Nomax honey comb structure

presented in between top and bottom face laminate. The emphasis of this study is on evaluation of deflection, bending stress and shear stress response under static four point bending condition. The 2D and 3D FE model predictions correlate with experimental results of Sandwich specimen. Predicted deflection in this study is success fully matching the response of CFC sandwich panels. The 3D FE model under static loading condition is closely matching with experimental deflection. It is found that the maximum percentage error is only 11.27%. Thus, in this study can be used with confidence in design analysis of the CFC sandwich panels.

[19] Performed Finite Element Analysis of Loading Area Effect on Sandwich Panel behaviors beyond the Yield Limit. The investigation is accomplished in sight of the core material nonlinearity and the geometric nonlinearity of the whole panel. High tech software ‘I-DEAS’ (Integrated Design Engineer Analysis software) is utilized to carry out the investigation. It is proved that the load carrying capacity of sandwich panel can be improved by loading the panel beyond the core yield limit. This load is going to be transmitted to the face sheet. Increasing the stiffness of the core material to a certain extent leads to face sheet yielding before the core material. It is proved that increasing core stiffness increases the load carrying capacity of the sandwich panel. Loading area plays good roll in the load carrying capacity of sandwich panel. Distributing loads over large area of panel surface leads to higher load carrying capacity.

[27]The three point bending test is conducted theoretically on aluminum, titanium and high tensile steel honeycomb sandwich panels and it is observed that titanium alloy has more strength to weight ratio. From the crushing tests on the aluminum honeycomb sandwich panel specimens under lateral crushing loads varying the cell thickness and height of the honeycomb core, it is seen that the core height is not an influential parameter on the crushing behavior of the honeycomb core. However the wall thickness of a honeycomb core cell is a critical variable affecting the crushing strength of the sandwich panels subject to lateral pressure loads.

2.7 Finite element formulation of sandwich panel

2.7.1 Problem Formulation

With The analytical development of a sandwich composite with constant depth starts the general depiction of a sandwich beam as shown in Figure 3.1

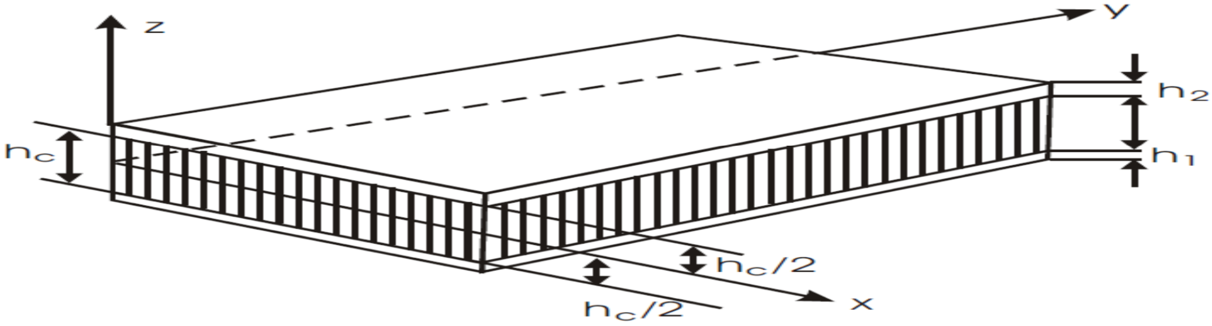

Figure 2.15 The nomenclature of sandwich material [19]

Assumptions

- The core carries the entire shear load in sandwich beams and plates.
- The face sheets carry the entire bending load.
- Core compression is negligible.[19]

The above–mentioned assumptions are true if:

1. The core and face sheets are elastic.
2. The overall length to thickness ratio is high.
3. The face sheet thickness is small compared to the overall thickness.
4. The ratio of mechanical properties between the face sheet and the core is high. [21]

The analysis is based on the above assumptions:

1. The face sheets are thin compared to the core, i.e., h_1, $h_2 << h_c$ and in a state of plane stress ($\boldsymbol{\sigma_z = \tau_{xz} = \tau_{yz} = 0}$).
2. The in-plane stresses, $\boldsymbol{\sigma_x}$, $\boldsymbol{\sigma_y}$, and $\boldsymbol{\tau_{xy}}$, in the core and negligible.
3. In-plane displacements, u and v, are uniform through the thickness of the face sheets, and assume their mid-plane (centroid for the corresponding facing) values.
4. The out-of-plane displacement, w, is independent of the z-coordinate, i.e., the thickness strain, $\varepsilon_z = \partial w/\partial z = 0$.
5. The in-plane displacements in the core, u and v, are linear in the thickness coordinate, z. [21]

The displacements of the core are,

$$u = u_o(x, y) + z\theta_x(x, y)$$

$$v = v_o(x, y) + z\theta_y(x, y)$$

$$w = w_o(x, y)$$

Where u_o, v_o and w_o are the displacements at the core mid-plane,

θx and θy are the rotations of cross sections originally perpendicular to the x and y axes, respectively. From continuity of displacements at the face/core interfaces ($z = \pm\ h_c/2$)

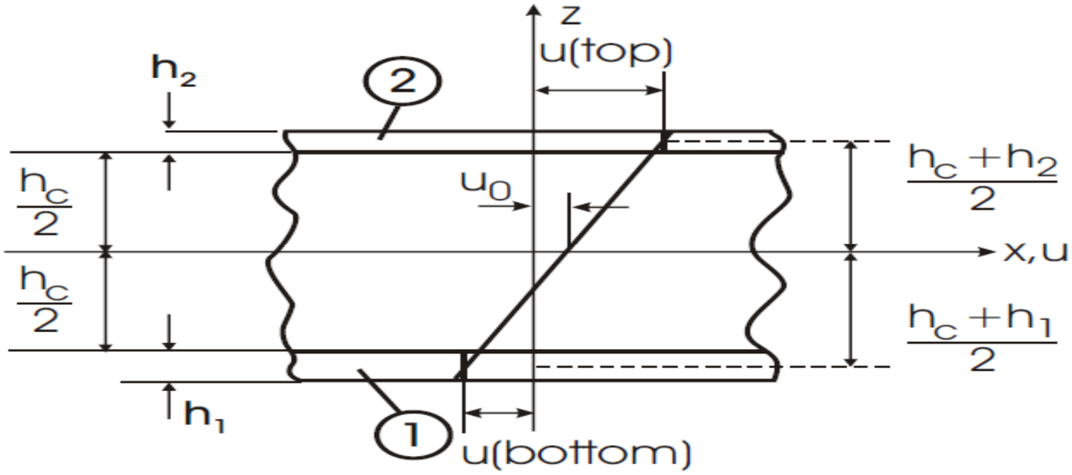

Figure 2.16 Displacement u for sandwich element oriented along the x-axis [21]

So that for top face (2) the u and v displacement component

$$U\ (top) = u_o + \left(\frac{hc+h2}{2}\right)\theta_x$$

$$V\ (top) = v_0 + \left(\frac{hc+h2}{2}\right)\theta_y$$

For bottom face

$$U\ (bottom) = u_o + \left(\frac{hc-h1}{2}\right)\theta_x$$

$$V\ (bottom) = v_0 + \left(\frac{hc-h2}{2}\right)\theta_y$$

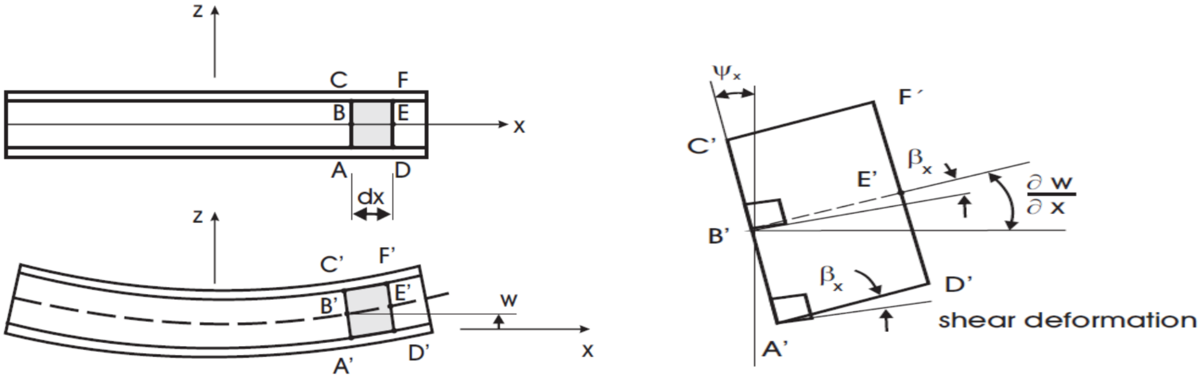

Figure 2.17 Deformation of core element in the xz plane[21]

The core element ACFD represents a section of the core with the surfaces AC and DF perpendicular to the x-axis before deformation. After deformation, point B displaces to assume a position at B′, and the vertical upwards displacement of point B (originally at $z = 0$) is w and that of the adjacent point E assuming the new position E' is: $w + (\partial w/\partial w)\, dx$, where $\partial w/\partial x$ is the slope of the panel along the x-axis.

It is assumed sandwich structures that the facings do not carry transverse shear or transverse normal stresses. The core usually works in transverse shear only. In addition, the core "holds" the structure together and supports thin and flexible facings against local deformations.

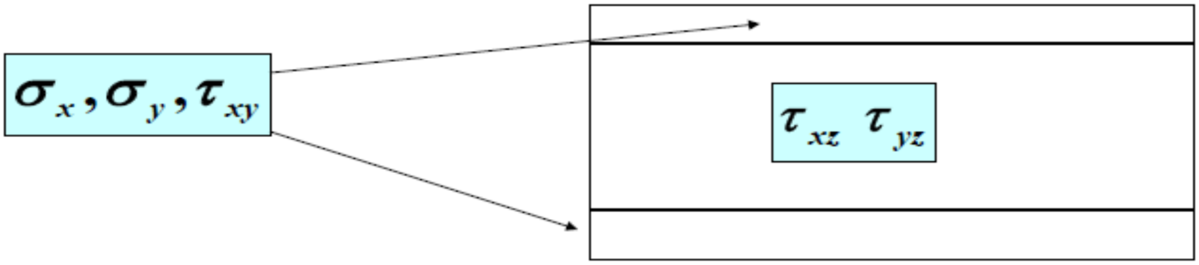

Figure 2.18 The face and the core stress [19]

2.7.2 Stress strain relation in sandwich panel

The stress resultants and stress couples for a sandwich element, Figure 2.19, are obtained by integrating the stresses over the element thickness.

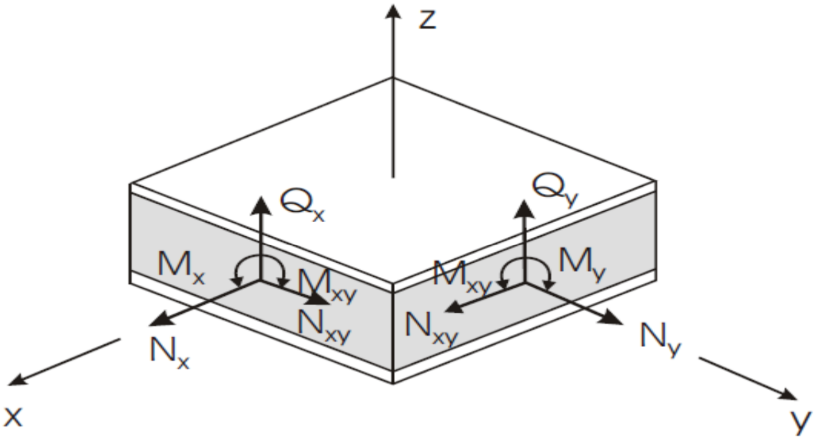

Figure.2.19 Stress resultants and stress couples for a sandwich element [21]

The linear plain strains at a distance z from the mid surfaces are given as follows

$\varepsilon_{xx}=u_{,x}=\varepsilon_{xx}^{0}+zk_{xx}$

$\varepsilon_{yy}=v_{,y}=\varepsilon_{yy}^{0}+zk_{yy}$

$\gamma xy=u_{,x}+v_{,y}=\gamma_{xy}^{0}+zk_{xy}$

Where ε_{xx}^{0}, ε_{yy}^{0}, γ_{xy}^{0} are the mid plane strains.

$$\varepsilon_{xx}^{0}=u_{,x}^{0}$$

$$\varepsilon_{yy}^{0}=v_{,y}^{0}$$

$$\gamma_{xy}^{0}=u_{,x}^{0}+v_{,y}^{0}$$

$u_{,x}^{0}$, $v_{,y}^{0}$ are the mid plane deformation along x and y direction

Notice that the in-plane normal and in plane shear stresses in the core are neglected. Neglecting the normal stresses perpendicular to the plane of the lamina, the stress-strain relations in the principal material.

The mid plane stress-strain relation

$$\begin{bmatrix}\sigma_x(1)\\ \sigma_y(1)\\ \tau_{xy}(1)\end{bmatrix}_k=\begin{bmatrix}Q11 & Q12 & Q13\\ Q12 & Q22 & Q26\\ Q16 & Q26 & Q66\end{bmatrix}_k\begin{Bmatrix}\varepsilon_{xx}\\ \varepsilon_{yy}\\ \gamma_{xy}\end{Bmatrix}_k$$

Where k is the ply index and i = 1 for the lower face, and i = 2 for the upper face.

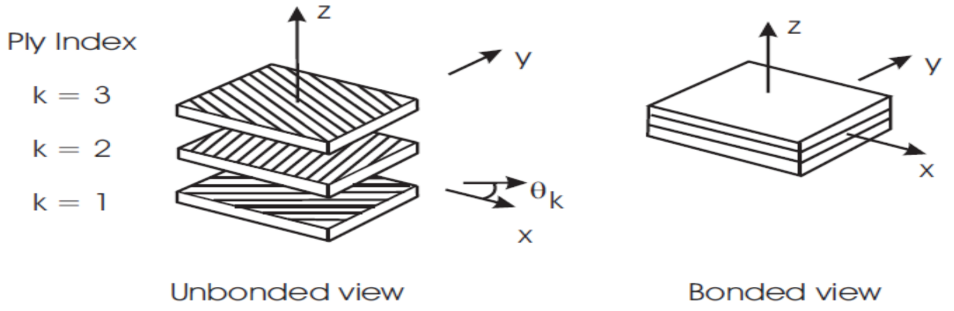

Figure 2.20 Ply notation [19]

Where $Q11=\frac{E_{11}}{(1-\upsilon_{12}V_{21})}$

$$Q12=\frac{\upsilon_{12}E_{22}}{(1-\upsilon_{12}V_{21})}$$

$$Q22 = \frac{E_{22}}{(1-\upsilon_{12}V_{21})}$$

The stress-strain relations of the lamina with respect to the x, y and z axes are as follows:-

$$\begin{bmatrix} \sigma_x \\ \sigma_y \\ \tau_{xy} \end{bmatrix}_k = \begin{bmatrix} \overline{Q11} & \overline{Q12} & \overline{Q13} \\ \overline{Q12} & \overline{Q22} & \overline{Q26} \\ \overline{Q16} & \overline{Q26} & \overline{Q66} \end{bmatrix}_k \begin{Bmatrix} \varepsilon_{xx} \\ \varepsilon_{yy} \\ \gamma_{xy} \end{Bmatrix}_k$$

$$\begin{Bmatrix} \overline{Q11} \\ \overline{Q22} \\ \overline{Q12} \\ \overline{Q66} \\ \overline{Q16} \\ \overline{Q26} \end{Bmatrix} = \begin{bmatrix} m^4 & n^4 & 2m^2n^2 & 4m^2n^2 & -4m^3n & -4m^3n \\ n^4 & m^4 & 2m^2n^2 & 4m^2n^2 & 4mn^3 & 4mn^3 \\ m^2n^2 & m^2n^2 & m^4+n^4 & -4m^2n^2 & 2(m^3n-mn^3) & 2(n^3m-nm^3) \\ m^2n^2 & m^2n^2 & -2m^2n^2 & (m^2-n^2)^2 & 2(m^3n-mn^3) & 2(n^3m-nm^3) \\ m^3n & -mn^3 & n^3m-nm^3 & 2(n^3m-nm^3) & m^4-3m^2n^2 & 3m^2n^2-n^4 \\ mn^3 & -m^3n & m^3n-mn^3 & 2(m^3n-mn^3) & 3m^2n^2-n^4 & m^4-3m^2n^2 \end{bmatrix} \begin{Bmatrix} Q11 \\ Q22 \\ Q12 \\ Q66 \\ Q16 \\ Q26 \end{Bmatrix}$$

Where m= cos θ

n =sin θ

Transverse shear stress resultants due to transverse shear stresses in the core .Thus we obtain [19]

$$\begin{bmatrix} Qy \\ Qx \end{bmatrix} = \mathrm{Cs} \begin{bmatrix} A44 & A45 \\ A45 & A55 \end{bmatrix} \begin{bmatrix} \varepsilon_{yz} \\ \varepsilon_{xz} \end{bmatrix}$$

Where A44= G_{yz}^{c} h_c

A55=G_{xz}^{c} hc

A45 =$\int Q45$ dz

Q45 = (Q55 –Q44) sin θcos θ typically A45 =0

CS =shear correction factor.

The distance other than mid plane the stress –strain relation

$$\begin{bmatrix} \sigma_x \\ \sigma_y \\ \tau_{xy} \end{bmatrix} = \begin{bmatrix} \overline{Q11} & \overline{Q12} & \overline{Q13} \\ \overline{Q12} & \overline{Q22} & \overline{Q26} \\ \overline{Q16} & \overline{Q26} & \overline{Q66} \end{bmatrix} \begin{Bmatrix} \varepsilon_{xx} \\ \varepsilon_{yy} \\ \gamma_{xy} \end{Bmatrix} = \begin{bmatrix} \varepsilon_{xx}^{o} \\ \varepsilon_{yy}^{o} \\ \gamma_{xy}^{o} \end{bmatrix} + z \begin{Bmatrix} k_{xx} \\ k_{yy} \\ k_{xy} \end{Bmatrix}$$

The in-plane displacements in the core, u and v, are linear in the thickness coordinate.The transversal shear deformation along z is assumed constant. So the

$\tau_{xz}=\Phi_x$

$\tau_{yz}=\Phi_y$

$$\begin{bmatrix}\tau_{xz}\\ \tau_{yz}\end{bmatrix}= Cs\begin{bmatrix}\overline{Q44} & \overline{Q45}\\ \overline{Q45} & \overline{Q55}\end{bmatrix}\begin{bmatrix}\Phi_x\\ \Phi_y\end{bmatrix}$$

The internal force and moment resultants of the laminate are obtained by integrating elemental forces and moments over the thickness of the laminate [19].

Due to the facing contribute

$$(Nx, Ny, Nxy) =\int_{-(\frac{hc}{2}+h1)}^{-hc/2}(\sigma x(1), \sigma y(1), \tau_{xy}(1)\ dz +\int_{hc/2}^{\frac{hc}{2}+h1}(\sigma x(1), \sigma y(1), \tau_{xy}(1))dz$$

$$(Mx, My, Mxy) =\int_{-(\frac{hc}{2}+h1)}^{-hc/2}(\sigma x(1), \sigma y(1), \tau_{xy}(1))\ zdz +\int_{hc/2}^{\frac{hc}{2}+h1}(\sigma x(1), \sigma y(1), \tau_{xy}(1))zdz$$

Due to the core contribute

$$(Qx, Qy)= \int_{-hc/2}^{\frac{hc}{2}}(\tau_{xz}, \tau_{yz})\ dz$$

In matrix other form

$$\{N_x \quad N_y \quad N_{xy}\}^T =\int_{-h/_2}^{h/_2}\{\sigma_x \quad \sigma_y \quad \tau_{xy}\}^T\ dz$$

$$\{M_x \quad M_y \quad M_{xy}\}^T =\int_{-h/_2}^{h/_2}\{\sigma_x \quad \sigma_y \quad \tau_{xy}\}^T\ dz$$

$$\{Q_X \quad Q_y\}^T =\int_{-h/_2}^{h/_2}\{\tau_{xz} \quad \tau_{yz}\}^T$$

From this three equations

$$\{P\} = \{D\}\{\varepsilon\}$$

P is the internal force and moment resultant of the lamination

ε is the resultant strains

D is deformation

$$\begin{Bmatrix}N_x\\ N_y\\ N_{xy}\\ M_x\\ M_y\\ M_{xy}\\ Q_X\\ Q_y\end{Bmatrix}=\begin{bmatrix}A11 & A12 & A16 & B11 & B12 & B16 & 0 & 0\\ A12 & A22 & A26 & B12 & B22 & B26 & 0 & 0\\ A16 & A26 & A66 & B16 & B26 & B66 & 0 & 0\\ B12 & B12 & B16 & D11 & D12 & D16 & 0 & 0\\ B13 & B22 & B26 & D12 & D22 & D26 & 0 & 0\\ B16 & B26 & B66 & D16 & D66 & D66 & 0 & 0\\ 0 & 0 & 0 & 0 & 0 & 0 & A44 & 0\\ 0 & 0 & 0 & 0 & 0 & 0 & 0 & A55\end{bmatrix}\begin{Bmatrix}\varepsilon_{xx}\\ \varepsilon_{yy}\\ \gamma_{xy}\\ k_{xx}\\ k_{yy}\\ k_{xy}\\ \Phi_x\\ \Phi_y\end{Bmatrix}$$

Where A are the mid plane deflection

$A_{ij} = A_{ij}(1) + A_{ij}(2)$ (i.e 1 and 2 is the deflection at bottom and the top surface respectively)

B and D is the deflection other than middle plane

$$B_{ij} = \left(\frac{hc+h2}{2}\right)A_{ij}(2) - \left(\frac{hc+h1}{2}\right)A_{ij}(1)$$

Evaluation of stiffness terms for a sandwich panel with N layers in two facings (h_k and h_{k-1} are coordinates of the interfaces of the k-th layer):

$$A_{ij}=\sum_{k=1}^{n}\int_{z_{k-1}}^{z_k}\left[\overline{Q_{ij}}\right]_k dz$$

$$B_{ij}=\sum_{k=1}^{n}\int_{z_{k-1}}^{z_k}\left[\overline{Q_{ij}}\right]_k z\,dz$$

$$D_{ij}=\sum_{k=1}^{n}\int_{z_{k-1}}^{z_k}\left[\overline{Q_{ij}}\right]_k z^2\,dz$$

$i,j = 1,2,6$

2.7.3 Finite element shape function

In the simpler classical theory, the neglect of transverse shear deformation effects means that ε_{xz}, ε_{yz} .From the above description five independent displacements such as, u_o, v_o, w_o, θx and θy.

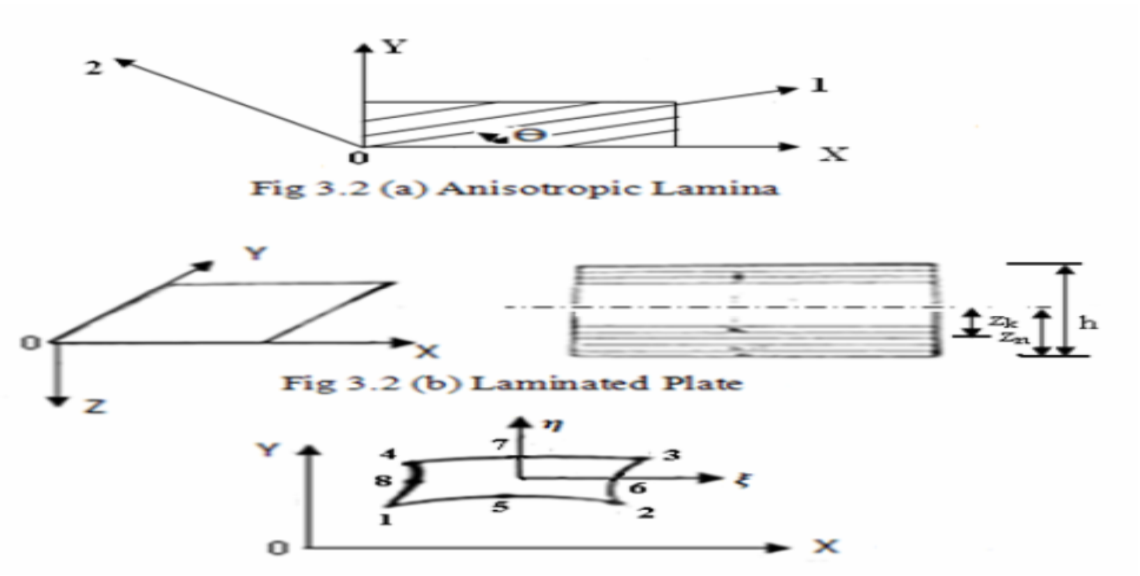

Figure 2.21 Eight nodded isoperimetric shell element [21]

Geometry of the element

$x=\sum_{i=0}^{8} N_i x_i$

$y=\sum_{i=0}^{8} N_i y_i$

Variation of displacement

$$u_0 = \sum_{i=0}^{8} N_i u_i$$

$$v_0 = \sum_{i=0}^{8} N_i v_i$$

$$w_0 = \sum_{i=0}^{8} N_i w_i$$

$$\theta\text{x} = \sum_{i=0}^{8} N_i \theta_{xi}$$

$$\theta\text{y} = \sum_{i=0}^{8} N_i \theta_{yi}$$

Where u_o, v_o and w_o are the displacements at the core mid-plane,

θx and θy are the rotations of cross sections originally perpendicular to the x and y axes, respectively. N_i are the shape functions

From the above diagram the shape function for eight nodded parametric shell element

$N_1 = \frac{1}{4}(1-\xi)(1-\eta)(-\xi-\eta-1)$

$N_2 = \frac{1}{4}(1+\xi)(1-\eta)(\xi-\eta-1)$

$N_3 = \frac{1}{4}(1+\xi)(1+\eta)(\xi-\eta-1)$

$N_4 = \frac{1}{4}(1-\xi)(1+\eta)(-\xi-\eta-1)$

$N_5 = \frac{1}{2}(1+\xi)(1-\xi)(1-\eta)$

$N_6 = \frac{1}{2}(1+\xi)(1+\eta)(1-\eta)$

$N_7 = \frac{1}{2}(1+\xi)(1+\eta)(1-\xi)$

$N_8 = \frac{1}{2}(1-\xi)(1+\eta)(1-\eta)$

2.7.4 The static analysis of sandwich panel

The strain element (ε) defined interms of displacement (u)

$\{\varepsilon\} = [\Delta]\{u\}$

Where u is the displacement and it define as

$\{u\} = [\text{N}]\{D_e\}$

$[B] = [\Delta][N]$

So that combines the above strain-displacement relation

$\{\varepsilon\} = [\Delta][N]\{D_e\}$

Stress – strain relation

$\{\sigma\} = [E]\{\varepsilon\}$

$=[E][\Delta][N]\{D_e\} \quad =[E][B]\{D_e\}$

Where E= Elastic stiffness

Δ=differential operation

N= Shape function

D_e= elemental nodal displacement

The total potential of the element is given by Rayleigh-Ritz variation approach

$$\pi_e = \frac{1}{2}\int\{\sigma\}^T\{\varepsilon\}dv - \int\{u\}^T\{q\}ds$$

$$\pi_e = \frac{1}{2}\int\{[E][B]\{d_e\}\}^T dv - \int[\mathrm{N}]\{d_e\}^{\,T}\{q\}ds$$

$$\pi_e = \frac{1}{2}\int\{d_e\}^T[B]^T[E][B]\{d_e\}dv - \int\{d_e\}^{\,T}[\mathrm{N}]^T\{q\}ds$$

From the minimum potential yield

$$[K_e]\{d_e\} = \{P_e\}$$

$$[K_e] = \frac{1}{2}\int[B]^T[E][B]dv$$

$$\{P_e\} = \int[\mathrm{N}]^T\{q\}ds$$

From the global coordinate system

$$[K]\{d\} = \{P\}$$

According to galerkin weight residual equation

$$\int[B]^T[E][B]\{d_e\}dv - \int[\mathrm{N}]^T\{q_i\}ds = 0$$

Boundary conditions

Force in the x-direction $\Longrightarrow \dfrac{\partial N_x}{\partial x}+\dfrac{\partial N_{xy}}{\partial y}=0$

Force in the y-direction $\Longrightarrow \dfrac{\partial N_{xy}}{\partial x}+\dfrac{\partial N_y}{\partial y}=0$

Moment about the x-axis $\Longrightarrow \dfrac{\partial M_x}{\partial x}+\dfrac{\partial M_{xy}}{\partial y}-Q_x=0$

Moment about the x-axis $\Longrightarrow \dfrac{\partial M_{xy}}{\partial x}+\dfrac{\partial M_y}{\partial y}-Q_y=0$

Force in the z-direction $\Longrightarrow \dfrac{\partial Q_x}{\partial x}+\dfrac{\partial Q_y}{\partial y}+N_x\dfrac{\partial^2 w}{\partial x^2}+2N_{xy}\dfrac{\partial^2 w}{\partial x\partial y}+N_y\dfrac{\partial^2 w}{\partial y^2}+q=0$

Static Analysis of Sandwich Plates of Composite Materials

$$D_{11}\frac{\partial^2\theta x}{\partial x^2} + D_{66}\frac{\partial^2\theta x}{\partial y^2} + (d_{12}+d_{66})\frac{\partial^2\theta y}{\partial x\partial y} - C_S A_{55}\left(\theta x + \frac{\partial w}{\partial x}\right) = 0$$

$$(d_{12}+d_{66})\frac{\partial^2\theta x}{\partial x\partial y} + D_{66}\frac{\partial^2\theta y}{\partial x^2} + D_{22}\frac{\partial^2\theta y}{\partial y^2} - C_S A_{44}\left(\theta y + \frac{\partial w}{\partial y}\right) = 0$$

$$C_S A_{55}\left(\frac{\partial\theta x}{\partial x} + \frac{\partial^2 w}{\partial x^2}\right) + C_S A_{44}\left(\frac{\partial\theta y}{\partial y} + \frac{\partial^2 w}{\partial y^2}\right) + p(x, y) = 0$$

In the literature review seen some of the advantage of sandwich material on railway vehicle body and past research works on the car body. The car body structure affect the energy utilization, passenger ride comfort, load carrying capacity and other related to maintenance and operation.

Researches were done on the sandwich material to get the advantage of its properties and also to minimizing the masses of the vehicle. Sandwich composites have high strength to weight ratio (which results in increase of payload, provides greater range and/or reduced fuel consumption), extended operational life, lower maintenance cost (due to less corrosion), as well as a range of integrated functions, such as thermal and sound insulation, excellent signature properties, fire safety, good energy absorption, directional properties of the face sheets enabling optimized design and production of complex and smooth hydrodynamic surfaces . The high specific bending stiffness of sandwich structures can with advantage is used in vehicles.

The basic sandwich structure theory presented in all these researches have described in the literature review is generally called the Classical sandwich theory. This theory assumes that:

- The core carries the entire shear load in sandwich beams and plates.
- The face sheets carry the entire bending load.
- Core compression is negligible.

Addis Ababa city tram car is a one directional, particularly low floor 3 tramcar set design. Tram sets are connected articulated system. Vehicle has angular steel construction with big windows.

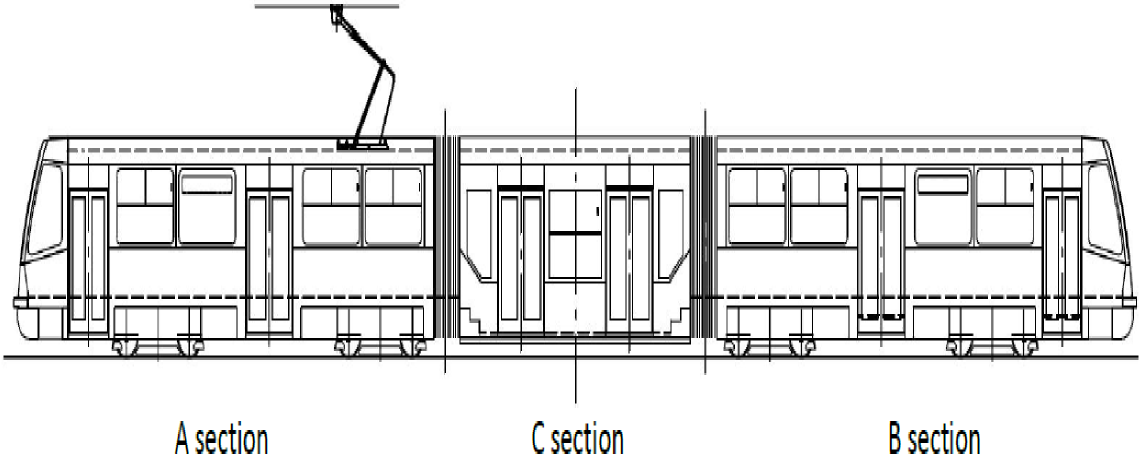

Figure 2.22 Cross section of Addis Ababa city tram

Chassis of A and B sections are mounted on two bogies and four axles. Middle section – C is suspended and supported with other sections. Car body section A and B are almost the same the only one difference is lack of roof electrical equipment on B section. In this research was analyzed the structure of Addis Ababa city tramcar of C-section by using its own material and by using aluminum honeycomb sandwich material and analyzed the effect of material in vehicle static of light rail train are computed.

CHAPTER THREE

3. Creating finite element model

This chapter deals with the FE method that is used to analyze the railway tram car in the commercial software ANSYS 14.5. A brief summary of the routines that have been used are presented. The finite element models were created in ANSYS which includes ANSYS Composite Prep Post (ACP).It is an add-in to ANSYS Workbench and is integrated with the standard analysis features. The entire workflow for sandwich structure can be completed from design to final information production as a result. This method of creating models is easier than coding an input file, especially when the models are large.

With the basic understanding of how finite element programs work, a finite element model must be created with appropriate parameters such as dimensions, loads, constraints, element choice, mesh selection, etc.

Modeling the vehicle body using exact steel material and honeycomb material are different. The modeling of the steel vehicle are finished on solid works and import as .STEP or .IJES file but to make the model for the honey comb used composite prep post (ACP) in addition to solid works

3.1 FE Analysis method of steel tram car

3.1.1 FE modeling of steel tram car

As stated earlier, to build the model of the tram car drawn in a computer-aided design (CAD) environment used SOLIDWORKS 11 and import the mode with a file format such as IGES, ACIS, or Parasolid.

Data of Tram car section C

Length=6900mm
Width=2180mm
Height between under frame to car top=2796 mm

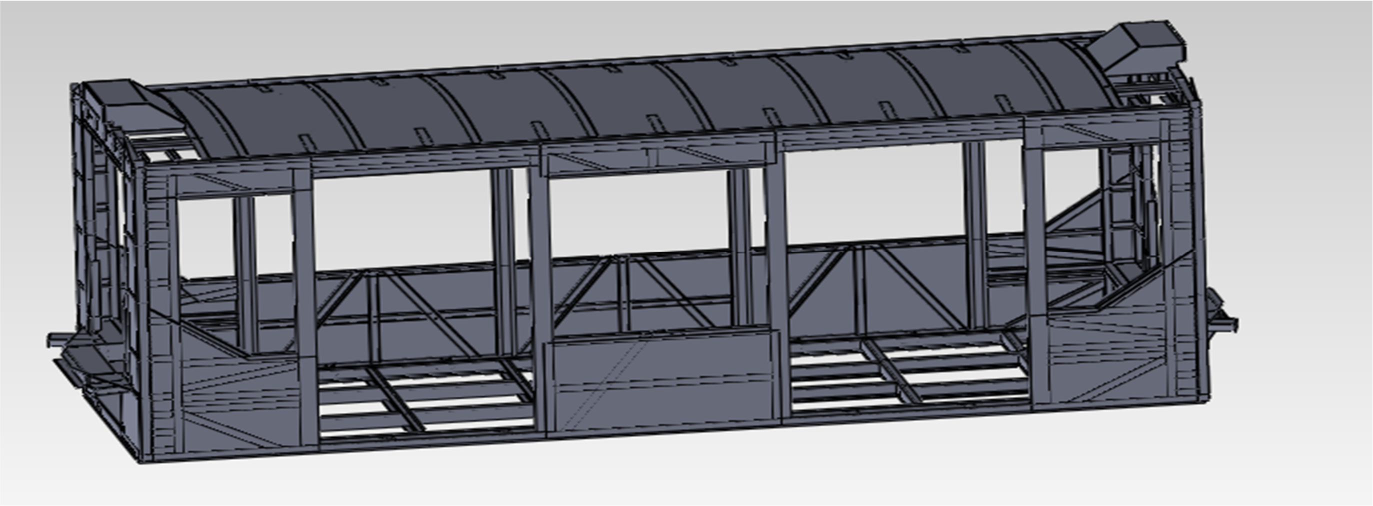

Figure 3.1 modeling of steel tram C-section using solid work

3.1.2 Define material property

Properties of material under study

Material is structural Steel according to EN 10025:2004 standard

Table 3.1 Material property of steel frame

	S235J2/d0001	S355J2
Min yield stress limit	235	355
Tensile strength	510	630
Impact strength (KV-J)	20	20
Modules of elasticity	210GPa	
Poisons ratio	0.3	
Density	7850kg/m	

Table 3.2 material property of sheet metal

	Nickel- chromium weathering steel (16NiCr4)
density	7800kg/m^3
Modules of elasticity	210GPa
Shear modulus	7.9 $*10^{10}$N/m^2
Tensile strength	$9*10^8$ N/m^2
Specific heat	440J/Kg

3.1.3 Mesh generation

The model consisted of 96168 elements and 347613 nodes and FEM analyzed quadrilateral shell elements. The mash with coarse sizing was selected and at different location an average element size between 10mm up to 20 mm and the face material sized element size of 10mm.

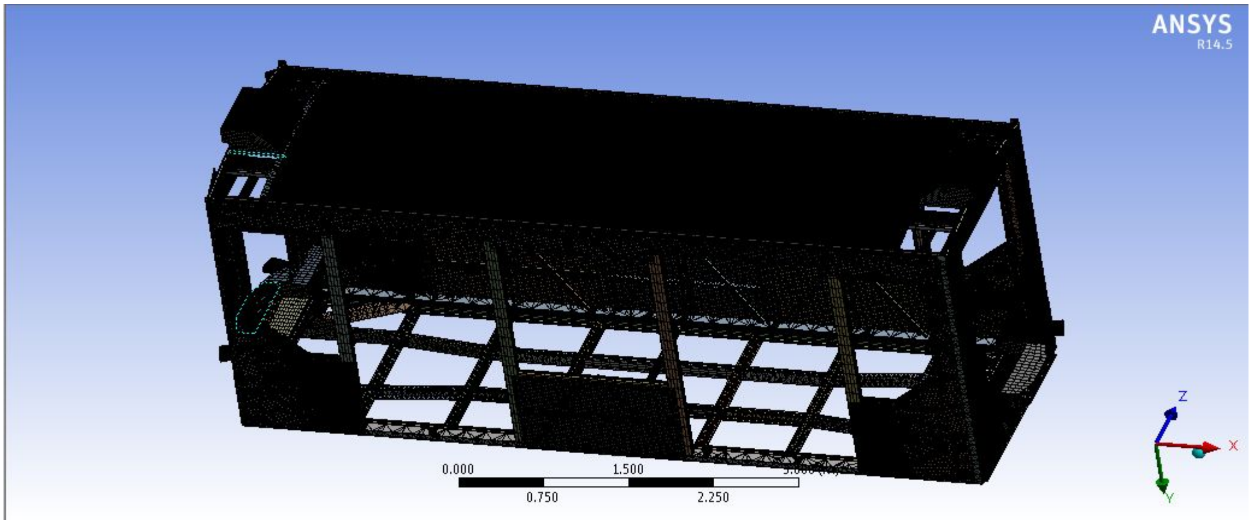

Figure 3.2 Meshing of steel vehicle body

3.1.4 Boundary condition

The tram car constraint was a fixed support at the coupling point between each tram. The C-section tram vehicle connected in both direction with A-section and B-section.

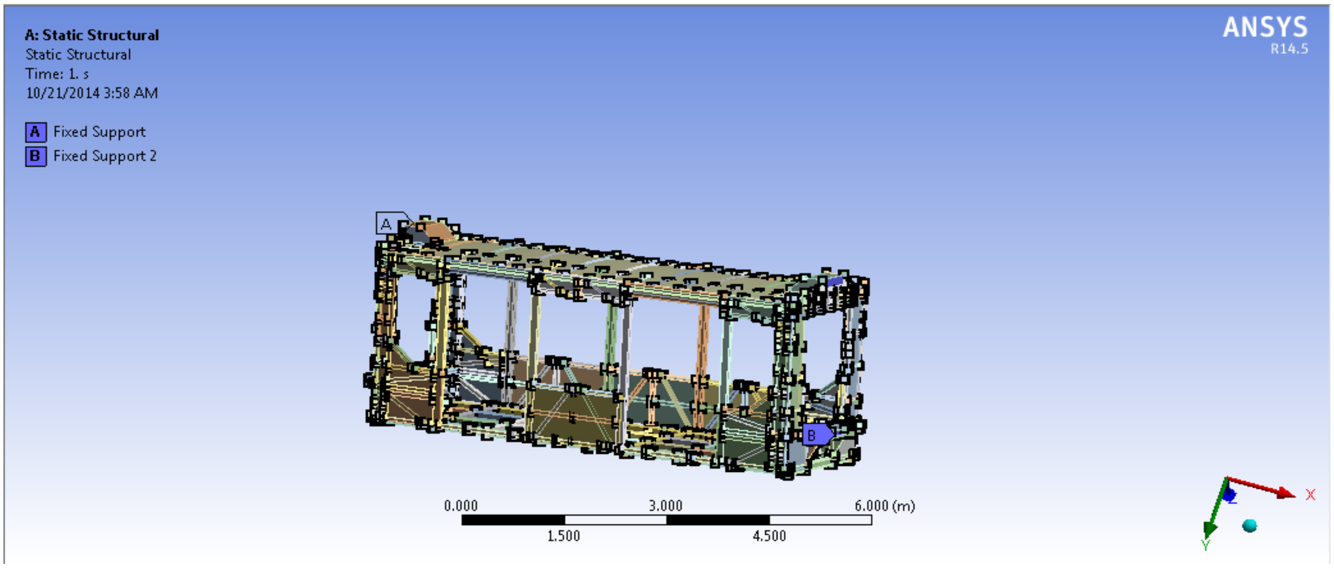

Figure 3.3 boundary conditions of the FE model

3.1.5 Support and load

One of the main parameters considered in the design of railway structures is the longitudinal yield strength or buff strength of the vehicle. This load requirement is important because when vehicles are properly designed to this load, they are protected against large-scale deformation, penetration, and damage during a variety of collision events ranging from hard couplings to end to- end collisions with other rail vehicles.

According to standard tram car categorized under P-V and we analyzed Addis Ababa LRT under these categories.

Table 3.3 load condition stated under EN 12663 for P-V type locomotive

Load	description	value
tensile load at coupling area	50KN tensile load in both direction	A value of 25 KN at each buffer
Compressive force at buffers	200KN compression force in both direction	A value of 100000N at each buffer
Turning right	0.15*gross vehicle weight in Y direction	1.4715m/s2
Turning left	0.15* gross vehicle weight in Y direction	1.4715 m/s2
Maximum operating load	1.3*gross vehicle weight in Z-direction	12.753m/s2

From the European standard In order to calculate the forces on the equipment attachments during operation of the vehicle, the masses of the components shall be multiplied by the specified accelerations in x, y and z direction.

X- Longitudinal direction

Y- Lateral direction

Z -vertical direction

Vertical load (F_Z) is the load uniformly distributed over the floor of the car body

$$F_Z = 1.3*(m_1 + m_4)$$

m_1 the design mass of the vehicle in working order according to EN15663 without bogie mass.

And m_4 the mass of exceptional pay load.

In Addis Ababa city tram m_4 take as the no of passenger at the peak hour which is 8person per meter square and According to EN 12663 standard average passenger's weight is 68 kg.

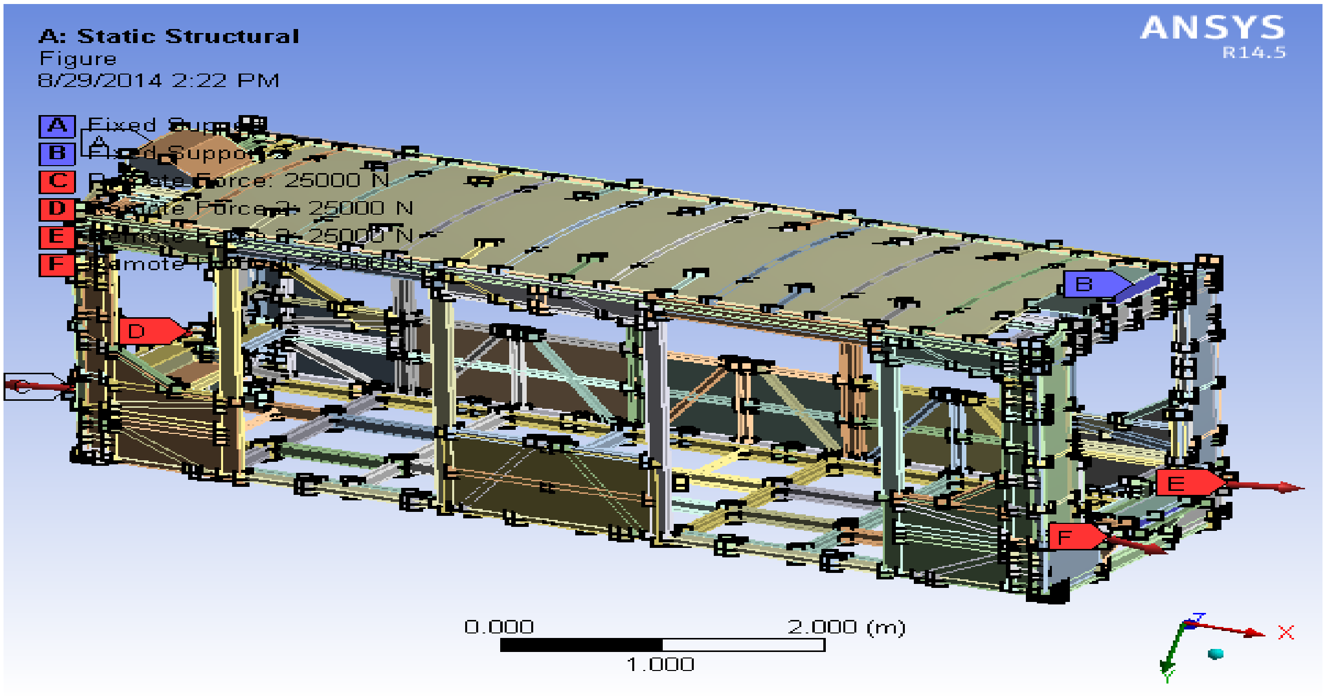

Figure 3.4 Tensile force at the buffer

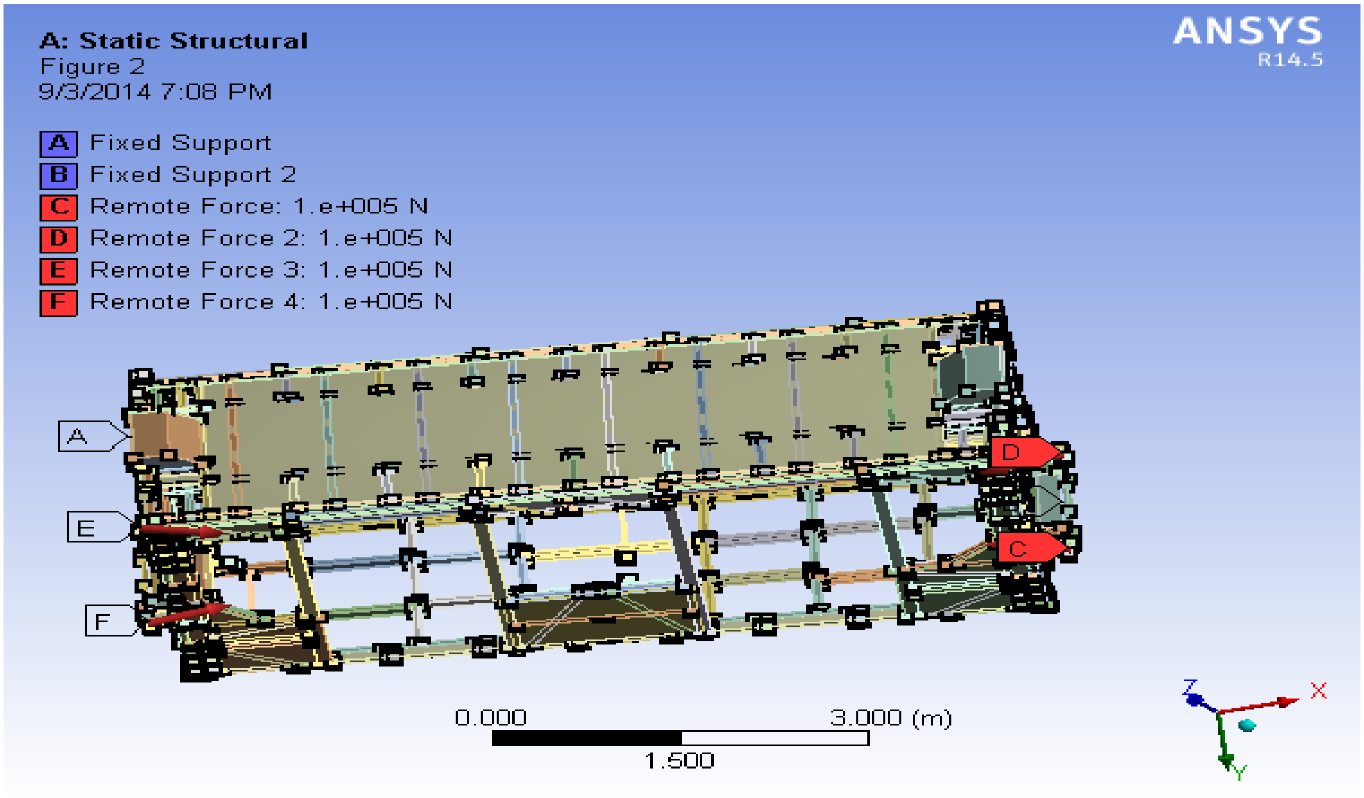

Figure 3.5 Compression force at the buffer

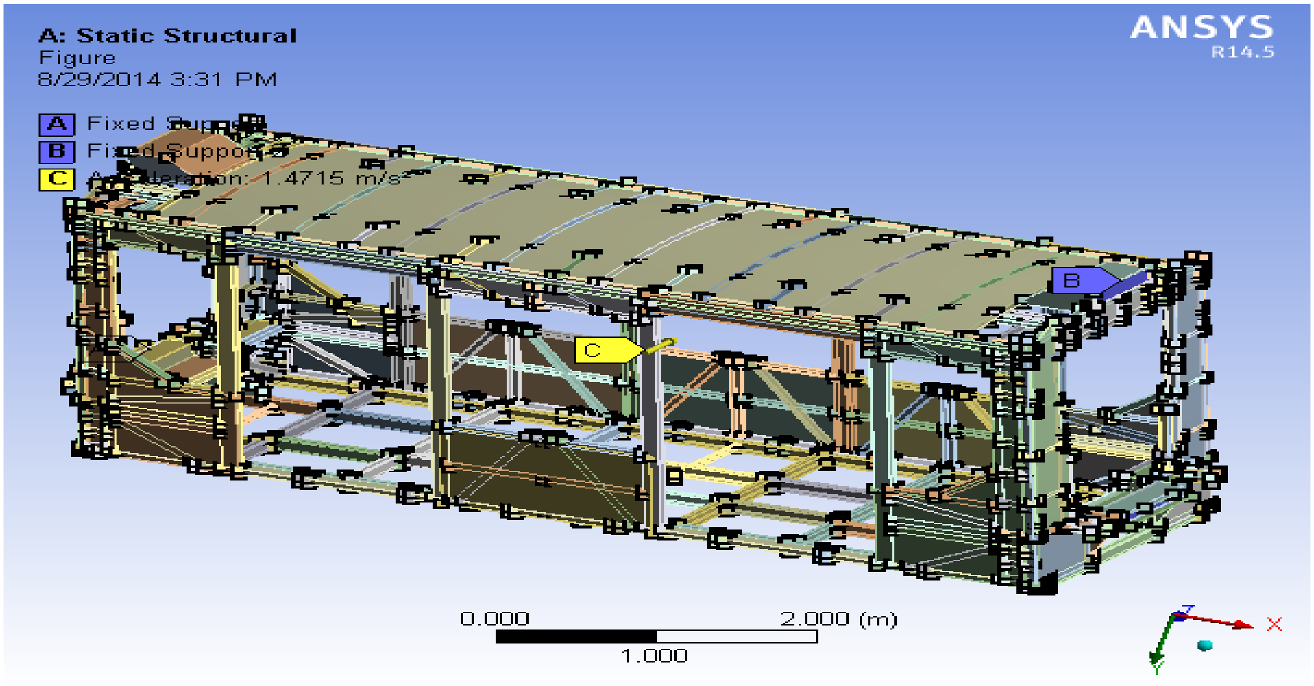

Figure 3.6 Load due to right turn and left turn

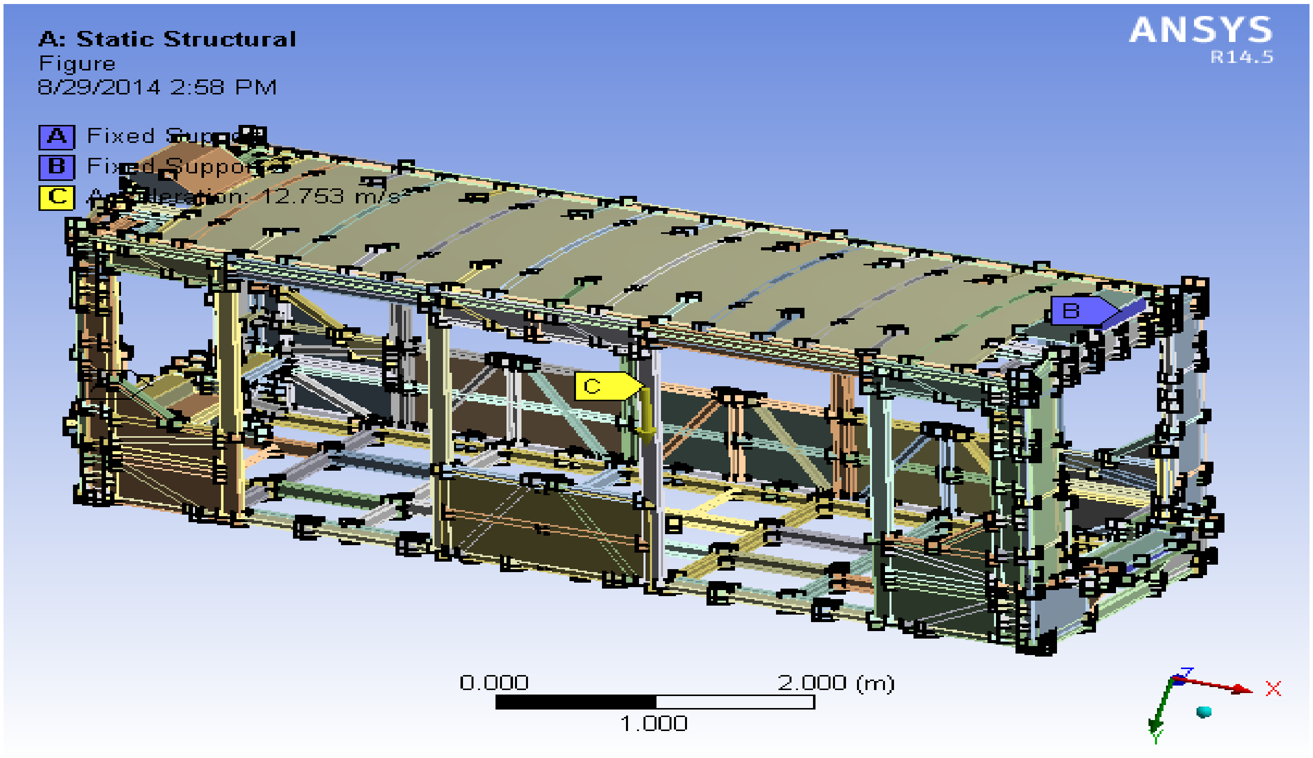

Figure 3.7 Load due to operating load

3.2 FE Analysis method of aluminum honeycomb

ANSYS Composite Prep Post (ACP) provides all necessary functionalities for the analysis of layered sandwich structures that include numerous layers, materials, thicknesses and orientations. Using the ACP we analyzed the aluminum honey comb tram car.

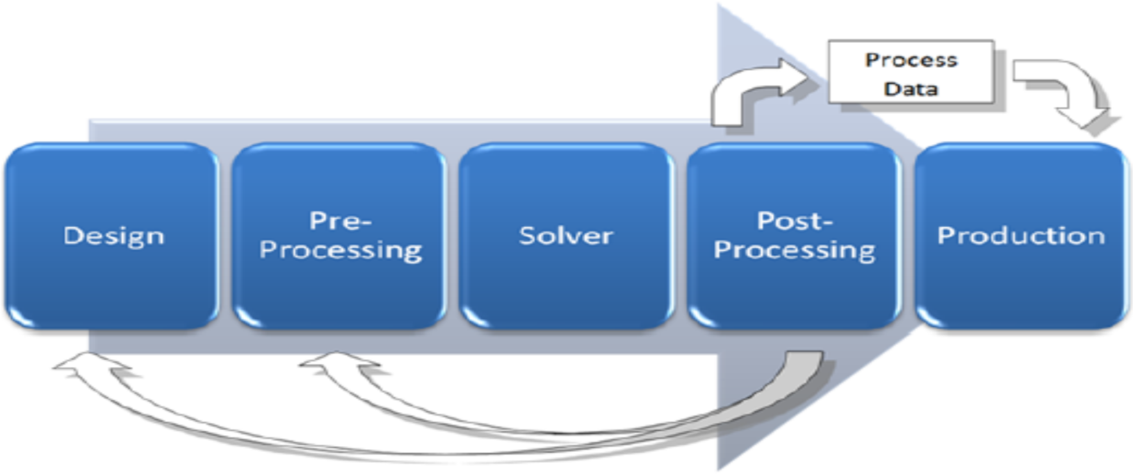

Figure 3.8 Finite element procedure used in ACP

The geometry of the tooling surfaces of a composite structure is the basis for analysis and production. Based on this geometry and a FE mesh, the boundary conditions and composite definitions are applied to the structure in the pre-processing stage and these composite definitions are transferred to the FE model and the solver input file. After a completed solution, the post-processing is used to evaluate the performance of the design and laminate results (failure, safety, strains and stresses) can be evaluated and visualized.

3.2.1 Aluminum honeycomb tram car model

In this research the two sides and the roof of the tram vehicle was changed into aluminum honeycomb material.

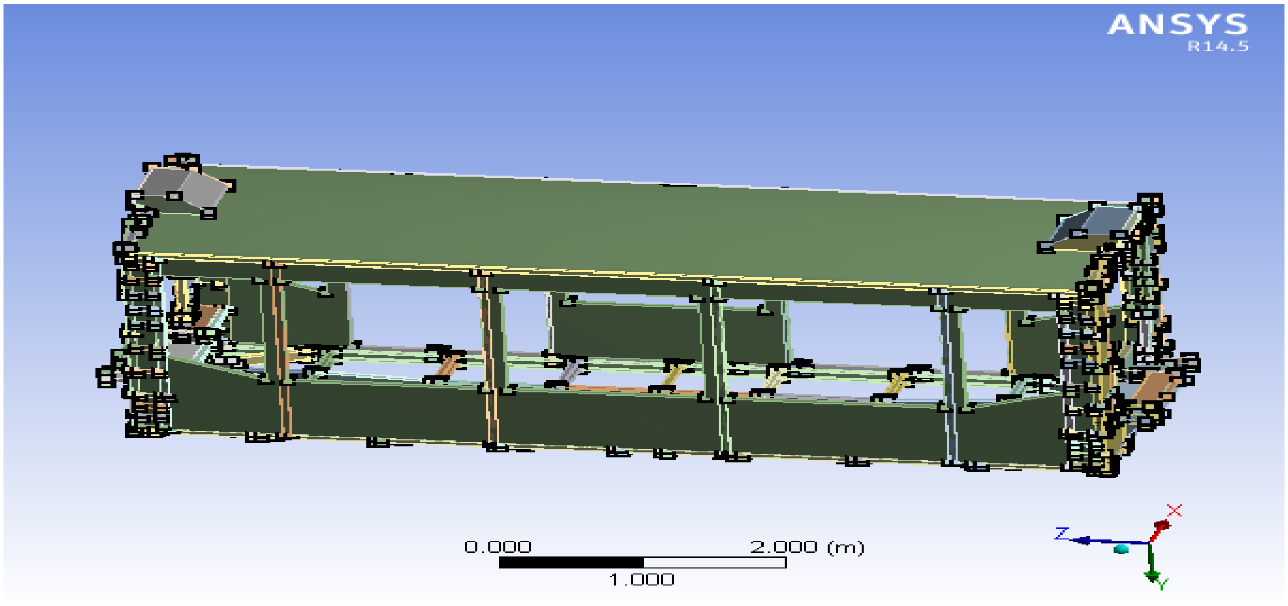

Figure 3.9 Aluminum honeycomb model

3.2.2 Define Engineering Data

Honeycomb material

Table 3.4 Mechanical properties of aluminum honeycomb core material A3003-H19

ITEM	properties
CORE density(kg/m^3	83.2
0.2% yield stress(MPa)	190
Elongation %	4
Compressive strength(MPa)	4.6
Compressive modulus (MPa)	1000
Shear strength, L (MPa)	2.4
Shear strength, w (MPa)	1.5
Shear modulus, L (MPa)	440
Shear modulus, w (MPa)	220

Mechanical property of facing plate material A5083-H321

Table 3.5 Face material of Aluminum alloy

Young's modulus(MPa)	Yield strength (MPa)	Tensile strength(MPa)	Elongation %
71070	268	367	13

3.2.3 Generate Mesh

The model consisted of 250374 elements and 1135826 nodes and FEM analyzed quadrilateral shell elements .The meshing element size of the aluminum honeycomb used 2mm

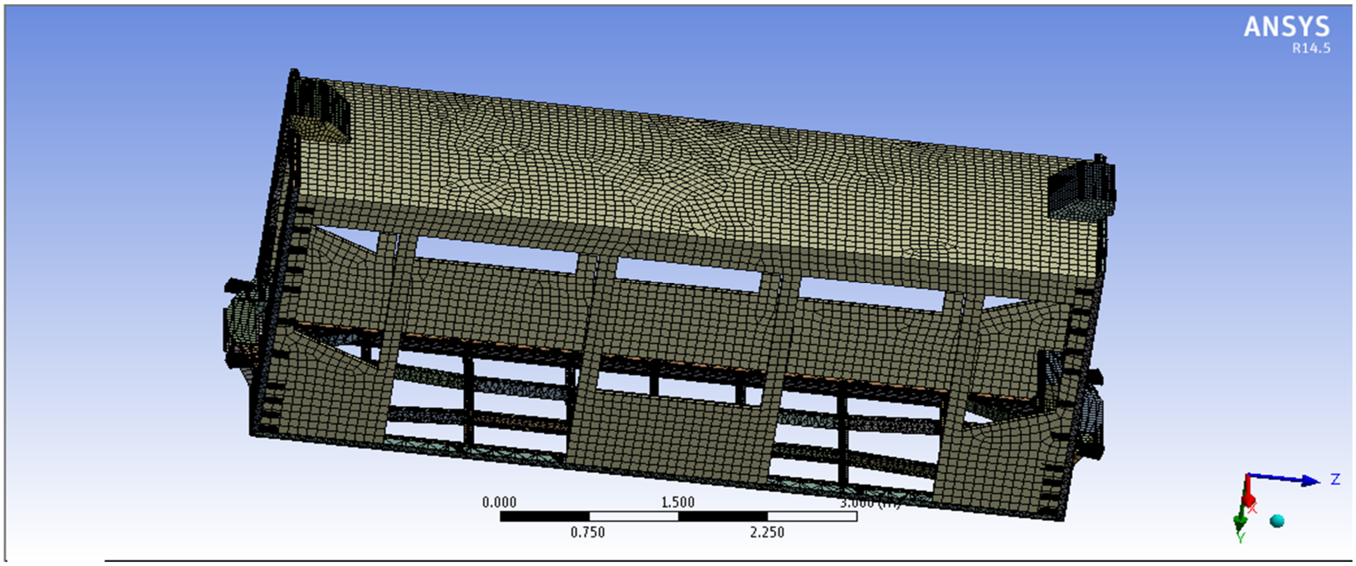

Figure 3.10 Meshing of aluminum sandwich tram car

3.2.4 ANSYS composite preprocess (ACP)

- Define Fabric

  Defined the two upper and the lower face material type and thickness are defined and also honeycomb core material type and thickness defined. The faces are a thickness of 2mm and a core of 40mm are selected.

- Define Rosettes and Oriented Element Sets

  Rosettes are coordinate systems that used to set the reference direction of Oriented Element Sets. In other words, Rosettes define the 0° direction for the composite layup and An Oriented Element Set is an Element Set with additional information about the element orientations.

–Create Modeling Plies

Ply Groups have no influence on the ply-ordering and definition but help to group the sandwich definitions. In the aluminum honeycomb used 3 ply groups the faces are defined as isotropic aluminum material defined in fabrics and for core used honeycomb ply type.

Workbench Analysis System

– Add the steel under frame and side end connect to the honeycomb sandwich material that drawn in ACP by aluminum honey comb material.

3.2.5 Define Boundary Conditions and loading condition

The load and the boundary condition are the same as that of steel tram vehicle used earlier.

3.3 Static stress analysis

The static analysis of the vehicle body was analyzed due to different loading condition stated on DIN EN 12663 and EN 15227 .The material properties of both steel and aluminum honeycomb stated earlier in table 3.1, 3.2.3.4, 3.5 has been used to determine the maximum principal stress and deformation.

3.3.1 Result of steel tram car due to tensile force at buffers

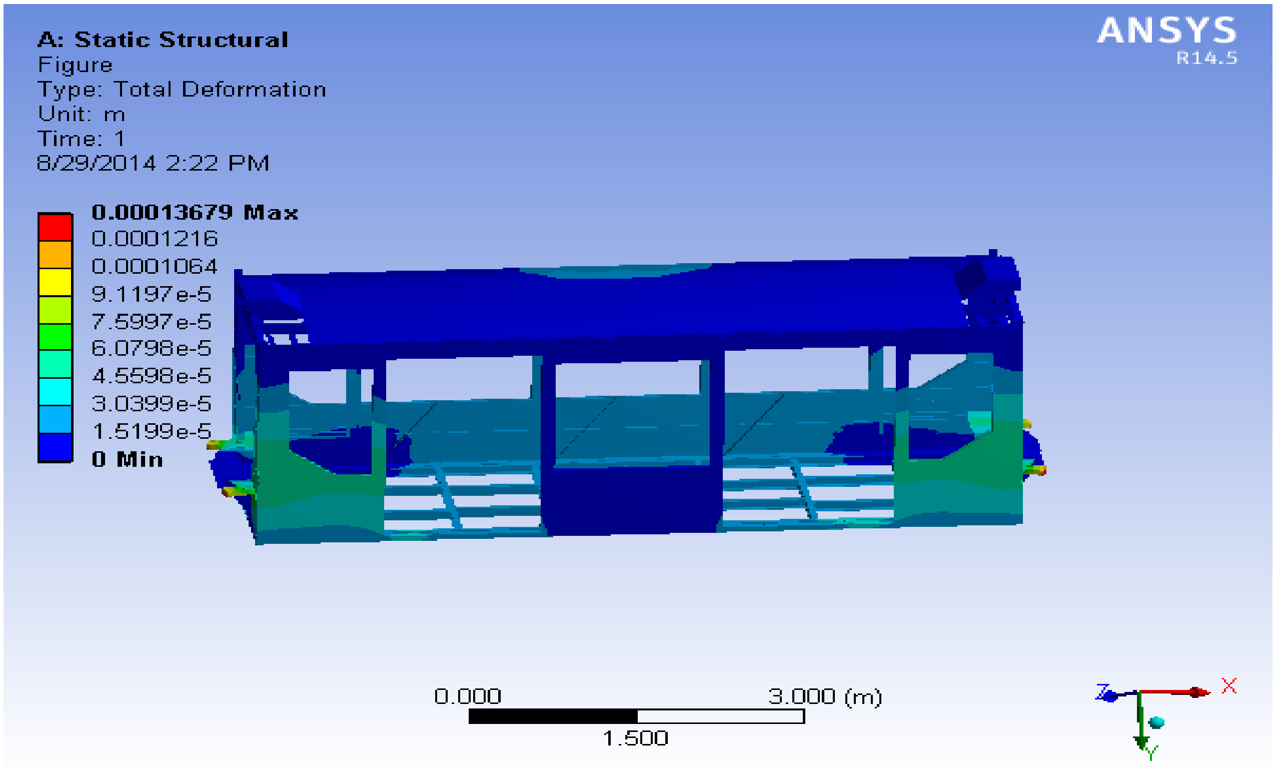

Figure 3.11 Total deformation due to tensile force at buffers

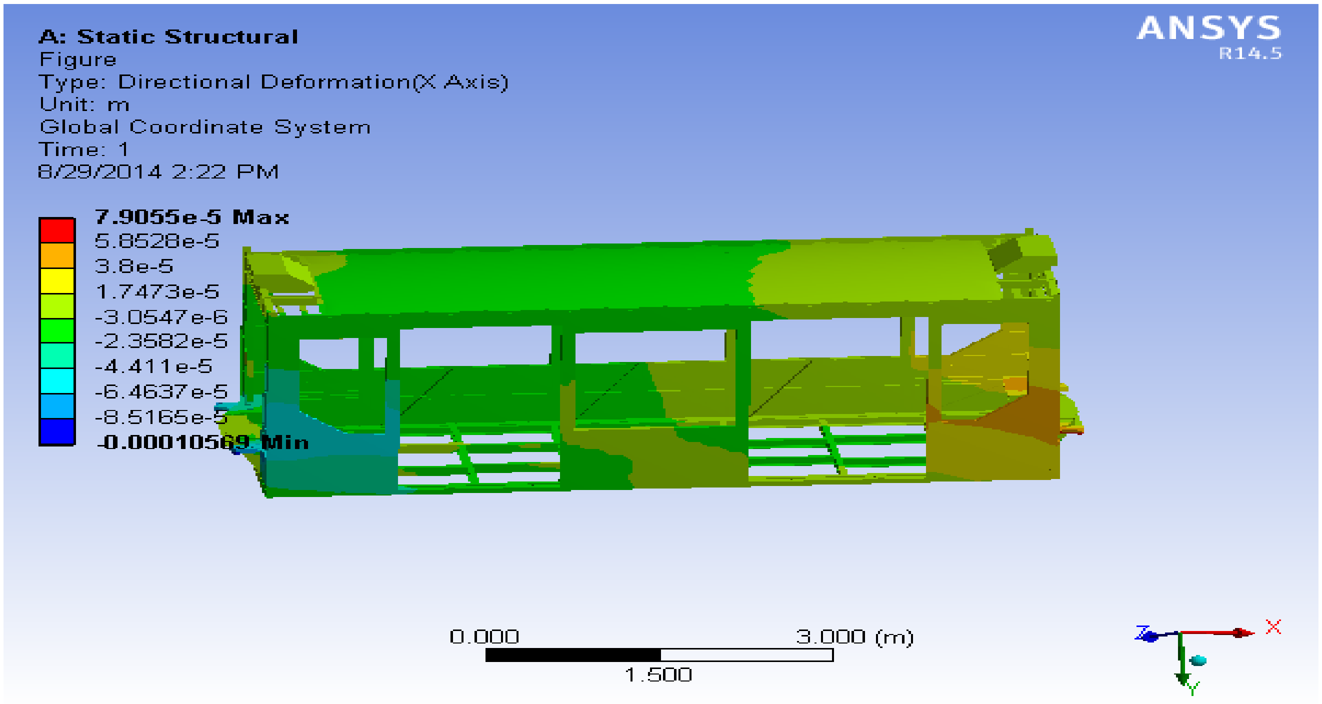

Figure 3.12 Directional deformation due to tensile force at buffers

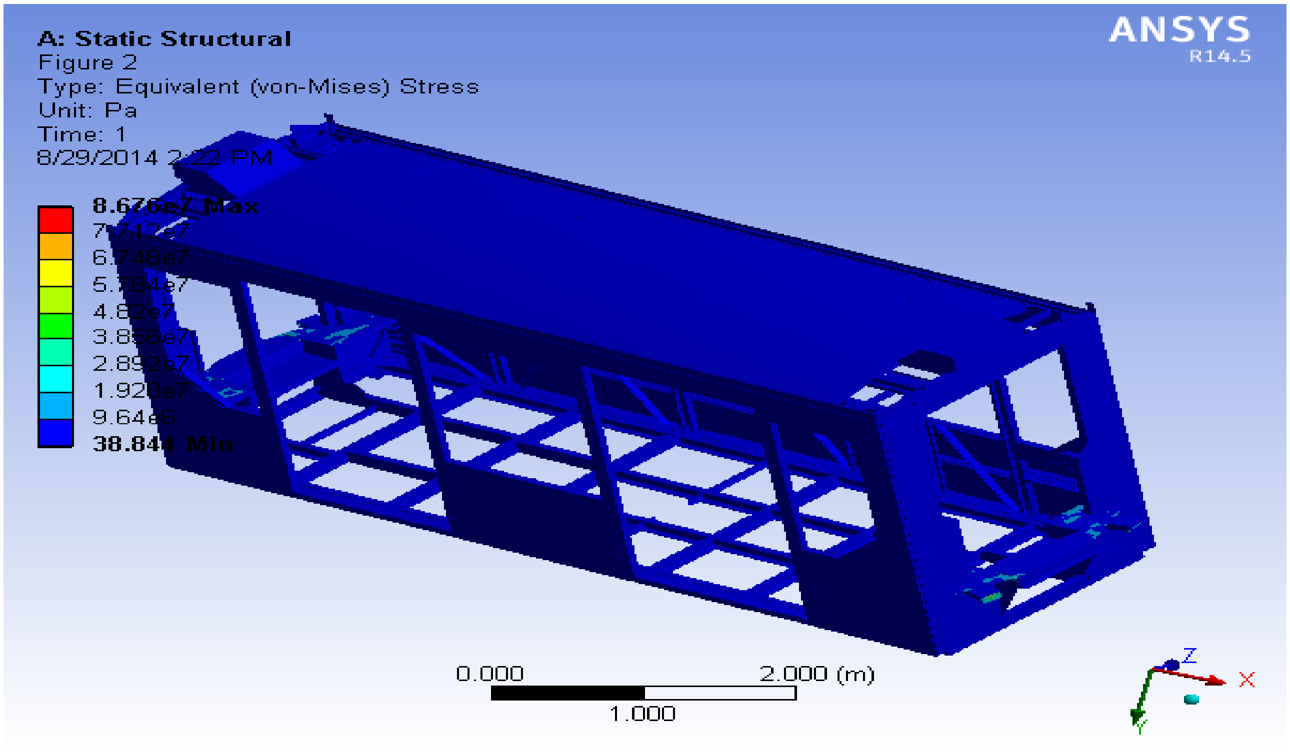

Figure 3.13 Equivalent von-moises stress due to tensile force at buffers

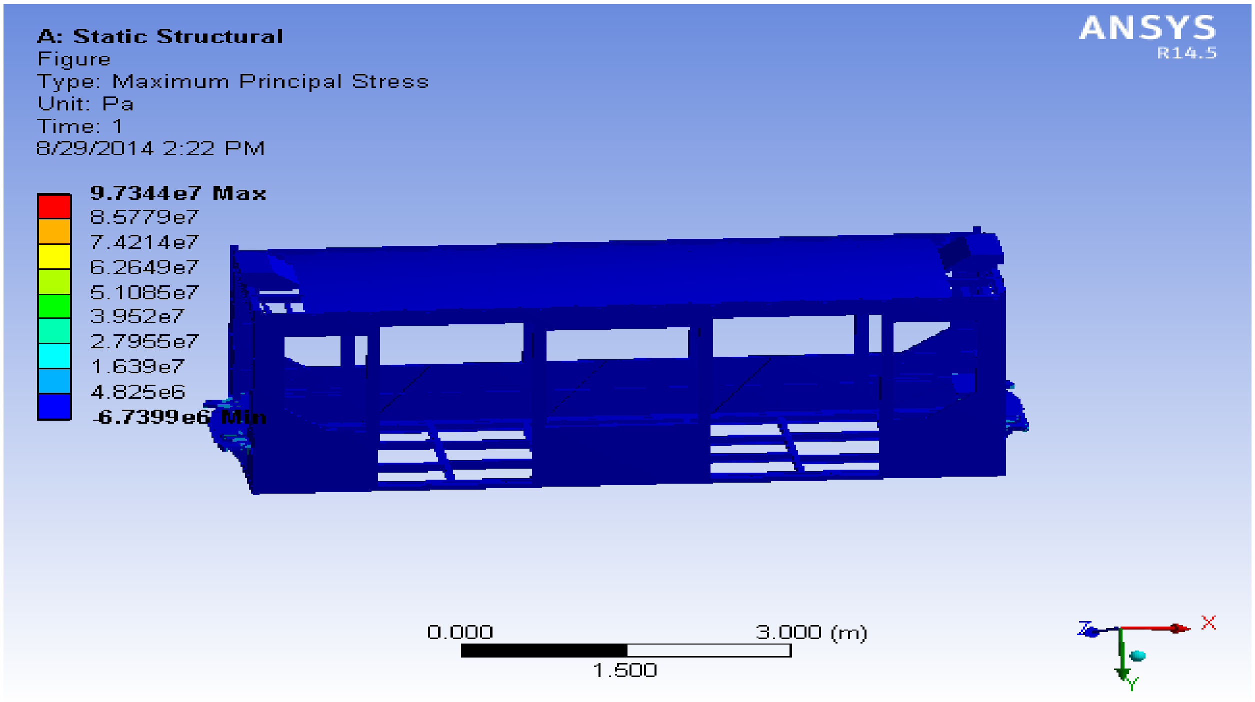

Figure 3.14 Maximum principal stress of steel tram vehicle

3.3.2 Result of steel tram car due to compression force at buffers

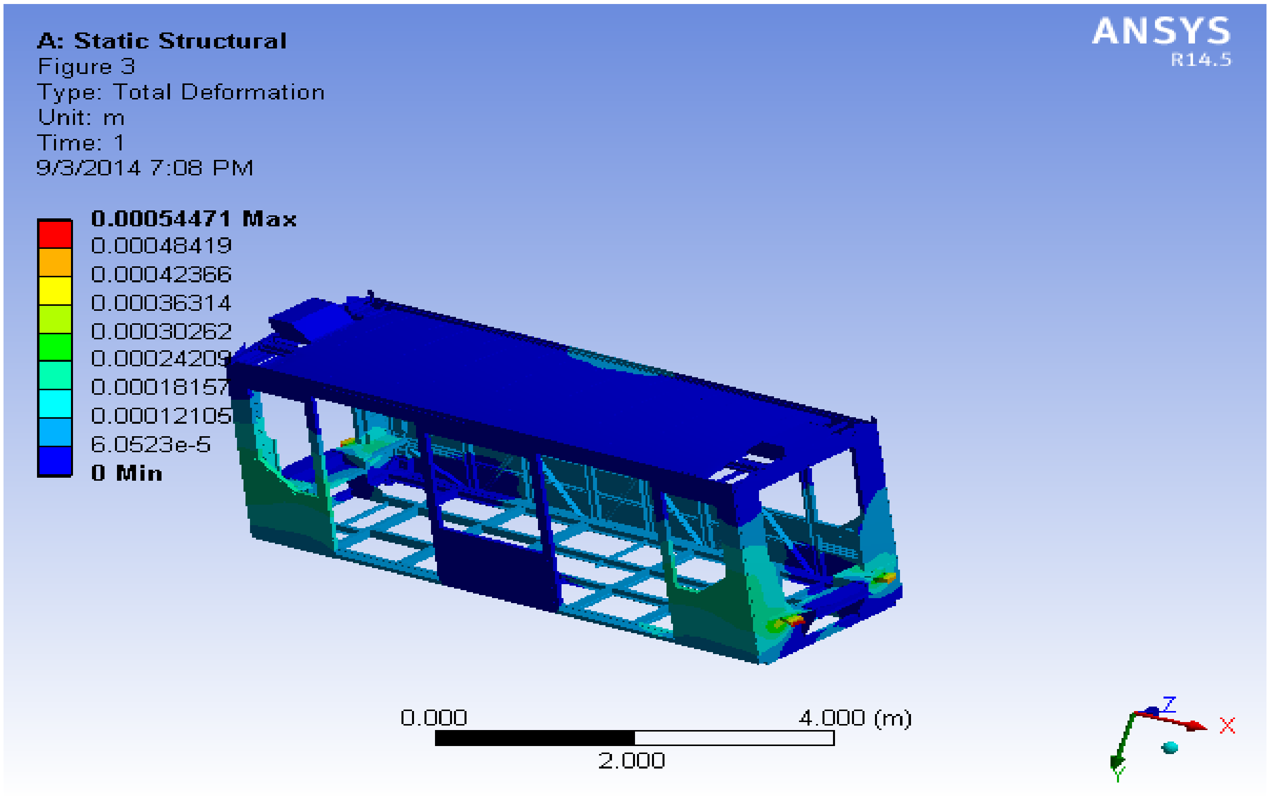

Figure 3.15 Total deformation due to compression force at buffers

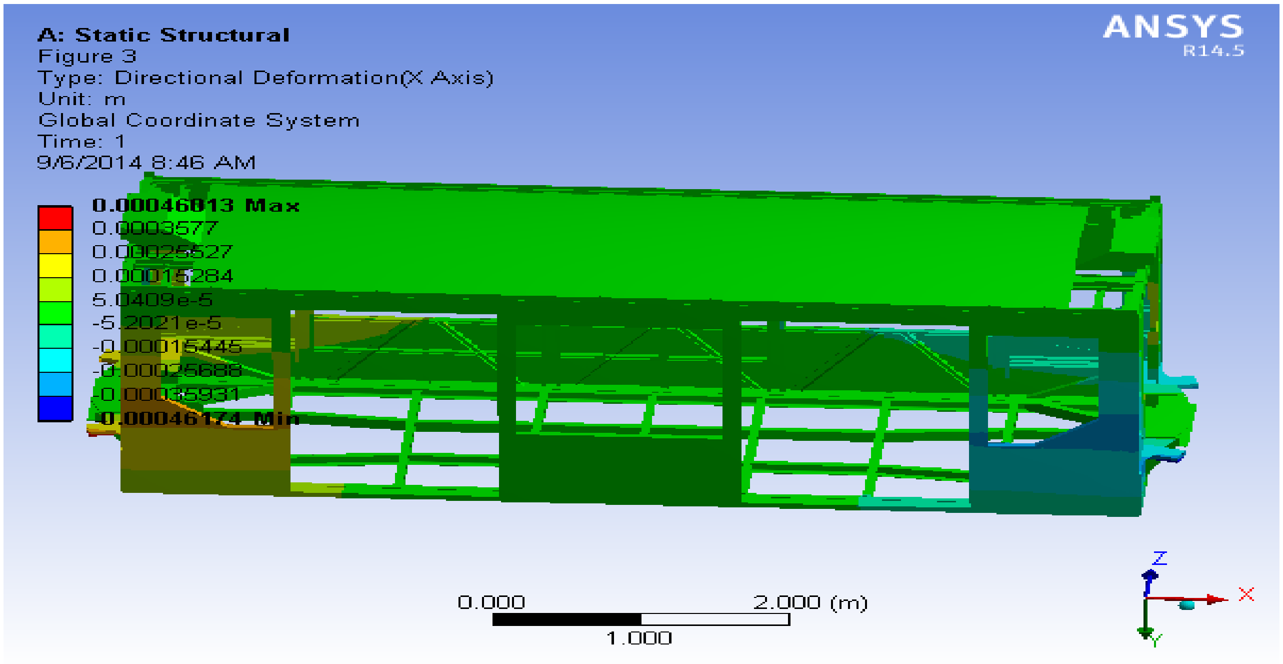

Figure 3.16 Directional deformation due to compression force at buffers

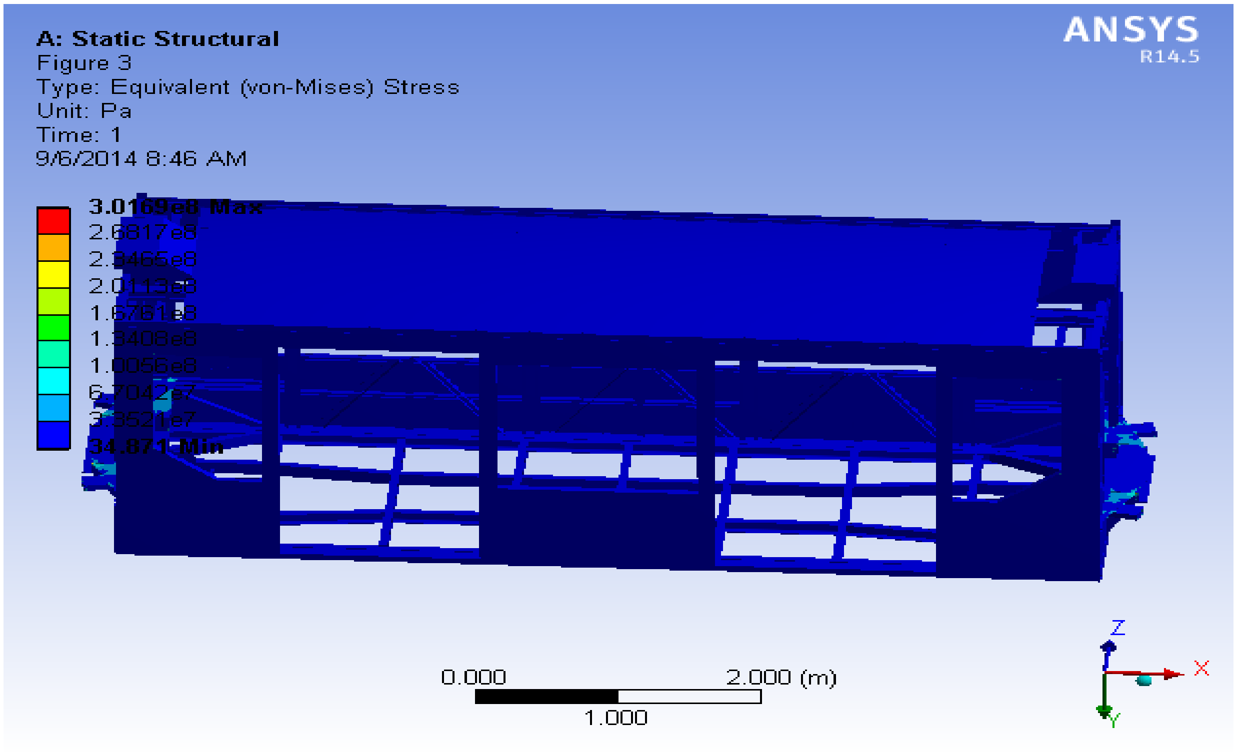

Figure 3.17 Equivalent (von-mises) stress due to compression force at buffers

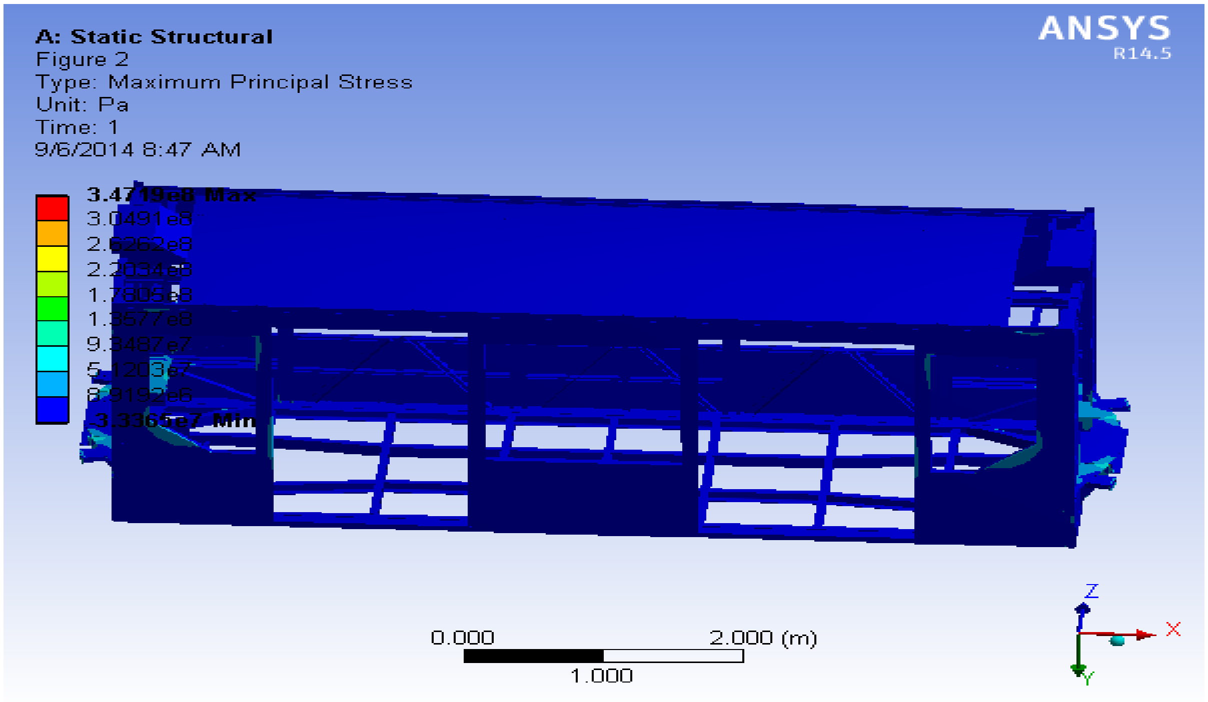

Figure 3.18 Maximum principal stress due to compression force at buffers

3.3.3 Result of steel tram car due to right turn

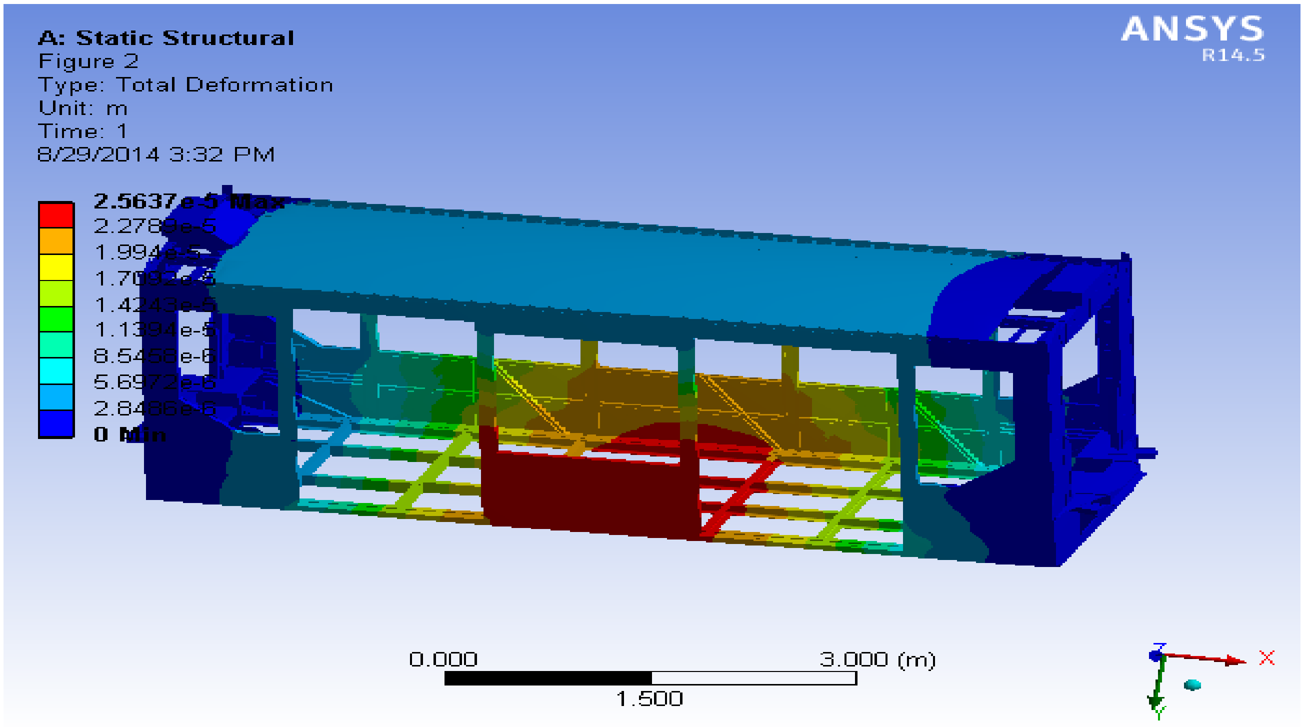

Figure 3.19 Total deflection due to right turn

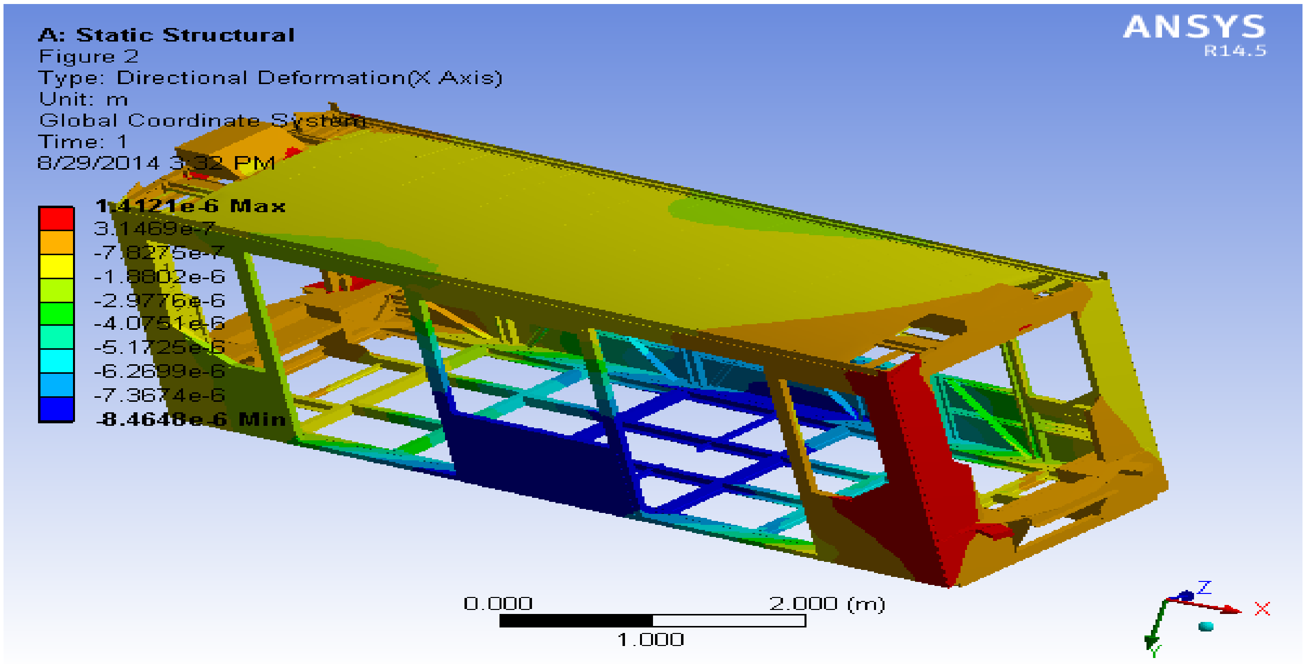

Figure 3.20 Directional deformations due to right turn

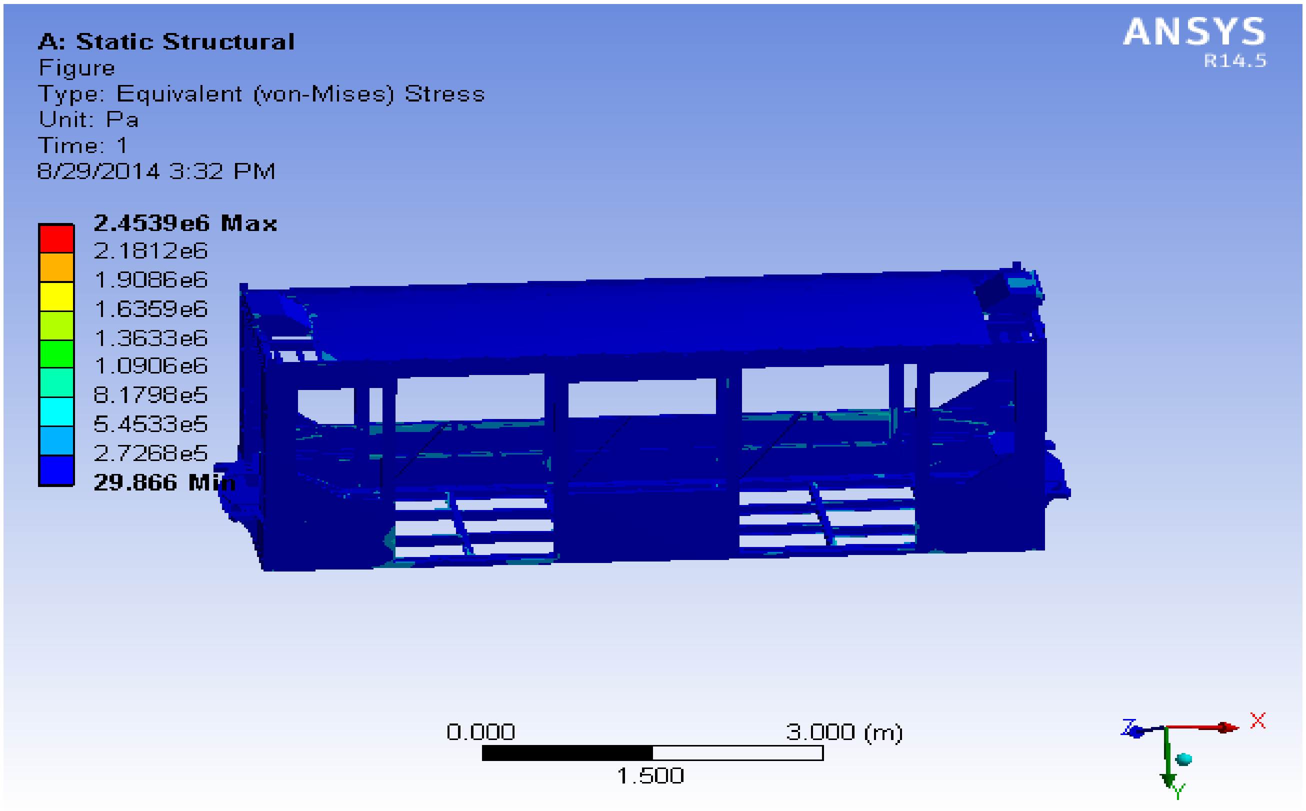

Figure 3.21 Equivalent von-moises stress due to right turn

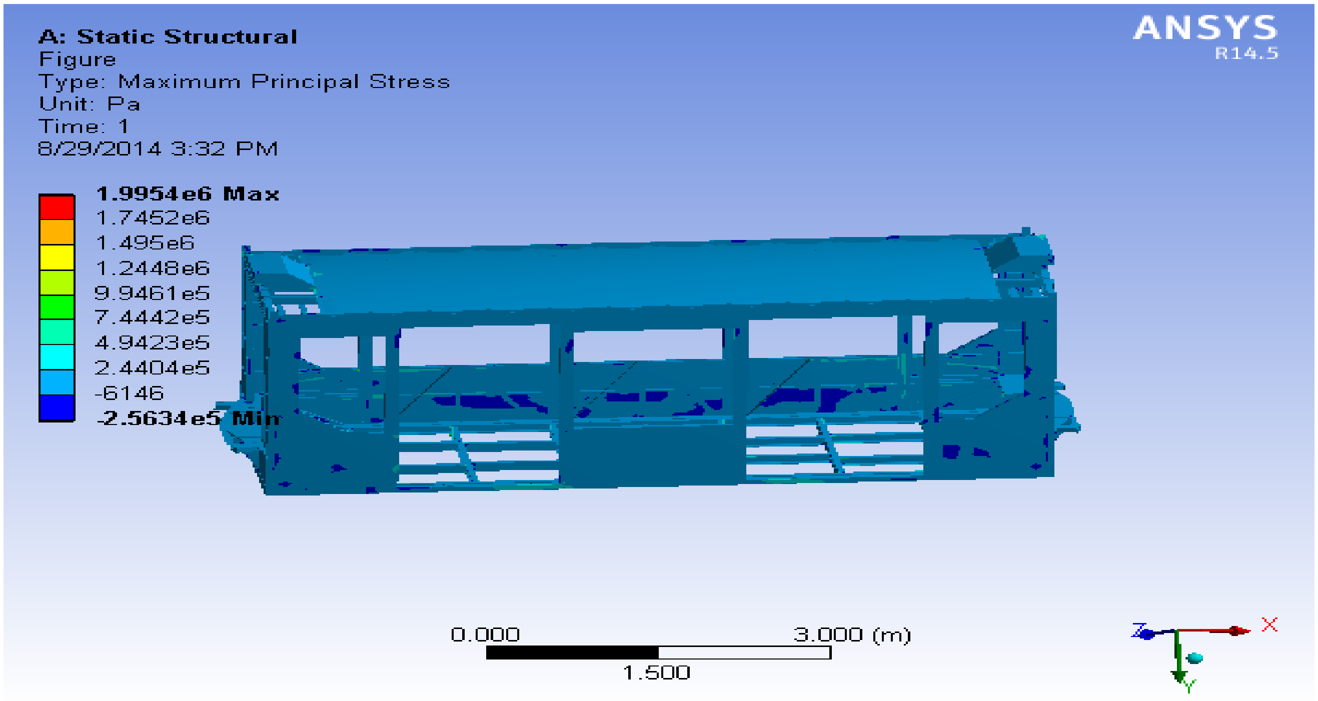

Figure 3.22 Maximum principal stress due to right turn

3.3.4 Result of steel tram car due to operating load

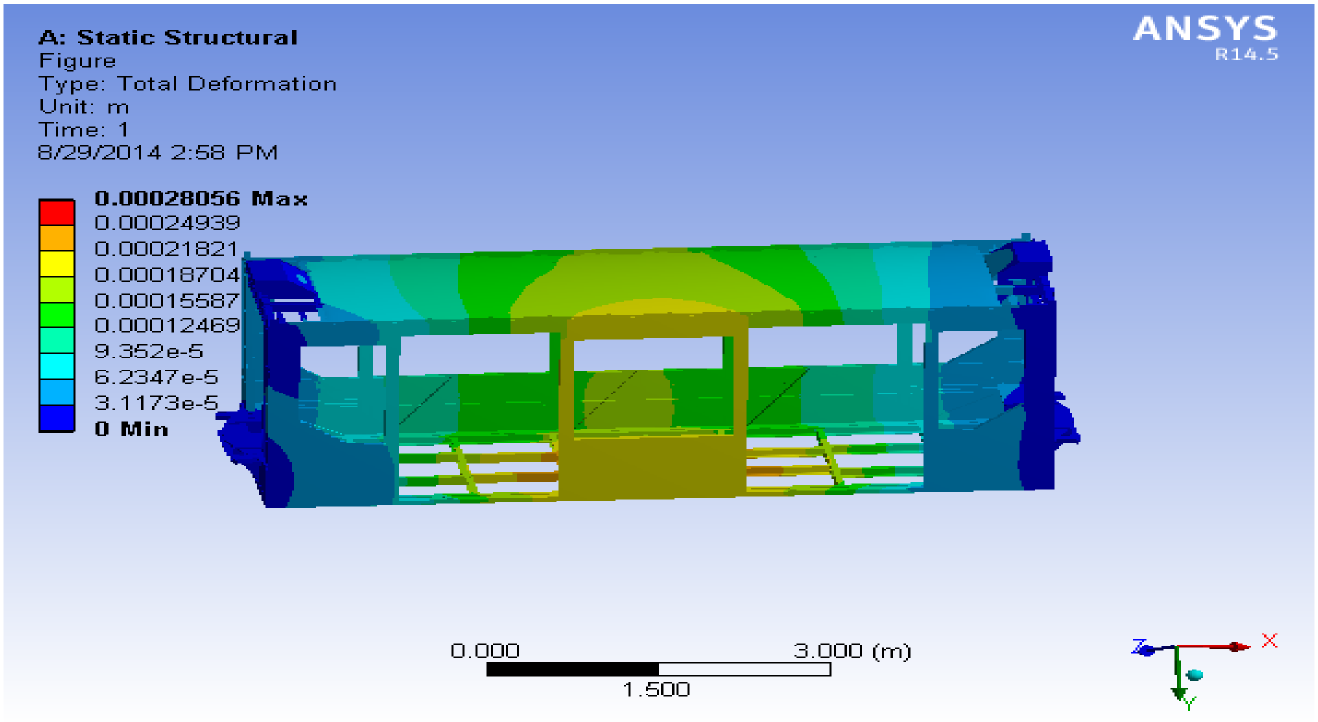

Figure 3.23 Total deformation due to operating load

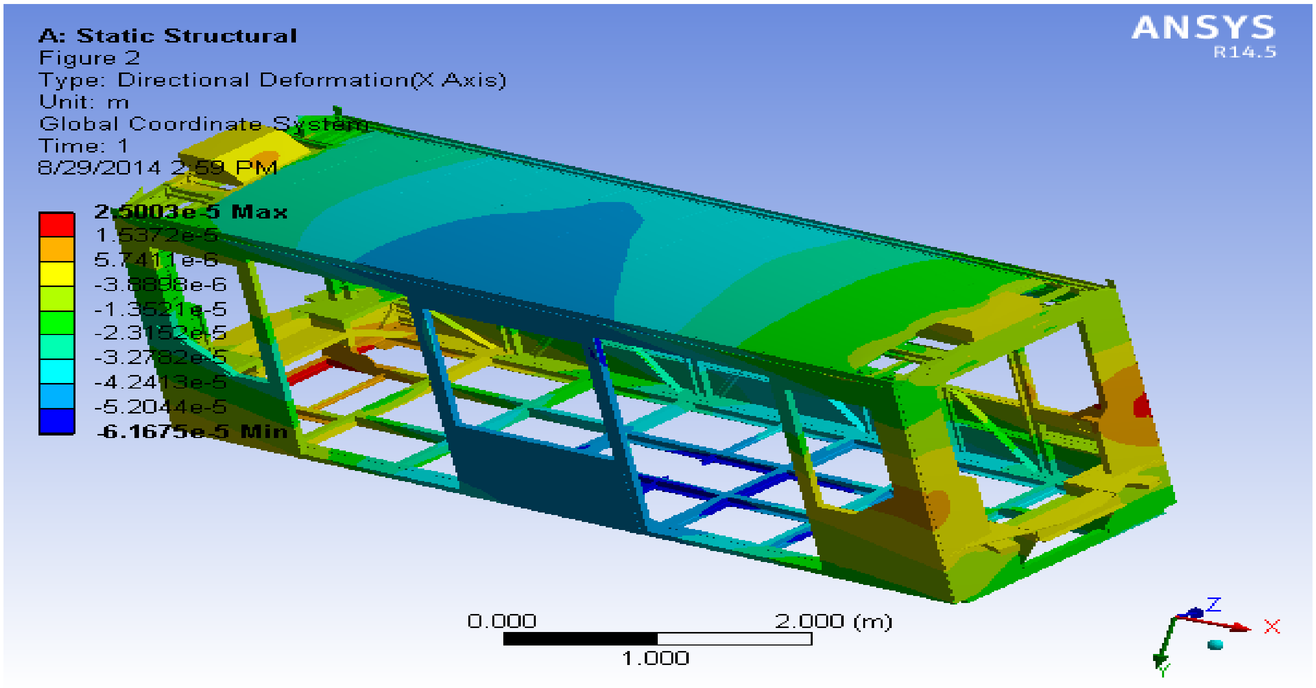

Figure 3.24 Directional deformation due to operating load

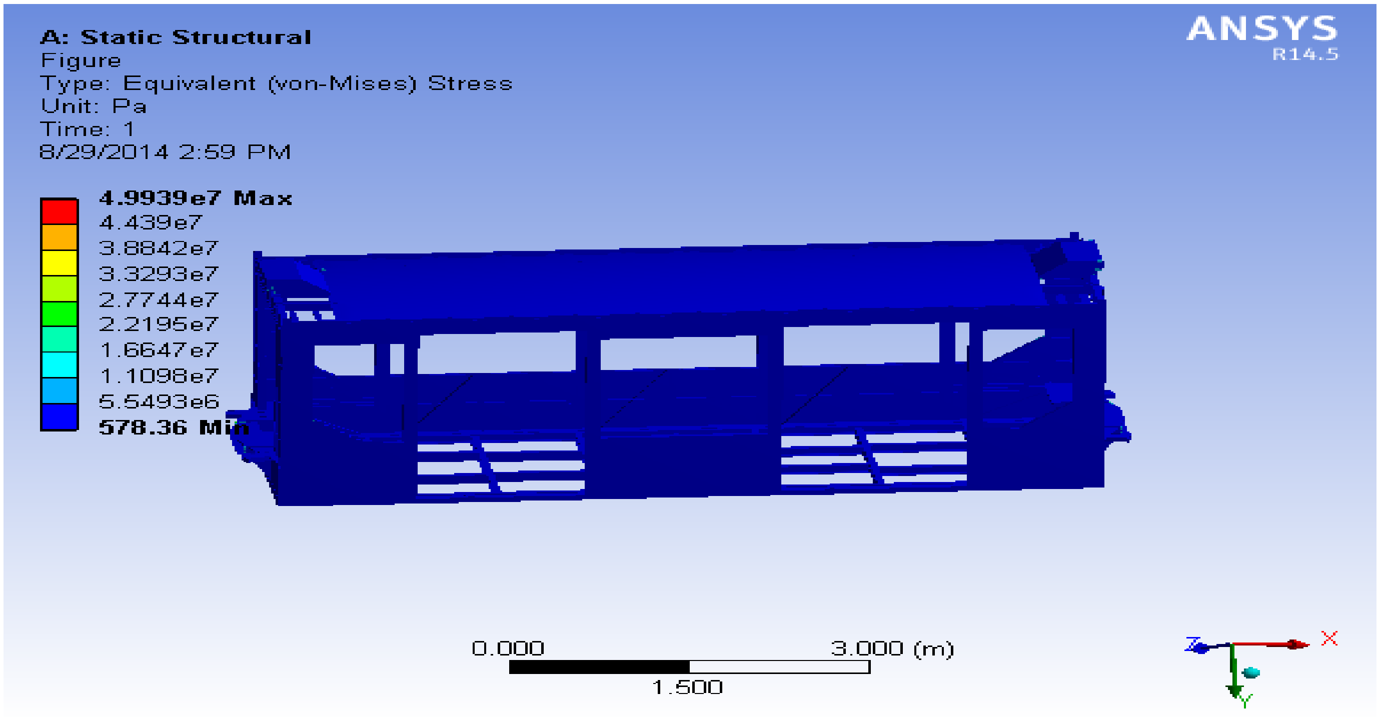

Figure 3.25 Equivalent (von-mises) stress due to operating load

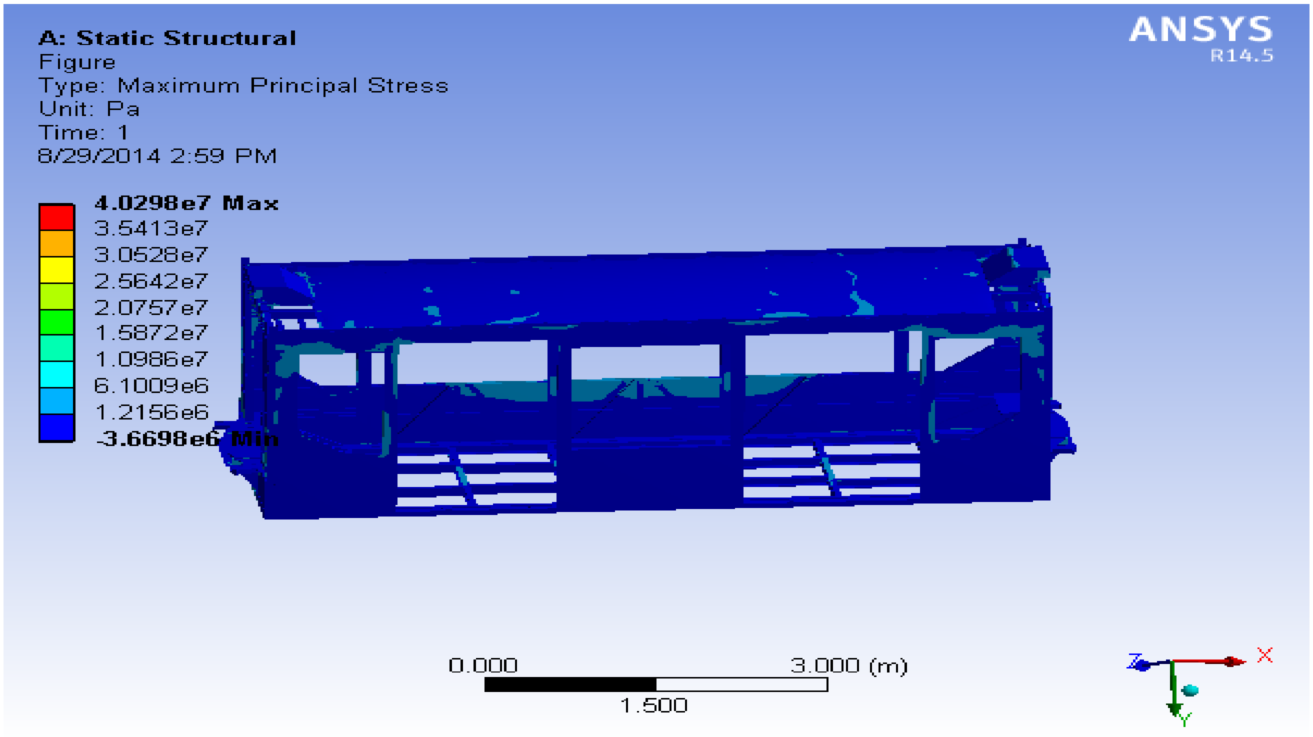

Figure 3.26 Maximum principal stress due to operating load

3.3.5 Result of aluminum honeycomb tram car due to tensile force at buffer

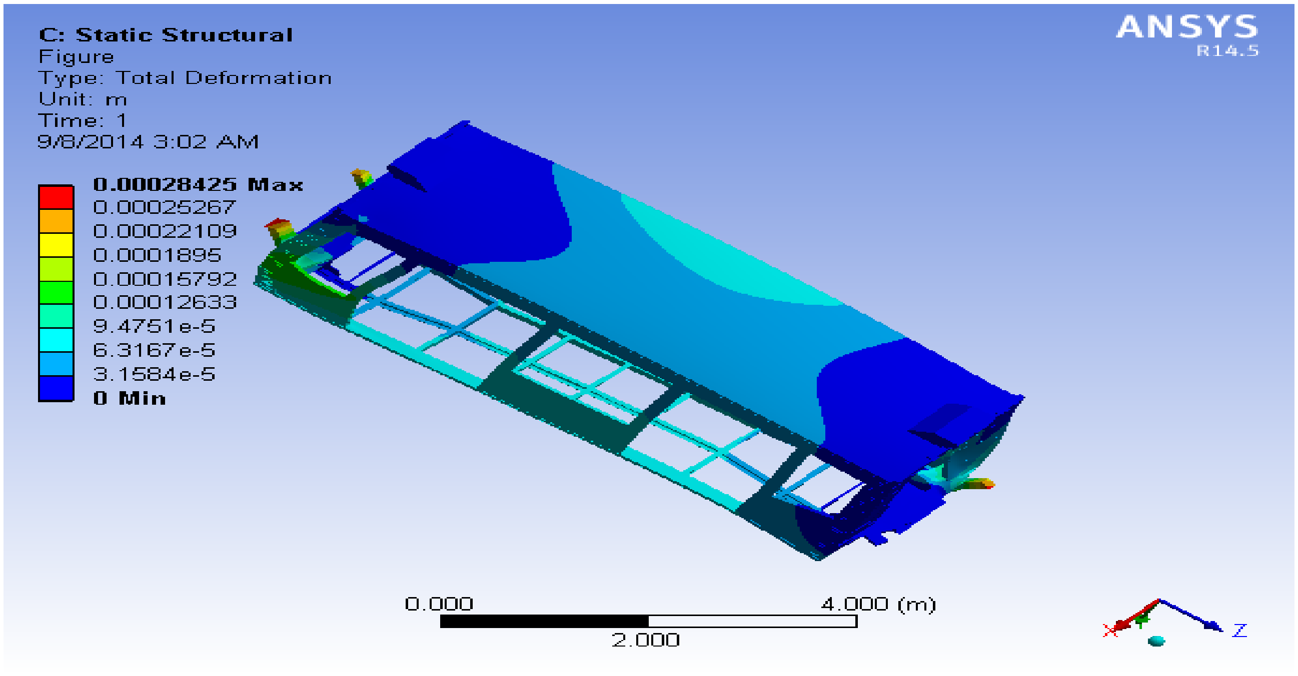

Figure 3.27 Total deformation due to tensile force at buffer

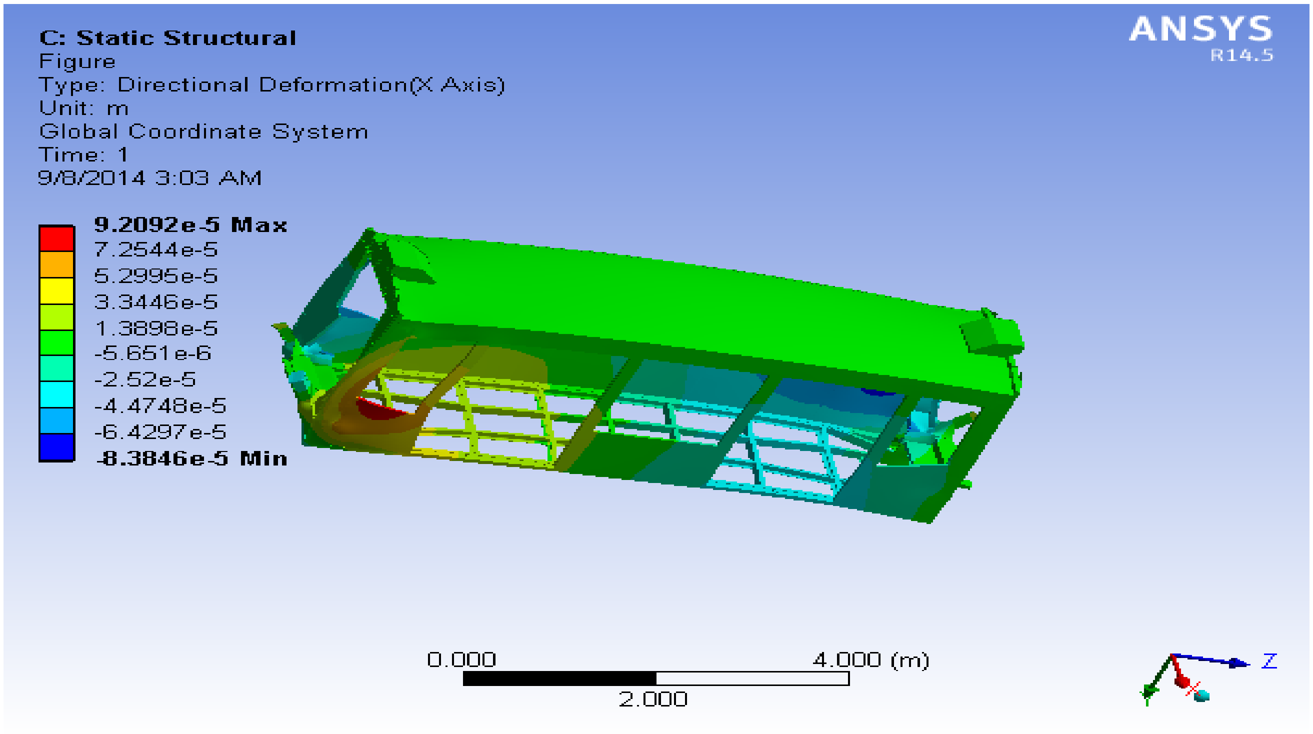

Figure 3.28 Directional deformation due to tensile force at buffer

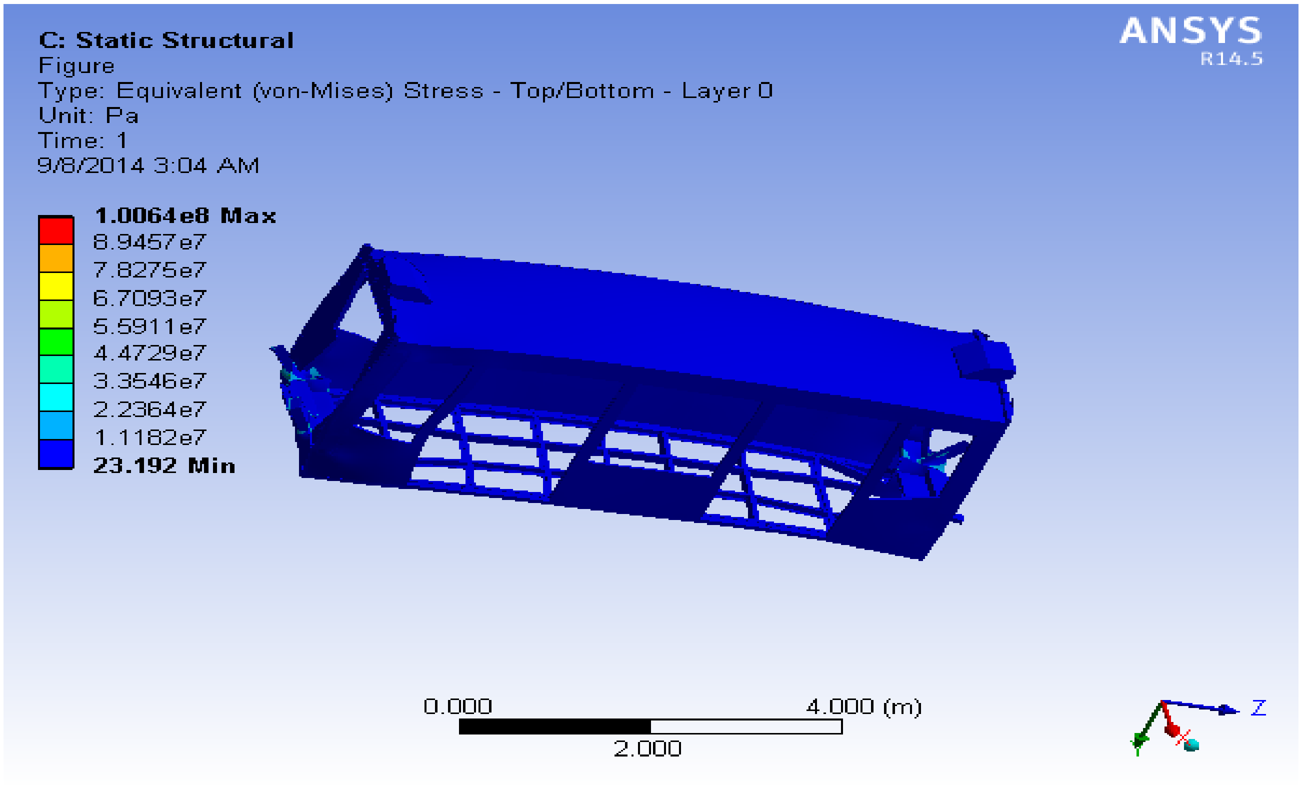

Figure 3.29 Equivalent (von-mises) stress due to tensile force at buffer

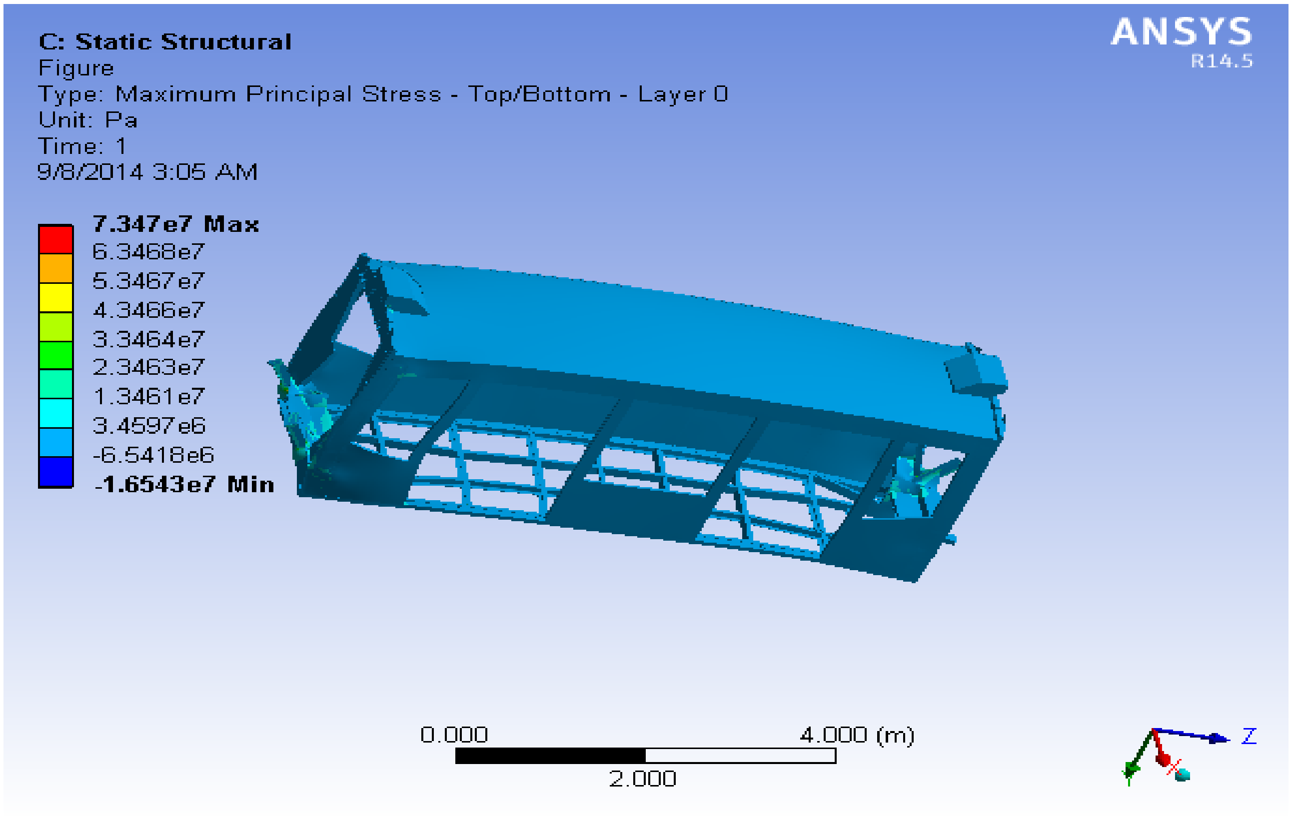

Figure 3.30 Maximum principal stress due to tensile force at buffer

3.3.6 Result of aluminum honeycomb tram car due to compression force at buffer

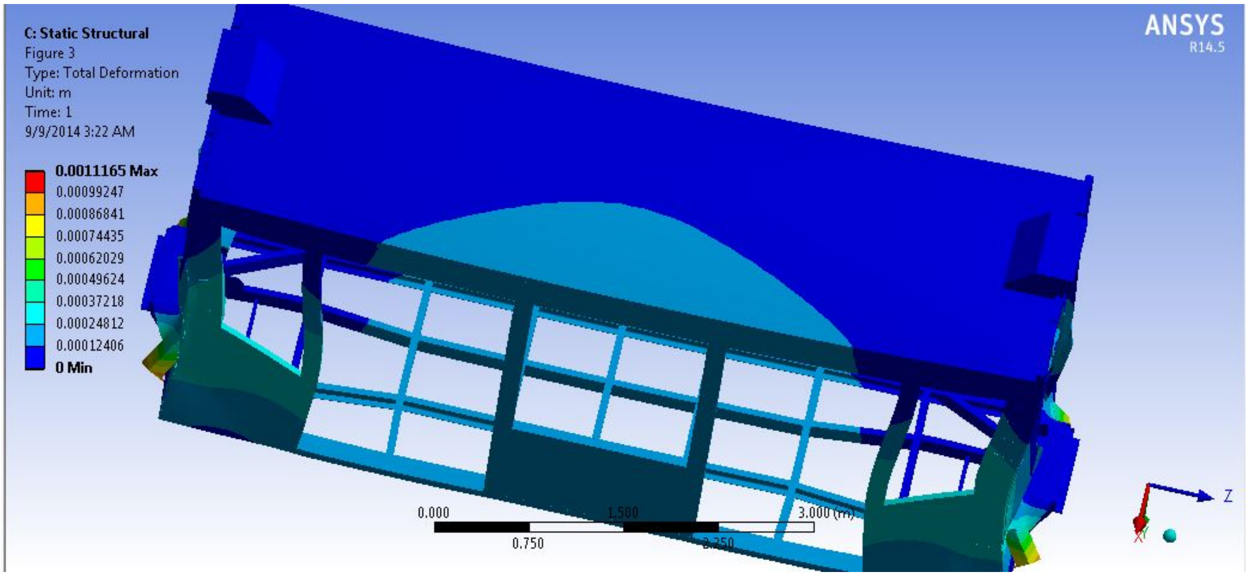

Figure 3.31 Total deformation due to compression force at buffer

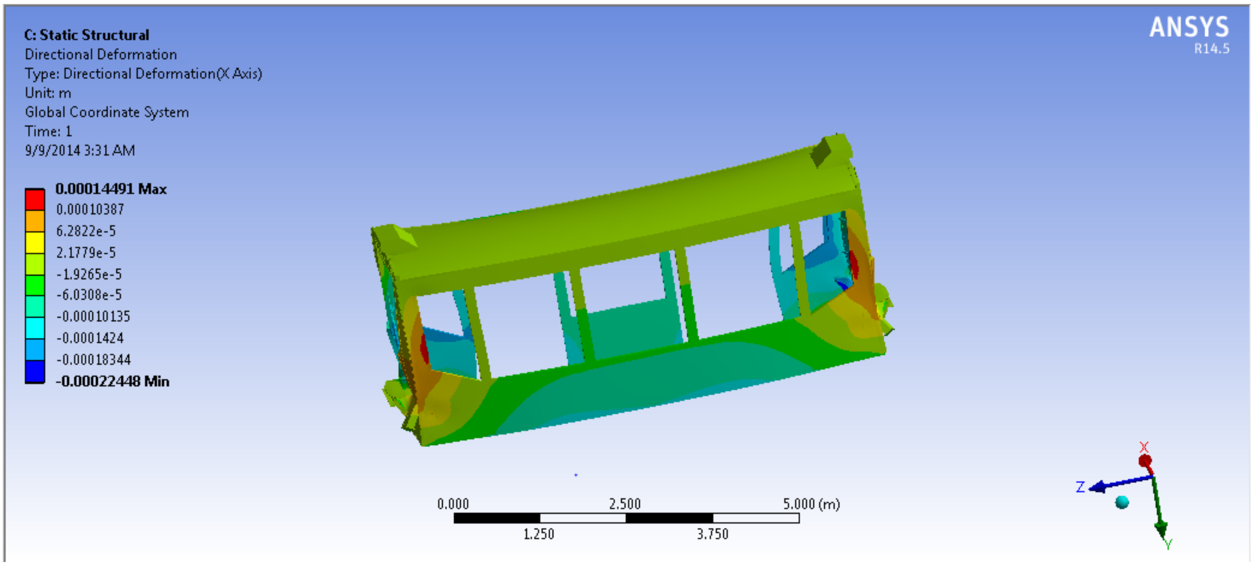

C: Static Structural
Directional Deformation
Type: Directional Deformation(X Axis)
Unit: m
Global Coordinate System
Time: 1
9/9/2014 3:31 AM

Figure 3.32 Directional deformation due to compression force at buffer

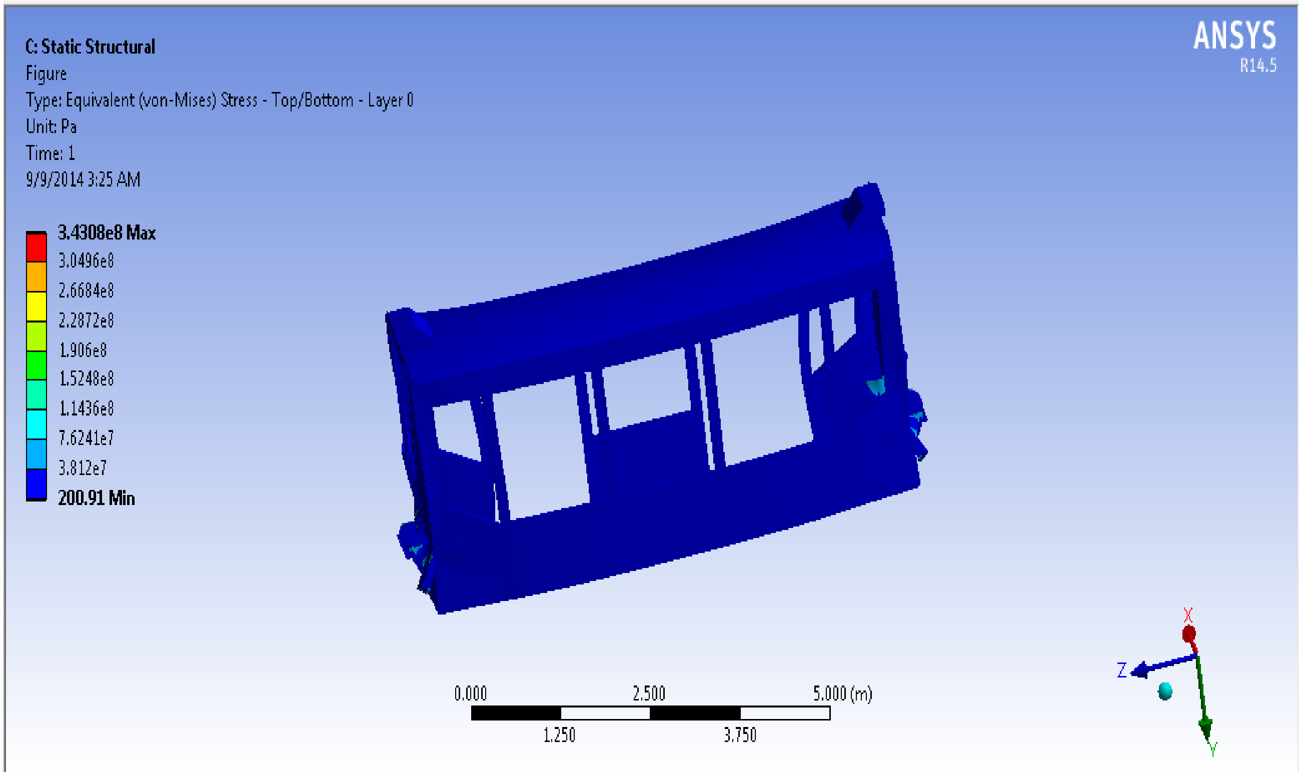

C: Static Structural
Figure
Type: Equivalent (von-Mises) Stress - Top/Bottom - Layer 0
Unit: Pa
Time: 1
9/9/2014 3:25 AM

Figure 3.33 Equivalent (von-mises) stress due to compression force at buffer

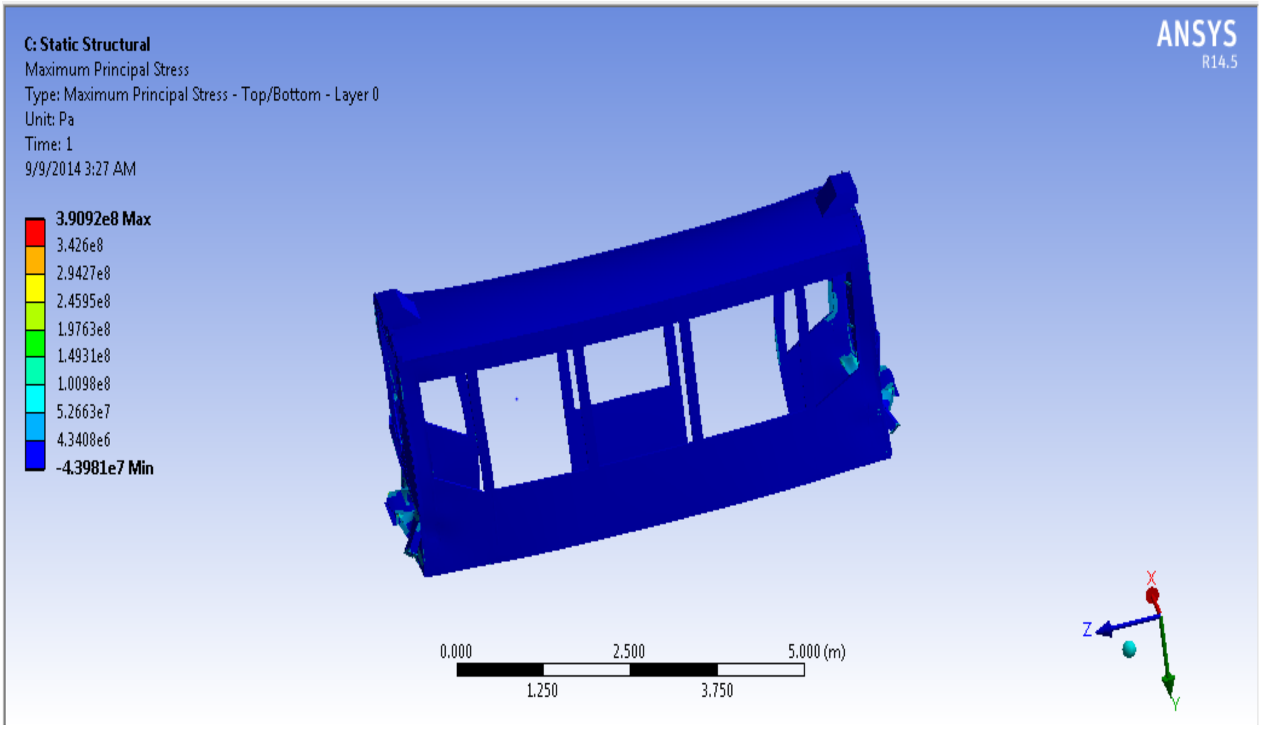

Figure 3.34 Maximum principal stress due to compression force at buffer

3.3.7 Result of aluminum honeycomb tram car due to right turn

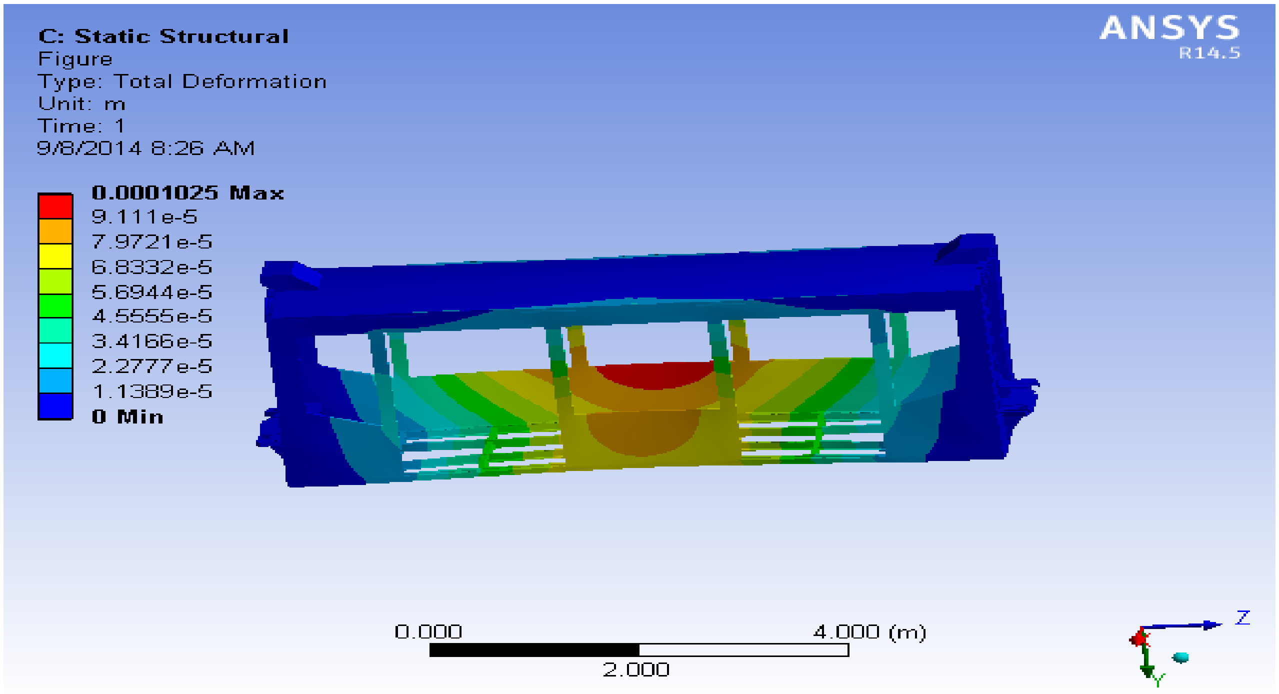

Figure 3.35 Total deformation due to right turn

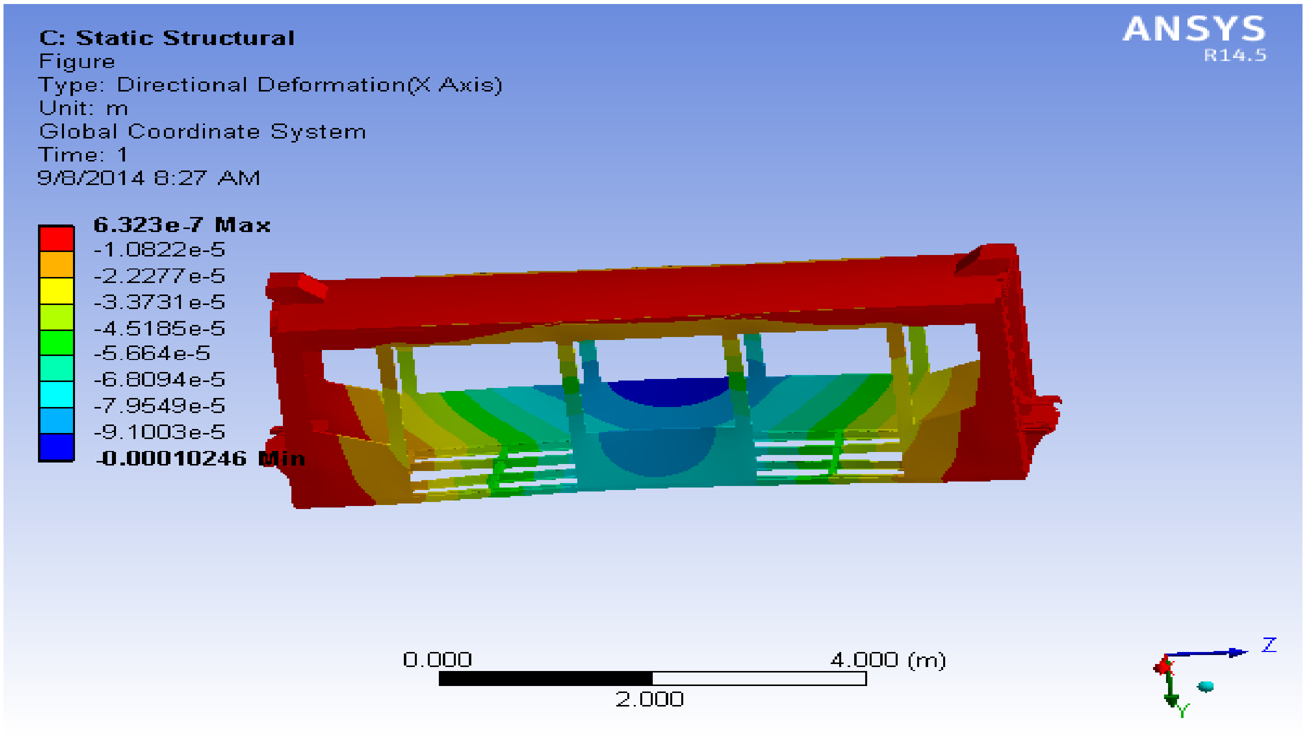

Figure 3.36 Directional deformation due to right turn

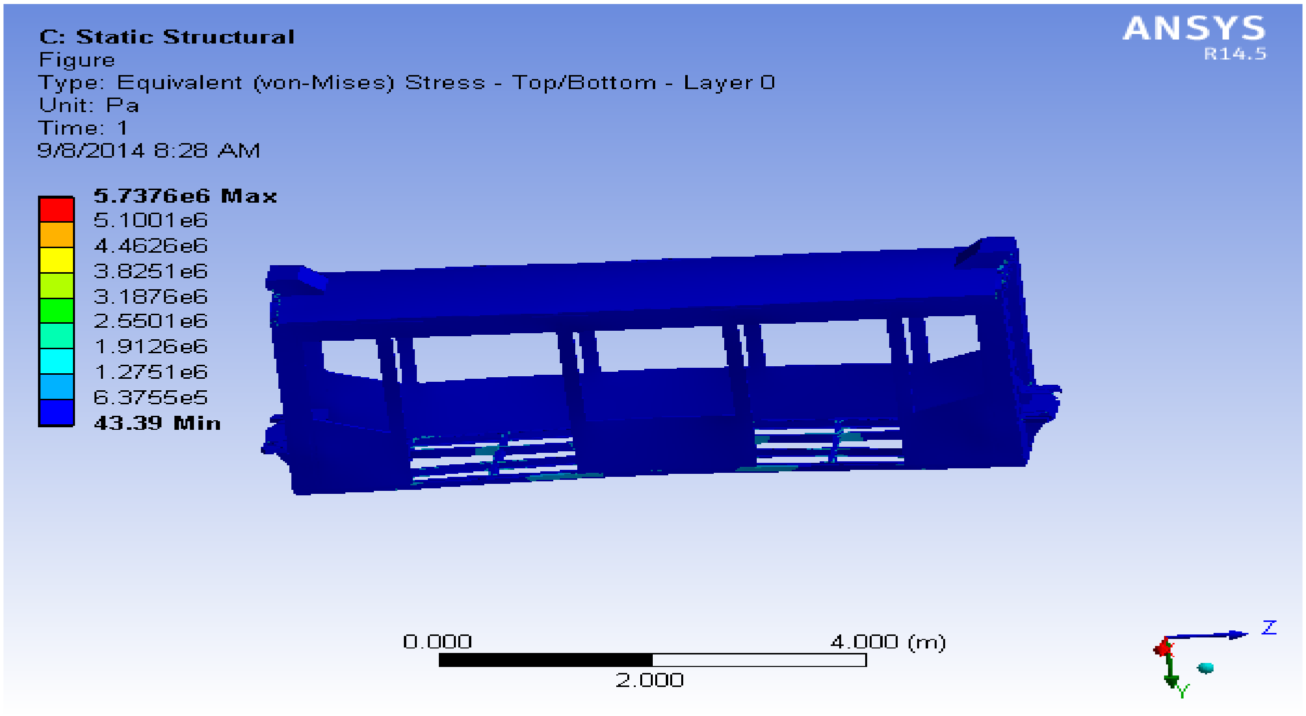

Figure 3.37 Equivalent (von-mises) stress due to right turn

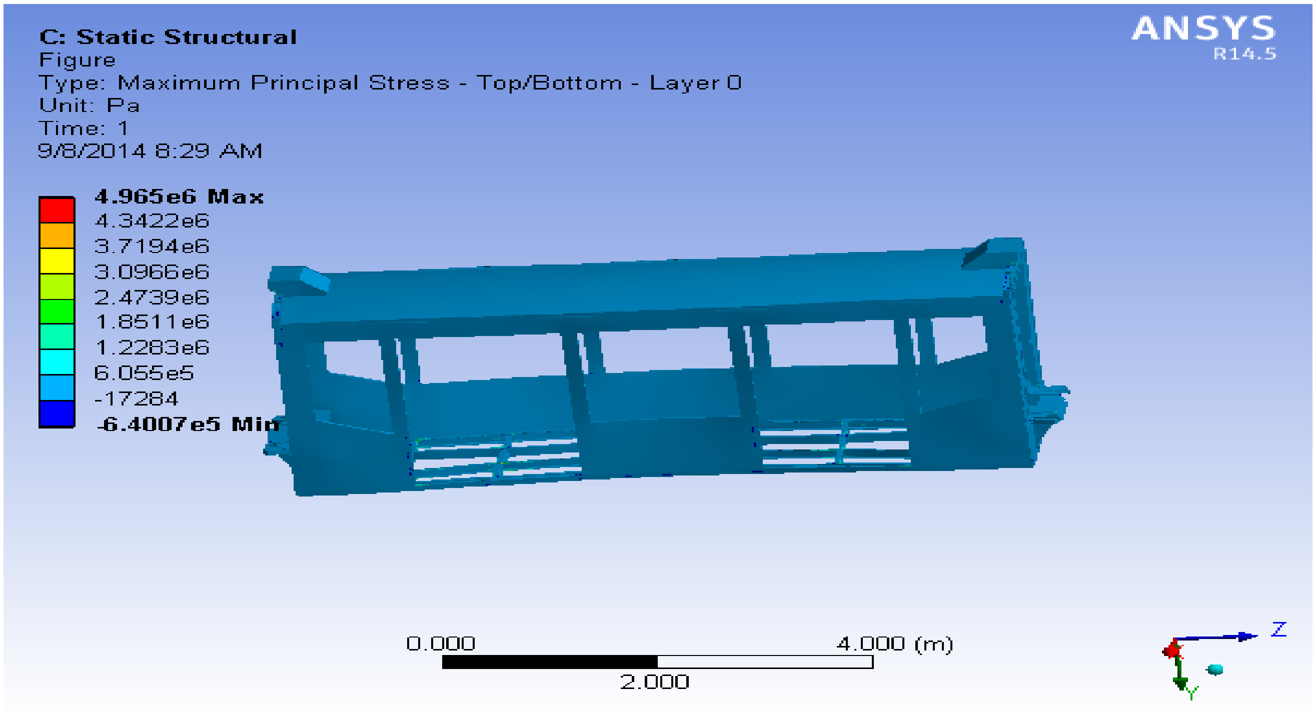

Figure 3.38 Maximum principal stress due to right turn

3.3.8 Result of aluminum honeycomb tram car due to operating load

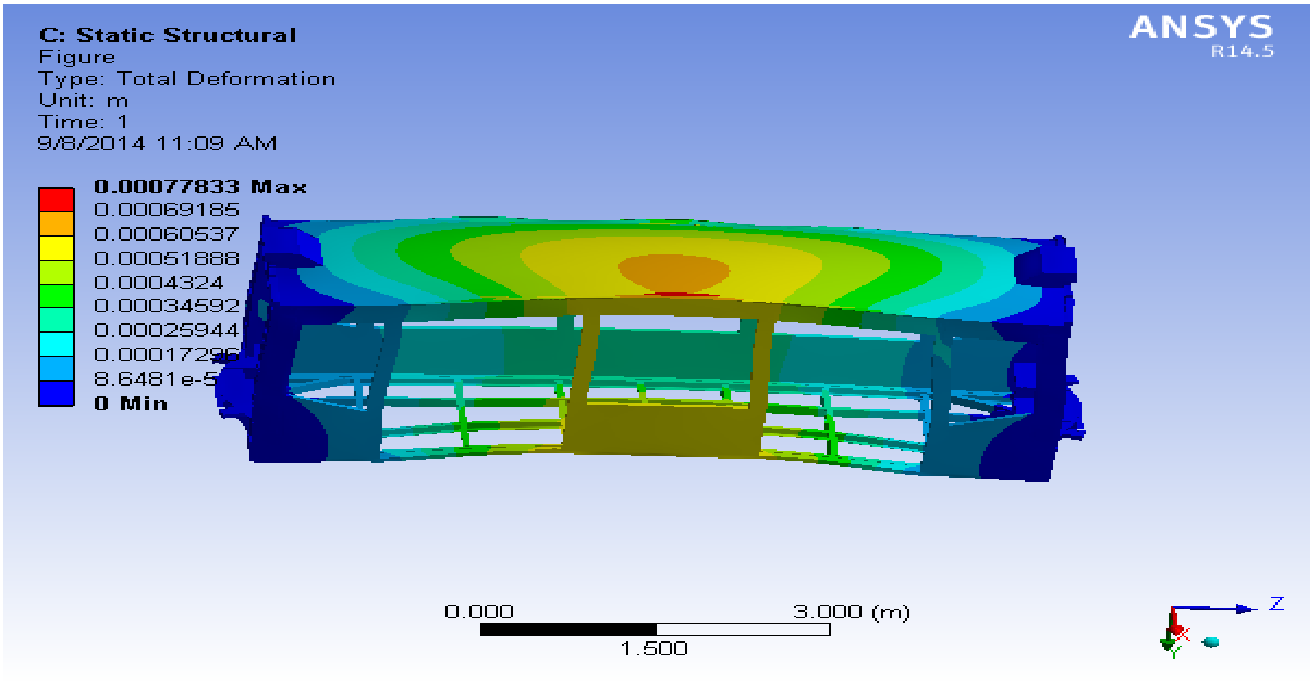

Figure 3.39 Total deformation due to operating load

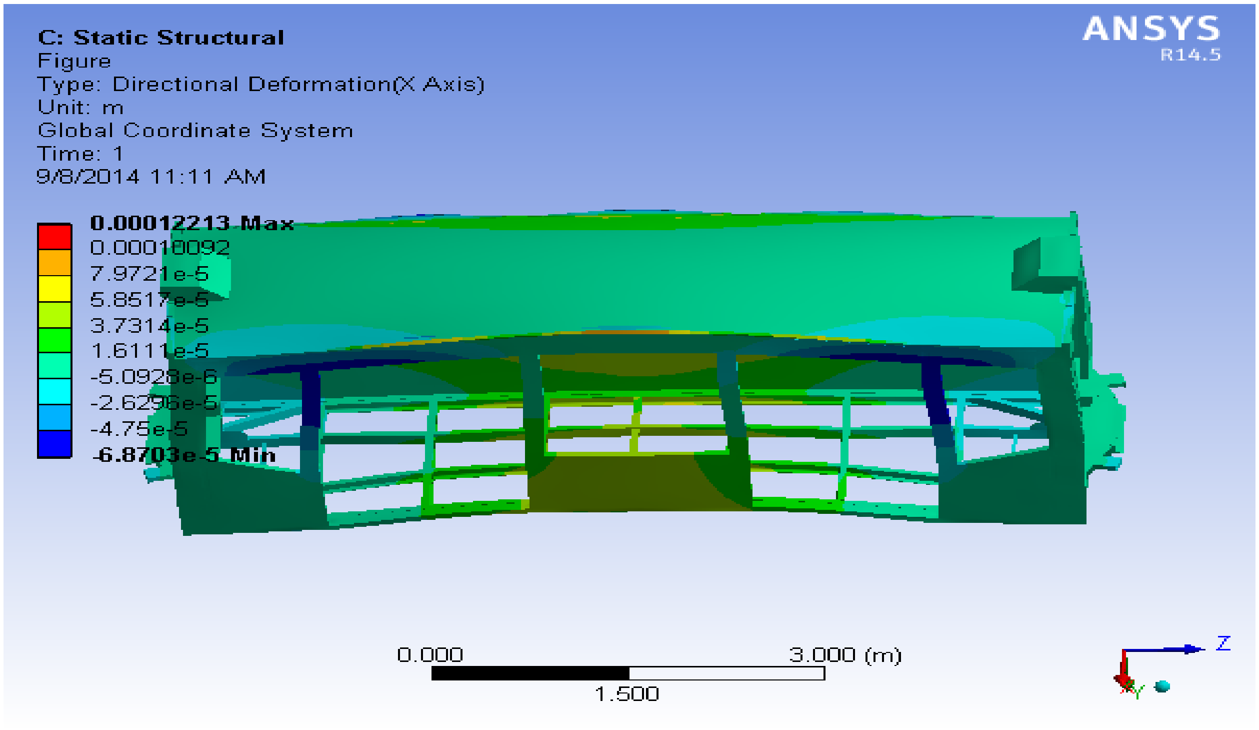

Figure 3.40 Directional deformation due to operating load

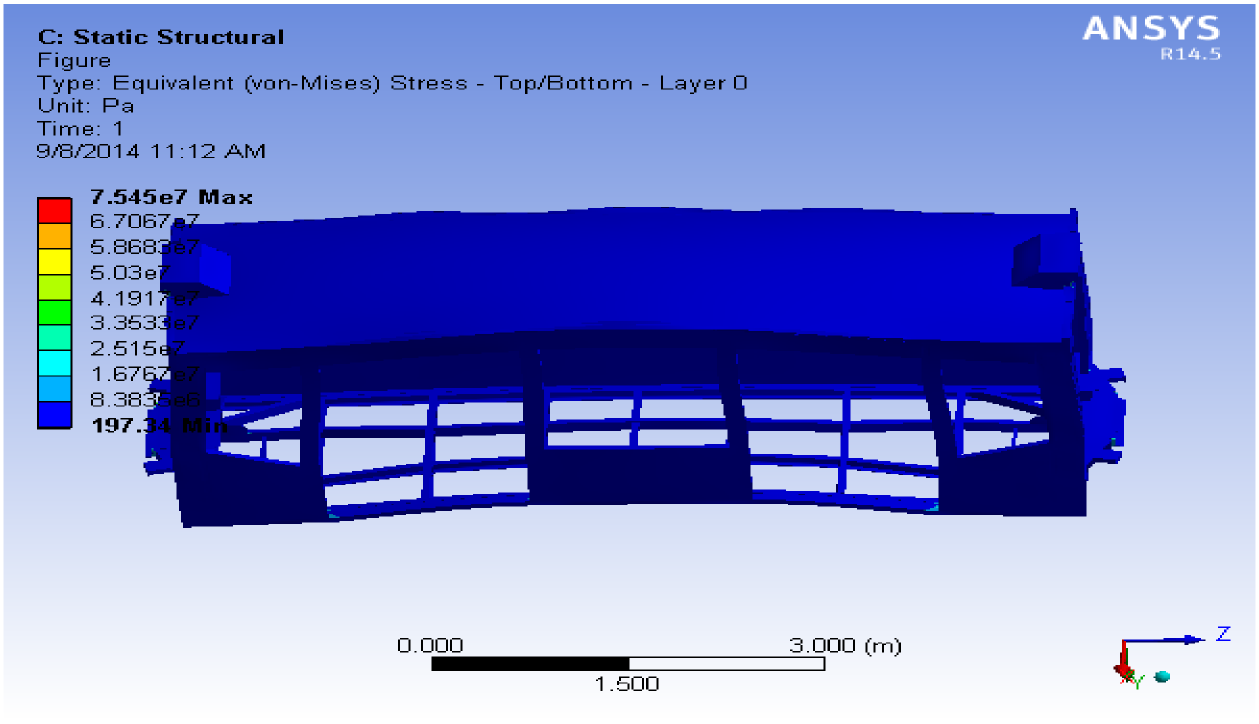

Figure 3.41 Equivalent (von-mises) stress due to operating load

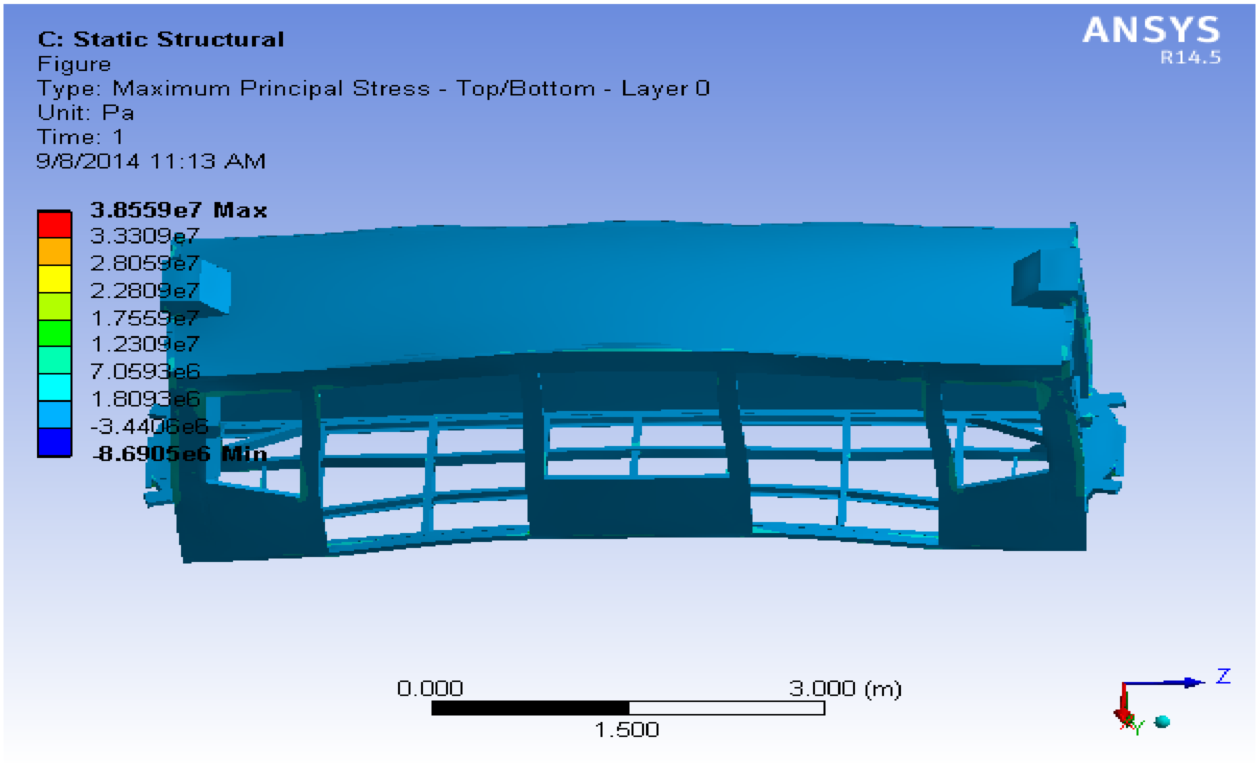

Figure 3.42 Maximum principal stress due to operating load

CHAPTER FOUR

4. Result and discussion

The results from the finite element modeling of the tram car using steel and aluminum sandwich material has been studied in ANSYS are presented. The purpose of the modeling is to verifying the vehicle body with the standard and the testing are based on proven experience supported by the evaluation of experimental data and published information. The stress analyzed under five different load condition stated under Table 3.2.The goal of stress analysis and the deformation presented in this section is to investigate the maximum stress area and verified with the standard and parameterized study of change of stress with both material. The ANSYS result described in table form found below.

Table 4.1 Maximum principal stress values

Load condition	Steel material	Aluminum honeycomb
Due to operation load	40.2MPa	38.55MPa
Due to tensile force at the buffer	97.344MPa	100.64MPa
Due to compression force at the buffer	347.19MPa	397.2MPa
Due to left turn	2.457MPa	3.154MPa
Due to right turn	1.995MPa	4.96MPa

Table 4.2 total deformation value

Load condition	Steel material	Aluminum honeycomb
Due to operation load	0.000028	0.0007783
Due to tensile force at the buffer	0.00013679	0.000284
Due to compression force at the buffer	0.000544	0.00111
Due to left turn	0.00002563	0.0001025
Due to right turn	0.00002563	0.0001025

The density of aluminum honeycomb material is 83.2 kg/m^3 and the density of steel used was 7800kg/m^3.With the same volume the mass reduces by 93.75% but the combination of the total weight of the vehicle reduced by 12.76 %. (I.e. the total weight of steel tram vehicle is 7440kg and 6500kg that of aluminum honeycomb sandwich material)

The advantage of aluminum honeycomb is not only weight reduction but also remove the manufacturing complexity of the steel vehicle due to its parts used. From the analysis the maximum principal stress value due to compression force is greater than the other stress value in other load case.

According to the EN12663 proof or yield strength under the static load case stated earlier When comparing the calculated or measured stress to the permissible stress, the utilization of the component shall be less than or equal to 1 according to the following general equation:

$$U = \frac{\sigma_{CS_1}}{R} \leq 1$$

Where

U is the utilisation;

S_1 is the safety factor for yield and proof strength

R is the material yield (ReH) or 0. 2 % proof stress (N/mm^2)

For ultimate failure

$$U = \frac{\sigma_{CS_2}}{R_m} \leq 1$$

Where

U is the utilisation

S_2 is the is the safety factor for ultimate failure

Rm is the material ultimate stress (N/mm^2) (as defined in EN 10002-1)

σ_C is the calculated stress, in newton per square millimeter (N/mm^2)

From the analysis both steel material and the aluminum honeycomb safety factor S_1 and S_2 is greater than the safety factor stated under EN12663.

In the analysis used 2mm face material and aluminum honeycomb core thickness from 38-44 mm and the compromise between weight and maximum stress value 40 mm core thickness is used.

Due to operating load or the acceleration acting on the vertical direction the maximum stress of aluminum honey comb is 38.55MPa and using steel the value is 40.2 MPa .The aluminum honeycomb reduced the stress by 4.1%.

Due to a tensile load of 50KN force applied on both side of the tram car the maximum principal stress of steel material is 97.334MPa and using aluminum honeycomb its stress is 100.64 MPa and they variation is 3.34%.

Due to acceleration force in the lateral direction to the right and to the left 0.697MPa and 2.96MPa maximum stress variation between steel and aluminum honeycomb.

Due to a compression force of 200KN force applied on both side of the tram car the maximum principal stress of steel material is 347.19MPa and using aluminum honeycomb its value is 397.2 MPa and its variation is around 12.59 %.

The maximum principal stress due to compression force applied on tram car using aluminum honeycomb higher compare to steel material result .To reduce the variation add steel or other stiffener on the aluminum honeycomb material or Increasing either the core or the face material thickness further reduced the maximum stress value.

CHAPTER FIVE

5. Conclusion, recommendations and future work

The purpose of this thesis was the structure analysis of the tram car by using finite element methods and also parameterized study was done by varying the material using steel and aluminum honeycomb.

5.1 conclusions

The conclusions that can be drawn from this research are:

- Structural analysis of the tram car using Aluminum honeycomb reduce the gross weight by 12.14% with almost the same maximum principal stress subjected to tensile ,compression ,operating and left and right turn. Aluminum honeycomb direct and indirect advantage on the railway infrastructure due to its light weight.
- From the analysis of vehicle body using steel and aluminum honeycomb sandwich material subjected to tensile and compression load the maximum stress found on the two end of buffer.
- The tram car maximum deformation and maximum stress found on the End walls and side walls connections area, the vertical support at the door area and the two end window corner. From the analysis verify that no significant permanent deformation is present after removal of the maximum loads.
- The deflection value of both steel and aluminum honey comb material value are minimum than material distortion limit.
- The thickness of the aluminum sandwich tram car is 44 mm and that of steel is 62mm.it save 0.248 m^2 with in vehicle body helps to increase space for the passengers.

Generally, the use of aluminum honeycomb are helps to reduce the weight of the tram car and it has direct and indirect advantage related to operating energy, acceleration, axle load and passenger comfort.

5.2 Recommendations

- The implications of the finite element analysis were promising, but using further justification by material test on aluminum honey comb this will help demonstrating the varies benefit of aluminum honeycomb. These tests could also include full-scale Strain gauge test on the tram car.
- The maximum principal stress due to compression force applied on tram car using aluminum honeycomb higher compare to steel material result .To reduce the variation replace the material in higher stress area and multi-material approach will be used.

5.3 Future work

- modal frequency analysis of tram car using aluminum honeycomb material
- Fatigue strength analysis of the tram vehicle on the articulation joints between vehicle bodies,
- Crash analysis of tram vehicle car using aluminum honeycomb material.

References

[1].EN 12663-1: Railway applications -Structural requirements of railway vehicle bodies - Part 1: Locomotives and passenger Rolling stock, 2010

[2]. EN 15227 ‘Railway applications–crashworthiness requirements for railway vehicle bodies’, European Committee for Standardization (CEN), CEN/TC 256, Final Draft 9/2007

[3]. Jens Koenig, Horst E. Friedrich, ‘Integral consideration of the light weight design for railway vehicles’

[4].Jens König, Gerhard Kopp, Joachim Winter, Horst E. Friedrich, 2012, Methodology for force flow optimized car body structures and implementation, German Aerospace Center - Institute of Vehicle Concepts

[5].C. Baykasoglu, E. Sunbuloglu, S. E. Bozdag, F. Aruk, T. Toprak and A. Mugan , ‘Numerical static and dynamic stress analysis on railway passenger and freight car’, International Iron & Steel Symposium, , Karabük, Türkiye , April 2012

[6].safety standard for structural requirements for heavy rail transit vehicles "Draft No. 9, Rev. 2", December 2007

[7].David Weinberg, “light weight methodology in rail vehicle”, department of aeronautical and vehicle engineering, 2010

[8].Alexander schirrer, martin kozek, jurgen schoftner, mimo, “vibration control for flexible rail car body: design and experimental validation”, Austria

[9]. Anneli Orvnas, Methods for Reducing Vertical Carbody Vibrations of a Rail Vehicle, Dipak G. Vamja, G. G. Tejani, July 2013 International Journal of Innovative Research in Science, Engineering and Technology, Experimental Test on Sandwich Panel Composite Material, Vol. 2, Issue 7, 3047-3054, 2010

[10]. Emigliano Campus, Bernard Roure, Use of Composite Materials in Railway Applications.

[11]. Ronan Cunningham, Michael O’Sullivan, Prof. J.F. McNamara, Dr. Annette Harte; shape and thickness optimization of a composite light rail vehicle body-shell.

[12]. Dipak D. Bari, P.S.Bajaj, theoretical flexural behavior of sandwich panel using composite materials, International Journal of Research in Engineering and Technology eISSN: 2319-1163 pISSN: 2321-7308

[13]. D. Zenkert, “Sandwich Construction”, EMAS Publishing, UK, 1997

[14]. David Wennberg, A Light Weight Car Body for High-Speed Trains Literature study, 2009

[15]. D. Zenkert. An Introduction to Sandwich Construction. EMAS, 1995.

[16]. A H Harte, J F McNamara and I D Robby, “A multilevel approach to the optimization of a composite light rail vehicle body shell”, Composite Structures, Vol. 63, Issues 3-4, 2004 pp. 447-453

[17]. DavidWennberg, Per Wennhage and Sebastian Stichel, selection of sandwich panels for the load carrying structure of high –speed rail vehicles, 16th International Conference on Composite Structures ICCS16

[18]. Salih Akour and Hussein Maaitah, ‘Finite Element Analysis of Loading Area Effect on Sandwich Panel Behavior beyond the Yield Limit’

[19]. AMIT KUMAR JHA, free vibration analysis of sandwich panel free vibration, 2007

[20]. J.R. Vinson, “The Behavior of Sandwich Structures of Isotropic and Composite Materials, Technomic, Basel, 1999

[21]. Huyue Zhao, stress analysis of tapered sandwich panels with isotropic or laminated composite facings , 2002

[22]. J S Kim, N P Kim, S H Han, “Optimal stiffness design of composite laminates for a train carbody by an expert system and enumeration method”, Composite Structures, Volume 68, Issue 2, April 2005, pp. 147-156

[23]. Henrik Herranen,Ott Pabut,Martin Eerme,Jüri Majak,Meelis Pohlak ,Jaan Kers,Mart Saarna,Georg Allikas, are Aruniit, ‘Design and Testing of Sandwich Structures with Different Core Materials’, ISSN 1392–1320 material science. Vol. 18, No. 1, , 2012

[24]. K B Shin, S H Hahn, “Evaluation of the structural integrity of hybrid railway carriage structures including the ageing effects of composite materials”, Composite Structures, Volume 68, Issue 2, pp. 129-137, April 2005

[25]. P Wennhage, “Structural – Acoustic Optimization of sandwich Panels”, Doctoral Thesis Report , 2001

[26]. K.Kantha Ra, K. Jayathirtha Ra,A.G.Sarwade, M.Sarath Chandra,2012, Strength Analysis on Honeycomb Sandwich Panels of different Materials, International Journal of Engineering Research and Applications (IJERA) , Vol. 2, Issue 3

[27]. M.M. Venugopal, S K Maharana, K S Badarinarayan, 2013 ,Finite Element Evaluation of Composite Sandwich Panel Under Static Four Point Bending Load, JEST-M, Vol. 2, Issue 1, 2013

[28]. Belingardi, M P Cavatorta, R Duella", Composite Structures, Volume 61, Issues 1-2, July 2003, pp. 13-25)

Appendix

ANSYS input file data for modeling aluminum honeycomb in ACP

```
Import compolyx
compolyx.application.mode='pre'
db = compolyx.DB()
Inc\\v145\\ACP\\databases\\materials.acpMdb')
db.run_script(path=u'C:\\file location \\dp0\\ACP-Pre\\ACP\\runACP.py', locals=locals())
db.models[u'ACP Model'].selection.set([db.models[u'ACP Model'].material_data.fabrics])
db.models[u'ACP Model'].material_data.create_fabric( name='Fabric.1')
db.models[u'ACP Model'].selection.set([db.models[u'ACP
Model'].material_data.fabrics['Fabric.1']])
db.models[u'ACP Model'].selection.set([db.models[u'ACP
Model'].material_data.materials['aluminum']])
db.models[u'ACP Model'].material_data.fabrics['Fabric.1'].material = db.models[u'ACP
Model'].material_data.materials['aluminum']
db.models[u'ACP Model'].material_data.fabrics['Fabric.1'].thickness = 2.0
db.models[u'ACP Model'].update(objects=[db.models[u'ACP
Model'].material_data.fabrics['Fabric.1']])
db.models[u'ACP Model'].selection.set([db.models[u'ACP
Model'].material_data.fabrics['Fabric.1']])
db.models[u'ACP Model'].material_data.fabrics['Fabric.1'].create_plot(query={
'polar_properties':[] } )
db.models[u'ACP Model'].selection.set([db.models[u'ACP
Model'].material_data.fabrics['Fabric.1']])
db.models[u'ACP Model'].selection.set([db.models[u'ACP Model'].material_data.fabrics])
db.models[u'ACP Model'].selection.set([db.models[u'ACP
Model'].material_data.fabrics['Fabric.1']])
db.models[u'ACP Model'].material_data.fabrics['Fabric.1'].name = u'face 1'
```

```
db.models[u'ACP Model'].selection.set([db.models[u'ACP Model'].material_data.fabrics['face
1']])
db.models[u'ACP Model'].selection.set([db.models[u'ACP Model'].material_data.fabrics])
db.models[u'ACP Model'].material_data.create_fabric( name='Fabric.1')
db.models[u'ACP Model'].selection.set([db.models[u'ACP
Model'].material_data.fabrics['Fabric.1']])
db.models[u'ACP Model'].selection.set([db.models[u'ACP
Model'].material_data.materials['Honeycomb']])
db.models[u'ACP Model'].material_data.fabrics['Fabric.1'].material = db.models[u'ACP
Model'].material_data.materials['Honeycomb']
db.models[u'ACP Model'].material_data.fabrics['Fabric.1'].thickness = 40.0
db.models[u'ACP Model'].material_data.fabrics['Fabric.1'].name = u'core material'
db.models[u'ACP Model'].update(objects=[db.models[u'ACP Model'].material_data.fabrics['core
material']])
db.models[u'ACP Model'].selection.set([db.models[u'ACP Model'].material_data.fabrics['core
material']])
db.models[u'ACP Model'].material_data.fabrics['core material'].create_plot(query={
'polar_properties':[] } )
db.models[u'ACP Model'].selection.set([db.models[u'ACP Model'].material_data.fabrics['core
material']])
db.models[u'ACP Model'].selection.set([db.models[u'ACP Model'].material_data.fabrics])
db.models[u'ACP Model'].material_data.create_fabric( name='Fabric.1')
db.models[u'ACP Model'].selection.set([db.models[u'ACP
Model'].material_data.fabrics['Fabric.1']])
db.models[u'ACP Model'].selection.set([db.models[u'ACP
Model'].material_data.materials['aluminum']])
db.models[u'ACP Model'].material_data.fabrics['Fabric.1'].material = db.models[u'ACP
Model'].material_data.materials['aluminum']
db.models[u'ACP Model'].material_data.fabrics['Fabric.1'].thickness = 2.0
db.models[u'ACP Model'].material_data.fabrics['Fabric.1'].name = u'face2'
```

```
db.models[u'ACP Model'].update(objects=[db.models[u'ACP
Model'].material_data.fabrics['face2']])
db.models[u'ACP Model'].selection.set([db.models[u'ACP
Model'].material_data.fabrics['face2']])
db.models[u'ACP Model'].material_data.fabrics['face2'].create_plot(query={ 'polar_properties':[]
} )
db.models[u'ACP Model'].selection.set([db.models[u'ACP
Model'].material_data.fabrics['face2']])
db.models[u'ACP Model'].selection.set([db.models[u'ACP
Model'].element_sets['All_Elements']])
db.models[u'ACP Model'].update(objects=[db.models[u'ACP
Model'].element_sets['All_Elements']])
db.models[u'ACP Model'].selection.set([db.models[u'ACP
Model'].element_sets['All_Elements']])
db.models[u'ACP Model'].selection.set([db.models[u'ACP
Model'].element_sets['All_Elements']])
db.models[u'ACP Model'].selection.set([db.models[u'ACP Model'].rosettes['Rosette']])
db.models[u'ACP Model'].selection.set([db.models[u'ACP Model'].rosettes['Rosette']])
db.models[u'ACP Model'].selection.set([db.models[u'ACP Model'].oriented_element_sets])
db.models[u'ACP Model'].create_oriented_element_set(name='OrientedElementSet.1')
db.models[u'ACP Model'].selection.set([db.models[u'ACP
Model'].oriented_element_sets['OrientedElementSet.1']])
db.models[u'ACP Model'].selection.set([db.models[u'ACP
Model'].element_sets['All_Elements']])
db.models[u'ACP Model'].selection.set([db.models[u'ACP
Model'].element_sets['All_Elements']])
db.models[u'ACP Model'].selection.set([db.models[u'ACP Model'].rosettes['Rosette']])
db.models[u'ACP Model'].oriented_element_sets['OrientedElementSet.1'].element_sets =
(db.models[u'ACP Model'].element_sets['All_Elements'])
```

```
db.models[u'ACP Model'].oriented_element_sets['OrientedElementSet.1'].rosettes=(db.models[u'ACP Model'].rosettes['Rosette'])
db.models[u'ACP Model'].update(objects=[db.models[u'ACP Model'].oriented_element_sets['OrientedElementSet.1']])
db.models[u'ACP Model'].selection.set([db.models[u'ACP Model'].oriented_element_sets['OrientedElementSet.1']])
db.models[u'ACP Model'].selection.set([db.models[u'ACP Model'].rosettes['Rosette']])
db.models[u'ACP Model'].oriented_element_sets['OrientedElementSet.1'].orientation_direction = (1.0, 0.0, 0.0)
db.models[u'ACP Model'].update(objects=[db.models[u'ACP Model'].oriented_element_sets['OrientedElementSet.1']])
db.models[u'ACP Model'].selection.set([db.models[u'ACP Model'].oriented_element_sets['OrientedElementSet.1']])
db.models[u'ACP Model'].selection.set([db.models[u'ACP Model'].oriented_element_sets['OrientedElementSet.1']])
db.models[u'ACP Model'].selection.set([db.models[u'ACP Model'].modeling_ply_groups])
db.models[u'ACP Model'].create_modeling_ply_group( name='PlyGroup.1' )
db.models[u'ACP Model'].selection.set([db.models[u'ACP Model'].modeling_ply_groups['PlyGroup.1']])
db.models[u'ACP Model'].modeling_ply_groups['PlyGroup.1'].name = u'face 1'
db.models[u'ACP Model'].selection.set([db.models[u'ACP Model'].modeling_ply_groups['face 1']])
db.models[u'ACP Model'].selection.set([db.models[u'ACP Model'].modeling_ply_groups])
db.models[u'ACP Model'].create_modeling_ply_group( name='PlyGroup.1' )
db.models[u'ACP Model'].selection.set([db.models[u'ACP Model'].modeling_ply_groups['PlyGroup.1']])
db.models[u'ACP Model'].modeling_ply_groups['PlyGroup.1'].name = u'core'
db.models[u'ACP Model'].selection.set([db.models[u'ACP Model'].modeling_ply_groups['core']])
```

```
db.models[u'ACP Model'].selection.set([])
db.models[u'ACP Model'].selection.set([db.models[u'ACP Model'].modeling_ply_groups])
db.models[u'ACP Model'].create_modeling_ply_group( name='PlyGroup.1' )
db.models[u'ACP Model'].selection.set([db.models[u'ACP
Model'].modeling_ply_groups['PlyGroup.1']])
db.models[u'ACP Model'].modeling_ply_groups['PlyGroup.1'].name = u'f'
db.models[u'ACP Model'].selection.set([db.models[u'ACP Model'].modeling_ply_groups['f']])
db.models[u'ACP Model'].selection.set([])
db.models[u'ACP Model'].create_modeling_ply_group( name='PlyGroup.1' )
db.models[u'ACP Model'].selection.set([db.models[u'ACP
Model'].modeling_ply_groups['PlyGroup.1']])
db.models[u'ACP Model'].modeling_ply_groups['PlyGroup.1'].name = u'face2'
db.models[u'ACP Model'].selection.set([db.models[u'ACP
Model'].modeling_ply_groups['face2']])
db.models[u'ACP Model'].selection.set([db.models[u'ACP Model'].modeling_ply_groups['face
1']])
mp_=db.models[u'ACP Model'].modeling_ply_groups['face 1'].create_modeling_ply()
db.models[u'ACP Model'].selection.set([db.models[u'ACP Model'].modeling_ply_groups['face
1'].plies['ModelingPly.1']])
db.models[u'ACP Model'].selection.set([db.models[u'ACP
Model'].oriented_element_sets['OrientedElementSet.1']])
db.models[u'ACP Model'].selection.set([db.models[u'ACP
Model'].oriented_element_sets['OrientedElementSet.1']])
db.models[u'ACP Model'].selection.set([db.models[u'ACP Model'].material_data.fabrics['face
1']])
db.models[u'ACP Model'].modeling_ply_groups['face 1'].plies['ModelingPly.1'].ply_material =
db.models[u'ACP Model'].material_data.fabrics['face 1']
db.models[u'ACP Model'].modeling_ply_groups['face
1'].plies['ModelingPly.1'].oriented_element_sets = (db.models[u'ACP
Model'].oriented_element_sets['OrientedElementSet.1'])
```

```
db.models[u'ACP Model'].selection.set([db.models[u'ACP Model'].modeling_ply_groups['face
1'].plies['ModelingPly.1']])
db.models[u'ACP Model'].selection.set([db.models[u'ACP
Model'].modeling_ply_groups['core']])
mp_=db.models[u'ACP Model'].modeling_ply_groups['core'].create_modeling_ply()
db.models[u'ACP Model'].selection.set([db.models[u'ACP
Model'].modeling_ply_groups['core'].plies['ModelingPly.2']])
db.models[u'ACP Model'].selection.set([db.models[u'ACP
Model'].oriented_element_sets['OrientedElementSet.1']])
db.models[u'ACP Model'].selection.set([db.models[u'ACP
Model'].oriented_element_sets['OrientedElementSet.1']])
db.models[u'ACP Model'].selection.set([db.models[u'ACP Model'].material_data.fabrics['core
material']])
db.models[u'ACP Model'].modeling_ply_groups['core'].plies['ModelingPly.2'].ply_material =
db.models[u'ACP Model'].material_data.fabrics['core material']
db.models[u'ACP
Model'].modeling_ply_groups['core'].plies['ModelingPly.2'].oriented_element_sets =
(db.models[u'ACP Model'].oriented_element_sets['OrientedElementSet.1'])
db.models[u'ACP Model'].selection.set([db.models[u'ACP
Model'].modeling_ply_groups['core'].plies['ModelingPly.2']])
db.models[u'ACP Model'].selection.set([db.models[u'ACP
Model'].modeling_ply_groups['face2']])
mp_=db.models[u'ACP Model'].modeling_ply_groups['face2'].create_modeling_ply()
db.models[u'ACP Model'].selection.set([db.models[u'ACP
Model'].modeling_ply_groups['face2'].plies['ModelingPly.3']])
db.models[u'ACP Model'].selection.set([db.models[u'ACP
Model'].oriented_element_sets['OrientedElementSet.1']])
db.models[u'ACP Model'].selection.set([db.models[u'ACP
Model'].material_data.fabrics['face2']])
```

```
db.models[u'ACP Model'].modeling_ply_groups['face2'].plies['ModelingPly.3'].ply_material =
db.models[u'ACP Model'].material_data.fabrics['face2']
db.models[u'ACP
Model'].modeling_ply_groups['face2'].plies['ModelingPly.3'].oriented_element_sets =
(db.models[u'ACP Model'].oriented_element_sets['OrientedElementSet.1'])
db.models[u'ACP Model'].selection.set([db.models[u'ACP
Model'].modeling_ply_groups['face2'].plies['ModelingPly.3']])
db.models[u'ACP Model'].selection.set([db.models[u'ACP Model'].solid_models])
db.models[u'ACP Model'].create_solid_model( name='SolidModel.1' )
db.models[u'ACP Model'].selection.set([db.models[u'ACP
Model'].solid_models['SolidModel.1']])
db.models[u'ACP Model'].selection.set([db.models[u'ACP
Model'].element_sets['All_Elements']])
db.models[u'ACP Model'].solid_models['SolidModel.1'].element_sets = [db.models[u'ACP
Model'].element_sets['All_Elements']]
db.models[u'ACP Model'].selection.set([db.models[u'ACP
Model'].solid_models['SolidModel.1']])
db.models[u'ACP Model'].selection.set([db.models[u'ACP Model'].solid_models])
db.models[u'ACP Model'].selection.set([db.models[u'ACP
Model'].solid_models['SolidModel.1']])
db.models[u'ACP Model'].update(objects=[db.models[u'ACP
Model'].solid_models['SolidModel.1']])
```